

DEPARTAMENT OF CHEMISTRY

CAROLINA DRUMONDE SOUSA

Degree in Biochemistry

ADVANCING CELL-BASED THERAPIES TOWARDS THE TREATMENT OF MYOCARDIAL INFARCTION

MASTER DEGREE IN BIOTECHNOLOGY

Universidade NOVA de Lisboa October, 2022

NOVA SCHOOL OF SCIENCE & TECHNOLOGY

DEPARTAMENT OF CHEMISTRY

ADVANCING CELL-BASED THERAPIES TOWARDS THE TREATMENT OF MYOCARDIAL INFARCTION

CAROLINA DRUMONDE SOUSA Degree in Biochemistry

Supervisor: Dr. Marta Costa, Senior Scientist,

iBET/ITQB-NOVA

Co-Supervisor: Dr. Margarida Serra, Principal Investigator,

iBET/ITQB-NOVA

Jury:

President: Prof. Dr. Carlos Alberto Gomes Salgueiro

Examiner: Dr. Miguel de Almeida FuzetaVogal: Dr. Marta Helena Guerreiro Costa

MASTER DEGREE IN BIOTECHNOLOGY

Universidade NOVA de Lisboa October, 2022

| Advancing cell-based therapies towards the treatment of myocardial infarction Copyright © Carolina Drumonde Sousa, Faculdade de Ciências e Tecnologia, Universidade NOVA de Lisboa. |
|---|
| A Faculdade de Ciências e Tecnologia e a Universidade NOVA de Lisboa têm o direito, perpétuo e sem limites geográficos, de arquivar e publicar esta dissertação através de exemplares impressos reproduzidos em papel ou de forma digital, ou por qualquer outro meio conhecido ou que venha a ser inventado, e de a divulgar através de repositórios científicos e de admitir a sua cópia e distribuição com objetivos educacionais ou de investigação, não comerciais, desde que seja dado crédito ao autor e editor. |

Acknowledgements

Primeiramente, gostaria de agradecer à Dr. Paula Alves e Prof. Manuel Carrondo por me darem possibilidade de realizar a minha dissertação de mestrado no laboratório de Tecnologia de Células Animais (TCA) no iBET.

Da mesma forma, gostaria também de deixar o meu agradecimento à Dr. Margarida Serra por tão bem me ter recebido no seu grupo. Pela disponibilidade e suporte que sempre demonstrou ao longo deste último ano.

À minha orientadora, Dr. Marta Costa, queria deixar o meu especial agradecimento por todos os ensinamentos e, além disto, agradecer por todo o apoio, orientação e disponibilidade constantes. Recebeu-me nesta instituição de braços abertos, sempre com palavras tranquilizadoras e boa disposição. De facto, este trabalho não teria sido possível sem ti.

Não posso também deixar de agradecer a todos os meus colegas do TCA e a todos no grupo das Stem, por me terem recebido tão bem e por estarem sempre dispostos a ajudar-me com absolutamente tudo. Um agradecimento especial à Margarida Costa e à Beatriz Painho, pois sem elas nada teria sido possível. Obrigada por tudo o que me ensinaram e por estarem sempre prontas a ajudar-me e apoiar-me, em tudo.

Gostaria de deixar o meu agradecimento também aos parceiros do projeto CardioPatch que contribuíram para o desenvolvimento e resultados gerados ao longo deste trabalhado, pela partilha de células, protocolos e todo o conhecimento que foram sem dúvida cruciais.

Aos meus pais, sem dúvida as pessoas mais importantes da minha vida, obrigada pelo apoio incondicional em todas as etapas da minha vida, especialmente durante todo o meu percurso académico. Mesmo fisicamente longe estiveram sempre presentes, sempre prontos amparar-me a dar-me força para continuar. Um obrigada nunca chegará por tudo o fazem por mim.

A todos os meus amigos, colegas de Bq e Biotec que contribuíram direta ou indiretamente nesta caminhada, obrigada por todos os bons momentos, por toda a ajuda e paciência comigo. E por fim, mas não menos importante, agradecer ao Pedro, que me acompanhou durante toda esta etapa, que me apoiou e deu forças para continuar.

Preface

The present work was performed at the Animal Cell Technology Unit at iBET/ITQB-NOVA (Oeiras, Portugal), supported by the CardioPatch Project (SOE4/P1/E1063), funded by Interreg Sudoe (UIDB/04462/2020) and iNOVA4Health (UIDP/04462/2020).

Abstract

Cardiovascular diseases remain the leading cause of death worldwide, with current available therapies failing to prevent or revert cardiac dysfunction. Thus, efforts have been made towards the development of new approaches with the potential to promote heart regeneration. Growing evidence suggests that the beneficial effects of transplanted cells are conducted by cells' secreted factors, such as extracellular vesicles (EVs). In this context, EV-based products are emerging as promising therapeutic strategies to repair cardiac damage after myocardial infarction.

Since the clinical translation of human adipose tissue-derived MSC (hAT-MSC) and hAT-MSC-derived EVs is currently limited by their scalability, in this work, two different strategies for manufacturing MSC-derived EVs with increased cardiac regenerative potential while maximizing EV secretion yields were explored. hAT-MSC were (i) transiently preconditioned, through glucose starvation and transfection with miR-145-5p inhibitor, known to impact their angiogenic potential and (ii) hAT-MSC were genetically modified with a lentiviral vector co-expressing apelin and FGF-2, two angiogenic and cardio-protective factors. hAT-MSC were expanded using a microcarrier-based culture system in stirred-tank bioreactors under hypoxic conditions. hAT-MSC-derived EVs were isolated from the conditioned medium by tangential flow filtration followed by size exclusion chromatography.

The different strategies implemented resulted in increased EV productivities (1.3-1.8-fold increase). We have observed that decreasing glucose concentration below 1 mM can not only impact the ability of MSC to secrete EVs, but also enhance their bioactivity towards cardiac regeneration, shedding light on the importance of standardizing cell culture conditions to develop more robust platforms for EV production. Additionally, we have shown that chemically-based non-viral gene delivery of miR-145-5p inhibitor can constitute a suitable approach to target the therapeutic potential of hAT-MSC-derived EVs. Finally, we have observed that genetically modified hAT-MSC can also secrete EVs with cardiac regeneration potential.

Keywords: Extracellular vesicles; Mesenchymal stem/stromal cells; Stirred-tank bioreactors; Preconditioning strategies; Genetically modified cells; Cardiac regenerative medicine.

Resumo

Atualmente, as doenças cardiovasculares são a principal causa de morte a nível mundial, sendo que as terapias atualmente empregues não conseguem prevenir ou reverter a disfunção cardíaca. Posto isto, esforços têm sido feitos de forma a desenvolver novas terapias capazes de promover a regeneração do tecido cardíaco. Estudos recentes sugerem que os efeitos benéficos das células transplantadas são induzidos por fatores por elas secretados, tais como as vesículas extracelulares (EVs). Por conseguinte, produtos terapêuticos à base de EVs surgem como alternativas promissoras.

Dado que a translação clínica de hMSCs do tecido adiposo (hAT-MSCs) e de EVs derivadas de hAT-MSCs é limitada pela sua escalabilidade, neste trabalho foram exploradas duas estratégias para a produção de EVs de forma a maximizar o seu potencial de regeneração cardíaco, bem como os rendimentos das EVs geradas. As hAT-MSCs foram (i) precondicionadas de forma transiente, através da deprivação de glucose e transfeção com o inibidor miR-145-5p, que tem um impacto no seu potencial pro-angiogénico e (ii) as hAT-MSCs foram geneticamente modificadas com um vetor lentiviral que co-expressa apelina e FGF-2, dois factores pro-angiogénicos e cardioprotectores. As hAT-MSCs foram expandidas num sistema de cultura em birreatores de tanque agitado baseado em microcarriers sob condições de hipóxia. As EVs produzidas foram isoladas do meio de cultura por filtração de fluxo tangencial seguida de uma cromatografia por exclusão de tamanho.

As diferentes estratégias implementadas resultaram no aumento da produtividade de EVs (aumento de 1.3-1.8 vezes). Foi possível observar que a diminuição da concentração de glucose abaixo de 1 mM tem impacto não só na capacidade de secreção de EVs, mas também aumenta a sua bioactividade direcionada à regeneração cardíaca, mostrando a importância de controlar as condições de cultura celular para desenvolver plataformas robustas para a produção de EVs. Além disso, demonstrámos que a transfeção celular com o inibidor miR-145-5p pode constituir uma abordagem adequada para aumentar o potencial terapêutico das EVs. Finalmente, foi observado que as hAT-MSCs geneticamente modificadas também possuem a capacidade de secretar EVs com potencial de regeneração cardíaco.

Palavras-Chave: Vesículas extracelulares; Células estaminais mesenquimais; Birreatores de tanque agitado; Estratégias de precondicionamento; Células geneticamente modificadas; Medicina regenerativa cardiovascular.



TABLE OF CONTENTS

| 1. | INTRODUCTION | 1 |
|--------|---|----|
| 1.1. | Cardiovascular Diseases | 1 |
| 1.2. | NOVEL THERAPIES FOR HEART REGENERATION AND REPAIR | 1 |
| 1.2.1 | Cell-based therapies | 1 |
| 1.2.2 | Cell-derived extracellular vesicles, overcoming the hurdles of cell-based therapies | 3 |
| 1.3. | THERAPEUTIC POTENTIAL OF MSC-DERIVED EVS | 6 |
| 1.4. | MANUFACTURING MSC-DERIVED EVS FOR THERAPEUTIC USE | 9 |
| 1.4.1. | Clinical translation of MSC-derived EVs | 9 |
| 1.4.2. | Large-scale production of MSC-derived EVs in stirred-tank bioreactors | 10 |
| 1.4.3. | Downstream processing of MSC-derived EVs | 11 |
| 1.5. | STRATEGIES TO IMPROVE THE THERAPEUTIC OUTCOME OF MSC-DERIVED EVS | 13 |
| 2. | AIM OF THE THESIS | 17 |
| 3. | MATERIALS AND METHODS | 19 |
| 3.1 | HAT-MSC CULTURE | 19 |
| 3.1.1 | hAT-MSC sources | 19 |
| 3.1.2 | hAT-MSC expansion in static culture systems | 19 |
| 3.1.3 | hAT-MSC expansion in STBR | 19 |
| 3.2 | HAT-MSC TRANSFECTION WITH MIR-145-5P INHIBITOR | 20 |
| 3.3 | ANALYTICAL TECHNIQUES FOR CHARACTERIZATION OF HAT-MSC | 20 |
| 3.3.1 | Cell concentration and viability | 20 |
| 3.3.2 | Qualitative assessment of cell viability | 21 |
| 3.3.3 | Analysis of extracellular metabolite concentration | 21 |
| 3.3.4 | Flow cytometry of hAT-MSC surface markers | 21 |
| 3.3.5 | Trilineage differentiation of hAT-MSCs | 21 |
| 3.3.6 | RT-PCR | 22 |
| 3.3.7 | Droplet digital PCR (ddPCR) | 23 |
| 3.4 | CONCENTRATION AND ISOLATION OF MSC-DERIVED EVS | 23 |
| 3.5 | MSC-DERIVED EV CHARACTERIZATION | 24 |
| 3.5.1 | Nanoparticle tracking analysis (NTA) | 24 |
| 3.5.2 | Protein quantification | 24 |
| 3.5.3 | Bead-based flow cytometry | 24 |
| 3.5.4 | Transmission Electron Microscopy (TEM) | 25 |
| 3.6 | FUNCTIONAL ASSAYS | 25 |
| 3.6.1 | Tube formation assay | 25 |

| 3.6.2 | Wound healing assay | 25 |
|----------|---|----|
| 3.7 | STATISTICAL ANALYSIS | |
| 4. | RESULTS AND DISCUSSION | 27 |
| 4.1 | PRODUCTION OF METABOLIC AND MIRNA PRE-CONDITIONED HAT-MSC AND THEIR | |
| DERIVED | EVs IN MICROCARRIER-SUPPORTED STIRRED-TANK BIOREACTORS | 30 |
| 4.1.1 N | Metabolic preconditioning of hAT-MSC and production of their derived EVs | 30 |
| 4.1.2 F | Preconditioning hAT-MSC with miR-145-5p inhibitor and production of their derived EVs | 40 |
| 4.2 | PRODUCTION OF GMMSC AND GMMSC-DERIVED EVS IN MICROCARRIER-SUPPORTED | |
| STIRRED- | TANK BIOREACTORS | 49 |
| 5. | CONCLUSIONS AND FUTURE WORK | 57 |
| 6. | BIBLIOGRAPHY | 59 |
| 7. | SUPPLEMENTAY INFORMATION | 69 |

LIST OF FIGURES

| FIGURE 1.1: SCHEMATIC REPRESENTATION OF EV BIOGENESIS | .5 |
|--|-----|
| FIGURE 1.2: UPTAKE OF EV BY RECIPIENT CELLS | .6 |
| FIGURE 2.1: SCHEMATIC OVERVIEW OF THE WORKFLOW OF THE THESIS | 18 |
| FIGURE 4.1: HAT-MSCs, TRANSFECTED HAT-MSC AND HAT-GMMSC CHARACTERIZATION2 | 29 |
| FIGURE 4.2: SCHEMATIC REPRESENTATION OF THE FEEDING STRATEGIES IMPLEMENTED DURING HAT-MS | C |
| CULTURE IN STBR – STANDARD AND STBR - GLUCOSE | 31 |
| FIGURE 4.3: HAT-MSC CULTURE CHARACTERIZATION AFTER EXPANSION IN STBR — STANDARD AND STBF | ₹ - |
| GLUCOSE | 32 |
| FIGURE 4.4: CHARACTERIZATION OF HAT-MSC-DERIVED EVS OBTAINED FROM STBR - STANDARD, STATIC | ; — |
| STANDARD, STBR – GLUCOSE AND STATIC – GLUCOSE AT DAY 7 OF CULTURE | 35 |
| FIGURE 4.5: EV PRODUCTION YIELDS OBTAINED IN STBR - STANDARD, STATIC - STANDARD, STBR | _ |
| GLUCOSE AND STATIC – GLUCOSE AT DAY 7 OF CULTURE. | 36 |
| FIGURE 4.6: FUNCTIONAL ANALYSIS OF EV BIOLOGICAL ACTIVITY AFTER EXPANSION IN STBR - STANDAR | D, |
| STATIC - STANDARD, STBR - GLUCOSE AND STATIC - GLUCOSE, ASSESSED BY TUBE FORMATION AND ADDRESS OF THE STATE O | ۱D |
| WOUND HEALING ASSAYS | 39 |
| FIGURE 4.7: HAT-MSC AND TRANSFECTED HAT-MSC CULTURE CHARACTERIZATION AFTER EXPANSION | IN |
| STATIC CONDITIONS | 11 |
| FIGURE 4.8: HAT-MSC AND TRANSFECTED HAT-MSC CULTURE CHARACTERIZATION AFTER STBR EXPANSION | NC |
| | 13 |
| FIGURE 4.9: CHARACTERIZATION OF HAT-MSC-DERIVED EVS OBTAINED FROM STBR - STANDARD, STATIC | ; — |
| STANDARD AND STBR – TRANSFECTED AT DAY 4 OF CULTURE | 14 |
| FIGURE 4.10: EV PRODUCTION YIELDS OBTAINED IN STBR - STANDARD, STATIC - STANDARD AND STBR | _ |
| TRANSFECTED AT DAY 4 OF CULTURE | 15 |
| FIGURE 4.11: FUNCTIONAL ANALYSIS OF EV BIOLOGICAL ACTIVITY AFTER EXPANSION FOR 4 DAYS IN STBR | . — |
| STANDARD, STATIC - STANDARD AND STBR - TRANSFECTED, ASSESSED BY TUBE FORMATION AND | ۷D |
| WOUND HEALING ASSAYS | 18 |
| FIGURE 4.12: HAT-MSC AND GMMSC CULTURE CHARACTERIZATION AFTER STBR EXPANSION | 50 |
| FIGURE 4.13: CHARACTERIZATION OF HAT-MSC-DERIVED EVS OBTAINED FROM STBR - STANDARD, STAT | 'IC |
| - STANDARD, STBR - GMMSC AND STATIC - GMMSC AT DAY 7 OF CULTURE | 51 |
| FIGURE 4.14 EV PRODUCTION YIELDS OBTAINED IN STBR - STANDARD, STATIC STANDARD, STBR - GMMS | C |
| AND STATIC – GMMSC AT DAY 7 OF CULTURE | 53 |
| FIGURE 4.15: FUNCTIONAL ANALYSIS OF EV BIOLOGICAL ACTIVITY AFTER EXPANSION IN STBR - GMMSC AND ANALYSIS OF EV BIOLOGICAL ACTIVITY AFTER EXPANSION IN STBR - GMMSC AND ANALYSIS OF EV BIOLOGICAL ACTIVITY AFTER EXPANSION IN STBR - GMMSC AND ANALYSIS OF EV BIOLOGICAL ACTIVITY AFTER EXPANSION IN STBR - GMMSC AND ANALYSIS OF EV BIOLOGICAL ACTIVITY AFTER EXPANSION IN STBR - GMMSC AND ANALYSIS OF EV BIOLOGICAL ACTIVITY AFTER EXPANSION IN STBR - GMMSC AND ANALYSIS OF EV BIOLOGICAL ACTIVITY AFTER EXPANSION IN STBR - GMMSC AND ANALYSIS OF EV BIOLOGICAL ACTIVITY AFTER EXPANSION IN STBR - GMMSC AND ANALYSIS OF EV BIOLOGICAL ACTIVITY AFTER EXPANSION IN STBR - GMMSC AND ANALYSIS OF EV BIOLOGICAL ACTIVITY AFTER EXPANSION IN STBR - GMMSC AND ANALYSIS OF EV BIOLOGICAL ACTIVITY AFTER EXPANSION IN STBR - GMMSC AND ANALYSIS OF EV BIOLOGICAL ACTIVITY AFTER EXPANSION IN STBR - GMMSC AND ANALYSIS OF EV BIOLOGICAL ACTIVITY AFTER EXPANSION IN STBR - GMMSC AND ANALYSIS OF EV BIOLOGICAL ACTIVITY AFTER EXPANSION IN STBR - GMMSC AND ANALYSIS OF EV BIOLOGICAL ACTIVITY AFTER EXPANSION IN STBR - GMMSC - | ۷D |
| STATIC - GMMSC, ASSESSED BY TUBE FORMATION AND WOUND HEALING ASSAYS | 55 |
| FIGURE 7.1 METABOLITE CONCENTRATION PROFILES DURING HAT-MSC CULTURE IN STATIC CULTUR | ٦E |
| SYSTEMS (STATIC - STANDARD AND STATIC - GLUCOSE) | 39 |



LIST OF TABLES

| TABLE 1.1: SUMMARY OF STUDIES IDENTIFYING BENEFICIAL EFFECTS OF MSC-DERIVED EVS | 8 |
|---|-----|
| TABLE 1.2: STRATEGIES TO ENHANCE THE THERAPEUTIC EFFICACY OF MSC-DERIVED EVS | .15 |
| TABLE 3.1: LIST OF ALL PRIMERS USED IN DDPCR | .23 |

Abbreviations

2D Two-dimensional
3D Three-dimensional
AB Apoptotic bodies
AKT Protein kinase B
ANGPT2 Angiopoietin-2
AT Adipose tissue

bFGF Basic fibroblast growth factor

BM Bone marrow

CCM Culture conditioned medium

CD Chemically-defined

cGMP Current good manufacturing practice

CM Cardiomyocyte

CPC Cardiac progenitor cell

Ct Cycle threshold

CVD Cardiovascular diseaseddPCR Droplet digital PCRDMSO Dimethyl sulfoxideDO Dissolved oxygen

DPBS Dulbecco's phosphate buffered saline

DSP Downstream processing
ESC Embryonic stem cells

ESCRT Endosomal sorting complex required for transport

FBS Fetal bovine serum
FDA Fluorescein diacetate
FGF-2 Fibroblast growth factor-2

GF Growth factor

gmMSC Genetically-modified mesenchymal stem/stromal cells

hAT-MSC Human adipose tissue-derived mesenchymal stem/stromal cells

HF Heart failure

HGFHepatocyte growth factorHIF-1αHypoxia inducible factorhPLHuman platelet lysate

HUVEC Human umbilical vein endothelial cell

ILV Intraluminal vesicles

iPSC Induced pluripotent stem cells

ISCT International Society of Cellular Therapy

LV Left Ventricular

LVEF Left ventricular ejection fraction

MHC Major histocompatibility complex

MI Myocardial infarction

miRNA Micro-RNA

MSC Mesenchymal stem/stromal cells

MV Microvesicles

MVB Multivesicular bodies

NTA Nanoparticle tracking analysis

PDGF Platelet-derived growth factor

PI Propidium iodide

PSC Pluripotent stem cells

RT Room temperature

SEC Size exclusion chromatography

STBR Stirred-tank bioreactor

TEM Transmission Electron Microscopy

TFF Tangential flow filtration

TGF- β Transforming growth factor- β

UCM Umbilical cord matrix

VEGF Vascular endothelial growth factor

VSMC Vascular smooth muscle cell

1. Introduction

1.1. Cardiovascular Diseases

Cardiovascular diseases (CVDs), such as myocardial infarction (MI), remain a major cause of morbidity and mortality globally and contribute significantly to impaired quality of life in surviving patients [1], resulting in a substantial financial burden either directly (medical bills) and indirectly (for instance, loss of income due to work absenteeism) [2]. As a result, it is of utmost importance not only to avoid risk factors to prevent the disease [2,3], but also to improve the treatments currently employed [4]. Among CVDs, in MI, due to occlusion of coronary artery, the affected area becomes deprived of blood flow. Consequently, oxygen and nutrient depletion lead to myocardial cells loss of function and death, which occurs through both apoptotic and necrotic mechanisms [5]. This substantial loss of cardiac muscle cannot be compensated given the minimal endogenous regenerative capability of the heart tissue [6]. Consequently, a fibrous scar tissue replaces the damaged area of the heart, causing loss of contractility, pathological cardiac dilatation, additional CM loss and mechanical dysfunction, all of which resulting in heart failure (HF) [7].

Current therapeutic approaches available to treat MI patients are, for example, cardioprotective therapies which include revascularization approaches that target the improvement of blood flow supply such as thrombolysis, cardiac intervention, and bypass surgery. Additionally, different pharmacological treatments have also been employed to limit MI size, such as angiotensin-converting enzyme inhibitors, angiotensin receptor-neprilysin inhibitors, β -blockers, and mineralocorticoid-receptor antagonists [8]. Even though these methods have improved patient survival and well-being, as their focus is in preventing the progressive process of cardiac remodeling to HF, they cannot reverse infarcted CMs. Heart transplantation remains the only long-term current solution for restoring normal cardiac function for end-stage HF patients. Thus, efforts have been made towards the finding of new approaches with the potential to promote heart regeneration and repair.

1.2. Novel therapies for heart regeneration and repair

1.2.1 Cell-based therapies

Cell-based therapies over the past years have been widely studied for cardiac repair and regeneration in patients with HF. In contrast to approaches solely providing a cardioprotective effect, cell-based therapies aim to generate new and functional myocardial tissue relying either on delivery of stem cell and/or cardiac progenitor cells (CPC) to physically replace irreversibly lost host cells (exogenous regenerative response) or on the paracrine activity of the supplied cells that activate repair signaling pathways in the recipient heart (endogenous regenerative response) [9].

One of the first cell types to be explored as potential sources for cell-based therapies were skeletal myoblasts, due to their phenotypic resemblance to the heart, ease of isolation and expansion, high *in vitro* scalability and resistance to hypoxic conditions [10]. Although positive effects were seen in

animal models [11], in the randomized phase II MAGIC clinical trial [12], cells failed to provide improvements in the left ventricular ejection fraction (LVEF).

Cardiac-committed cells, in particular cKIT+ CPCs and cardiosphere-derived cells (CDCs), were other cell type that entered cardiac regeneration trials. The knowledge that the mammalian heart harbors stem and/or progenitor cells led to the idea that recovery of heart function would be achieved more effectively through the use of these cells, since they are phenotypically similar to the cells they were intended to substitute [6]. The SCIPIO clinical trial [13] was the pioneer trial in the treatment of ischemic cardiomyopathy with cKIT+ CPCs. Even though the results suggested that intracoronary administration of these cells was effective in improving left ventricular (LV) function and decreasing infarct size, the paper was retracted because some results regarding the phenotype of CPCs were found to have been manipulated. Moreover, although several pre-clinical studies confirmed CPC's beneficial effects, the underlying mechanisms of these effects remain unclear and CPCs were found to fail to engraft the heart and do not differentiate into CMs. Subsequently, it was hypothesized that beneficial effects observed in cardiac function after injury could be attributed to CPCs paracrine actions that modulate cardiac contractility or through heart re-vascularization, as cells are more likely to differentiate into vascular cells rather than CMs [14,15]. On the other hand, CDCs were firstly studied in the CADUCEUS trial [16]. The investigators reported that the intracoronary administration of autologous CDCs resulted in a diminished fibrous scar size and thickening of the wall of the damaged area. Overall, there are promising results reported using cardiac-committed cells, however their true regenerative potential and the reproducibility of different trials reported still needs to be addressed [17].

Pluripotent stem cells (PSC), including embryonic stem cells (ESC) and induced pluripotent stem cells (iPSC), have been used to provide new CMs for cardiac regeneration. Due to their remarkable self-renewal capacity, these cells can provide unlimited generation of CMs. Furthermore, their application in cell-based therapies was considered appealing in terms of scalability, and because they provide the possibility to control their differentiation level and, thus, to transplant the cells at the desired level of cardiomyogenic commitment [9]. Numerous studies have shown that ESC implantation enhances LV function in HF animal models [18]. In addition, in the ESCORT trial [19], a fibrin scaffold containing ESCs was implanted on the epicardium of the infarcted area. Overall, even though encouraging results have been reported, there are still major issues associated with the use of these cells, namely the ethical issues related to the manipulation of embryos, graft rejection, arrhythmias and potential risk of teratomas [18]. These drawbacks have prompted the finding of new cell alternatives with similar pluripotent phenotype, which led to the use of iPSC. Similarly to ESCs, iPSCs have also shown positive outcomes in several animal models [20,21]. However, once again, biological safety concerns need to be addressed, such as teratoma formation.

In this work, we will focus on mesenchymal stem/stromal cells (MSCs). The growing interest in MSCs comes from their remarkable features, in particular, their straightforward availability, isolation, scalability, preservation with minimal loss of potency, low immunogenicity and, in addition, their paracrine and immunomodulatory functions [22]. The use of MSCs in clinical studies for the treatment of MI has grown significantly over the past ten years. More than 300 clinical trials (Phases 1-3) have been carried out with the goal of demonstrating the efficacy and safety of MSCs for therapeutical use in

several diseases [23]. In particular, more than 150 trials can be found in the clinical trials database evaluating MSCs as potential therapeutic candidates for CVDs [24].

MSCs can be obtained from multiple adult tissues, including bone marrow (BM), adipose tissue (AT), as well as neo-natal tissues such as umbilical cord matrix (UCM) and many others. For several years, BM was considered as the main source for the isolation of MSCs, however, the extremely invasive harvesting procedure, limited cell numbers, and maximal lifespan with increasing age led to the search for alternative sources. AT is an alternative source that presents several advantages compared to other sources, mainly due to its higher abundance and less invasive method for cell isolation [25].

Since MSCs were discovered, a consensus about their definition was never completely uniform among investigators. Therefore, to standardize their definition and methods of isolation and expansion, in 2006, the International Society of Cellular Therapy (ISCT) established three minimal criteria to define MSC: adherence to plastic under standard culture conditions using tissue culture flasks, expression of surface markers CD105, CD73 and CD90, lack of expression of CD45, CD34, CD14 or CD11b, CD79α or CD19 and HLA class II and, finally, *in vitro* differentiation into osteogenic, chondrogenic, and adipogenic cell lineages [26].

In the past, MSC's therapeutic effects were mainly correlated with their ability to differentiate and, consequently, restore lost tissue function. However, more recent studies have shown uncertainties regarding the mechanism of action behind this effect. Although transplanted MSCs have been shown to migrate preferentially to the injured area, they show poor survival and low engraftment rates [27]. In addition, there are other challenges regarding transplanted MSCs that include immune reactions, senescence-induced genetic instability or loss of function and the overall patient safety associated with the possibility of malignant transformation [28]. These observations have drawn the attention to their secretome and its possible role in tissue repair and recovery from injury. Indeed, several studies have been suggesting that the beneficial effects observed after MSC transplantation in experimental models of tissue injury might be related to MSC's paracrine activity, as they secrete a large variety of soluble factors that may either activate target cells or stimulate neighboring cells to start repairing damaged tissue [29-31]. These factors have been seen to exert modulatory effects on the tissue microenvironment, from anti-inflammatory to anti-apoptotic or even regeneration-stimulating, which are promising qualities for cardiovascular repair [29]. Becoming aware of these paracrine-mediated effects, along with all the drawbacks associated with cell-based therapies led to the study and development of cell-free therapies.

1.2.2 Cell-derived extracellular vesicles, overcoming the hurdles of cell-based therapies

Given the limited and mostly moderate beneficial effects reported in cell-based therapies, the paracrine activity of the cells has been suggested as the main mechanism behind MSC's clinically relevant properties, particularly through secretion of growth factors (GF), micro-RNAs (miRNAs) and extracellular vesicles (EVs). Indeed, in several preclinical studies it was demonstrated that MSC-derived culture

conditioned medium (CCM) treatment can improve organ function to an equal or greater extent compared with MSC treatment, providing encouraging results for the treatment of multiple diseases, including MI, using cell-free therapies [29,32].

EVs, being a reflection of the factors secreted by cells, have been increasingly drawing the attention of researchers due to their broad therapeutic potential. Furthermore, the application of cell-derived EVs rather than MSCs themselves in the context of regenerative medicine has numerous advantages, as it enables to avoid some of the limiting factors associated with cell therapy. First of all, due to their reduced abundance of transmembrane proteins such as major histocompatibility complexes (MHCs), EVs can be less immunogenic than whole cells. They present less risk of tumorigenesis as they are not able to replicate. Furthermore, because EVs are delimited by a bilayer membrane, their cargo components are protected from degradation and allows them to migrate long distances in tissues. Additionally, EVs exhibit high physicochemical stability and can be stored for a long time at -80° C without any toxic cryoprotectant agents while maintaining their bioactivity, presenting longer shelf-life than cells themselves [33,34].

EVs are a heterogenous collection of small membrane-bound organelles released from almost all cell types to the extracellular environment. These particles were firstly described in 1983 as part of a mechanism to discard undesirable materials from cells (proteins, nucleic acids and lipids). Later research, however, revealed that they are crucial for intercellular communication in both physiological and pathological processes [30].

EVs are typically categorized into three subtypes according to their size and biogenesis process: exosomes, microvesicles (MVs) and apoptotic bodies (ABs) (Figure 1.1). Among these three EV subtypes, exosomes are the smallest with a typical diameter of 30-150 nm. Exosomal vesicles, which are the best currently characterized EVs, have an endosomal origin, meaning that they are formed by inward budding of the plasma membrane to create early endosomes. Subsequently, these endosomes mature into late endosomes, through endosomal membrane invagination that creates intraluminal vesicles (ILVs). These structures are named multivesicular bodies (MVBs). During this process, specific cargos from the cytosol, such as proteins, lipids and RNAs, are incorporated into ILVs through two pathways: endosomal sorting complex required for transport (ESCRT)-dependent or ESCRTindependent processes. MVBs can then be released into the extracellular environment. Exosome release depends on transport and fusion of the MVBs with the plasma membrane, which involves several components, as molecular switches (small GTPases), cytoskeleton components (microtubule and microfilament), molecular motors (dynein and kinesin) and the membrane fusion apparatus (SNARE complex) [31]. Importantly, Rab GTPases, in particular Rab27a and Rab27b, have an important role in exosome release, controlling multiple steps of vesicular trafficking, including budding, motility, docking and fusion of different vesicular transport intermediates to acceptor membranes [35].

MVs are EVs with a typical size range between 100-1000 nm and are formed through outward budding of the cell's plasma membrane that is promoted by the formation of membrane domains with different lipid and protein composition. Subsequently, MVs are released as the interactions between the cytoskeletal proteins and the plasma membrane are broken. Importantly, this process is coordinated by the levels of intracellular Ca²⁺ [36].

Lastly, ABs represent the largest class of EVs, with approximately 50-5000 nm in diameter. These bodies are released during apoptosis into the extracellular space, through blebbing of the plasma membrane. Conversely to exosomes and MVs content, ABs contain intact organelles and nuclear components [37].

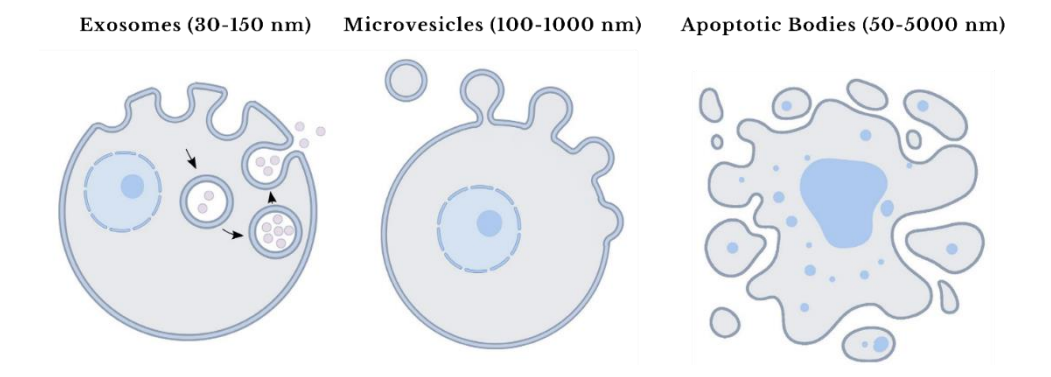


Figure 1.1: Schematic representation of EV biogenesis. EV subtypes are defined according to their biogenesis process, either from intraluminal vesicles formed within endosomal compartments (exosomes), direct budding of the plasma membrane (microvesicles) or the process of apoptotic cell disassembly (apoptotic bodies). Adapted from [32].

In addition to size and biogenesis, EVs are commonly identified according to their surface markers. Although there is still discussion about the precise specific markers of EV subtypes, flotillin, heat-shock proteins (HSP60, HSP70, HSP90), tetraspanins (CD9, CD63, CD81), numerous annexins and MHC class I and class II are known to be generic EV markers. Furthermore, it is challenging to experimentally distinguish the different EV subpopulations due to overlapping size, density and membrane composition. Following this, "EVs" has been used as a general term that include all EV subtypes [38,39].

EVs carry a cargo of lipids, proteins and genetic materials (mRNA, miRNA, pre-miRNA, and other noncoding RNA) that are transferred and released into recipient cells. Following their release into the extracellular environment, EVs can interact with target cells and, therefore, transfer their cargo via different pathways: EVs may enter cells by direct fusion to the cell membrane or via different endocytic pathways (Figure 1.2) [33,40].

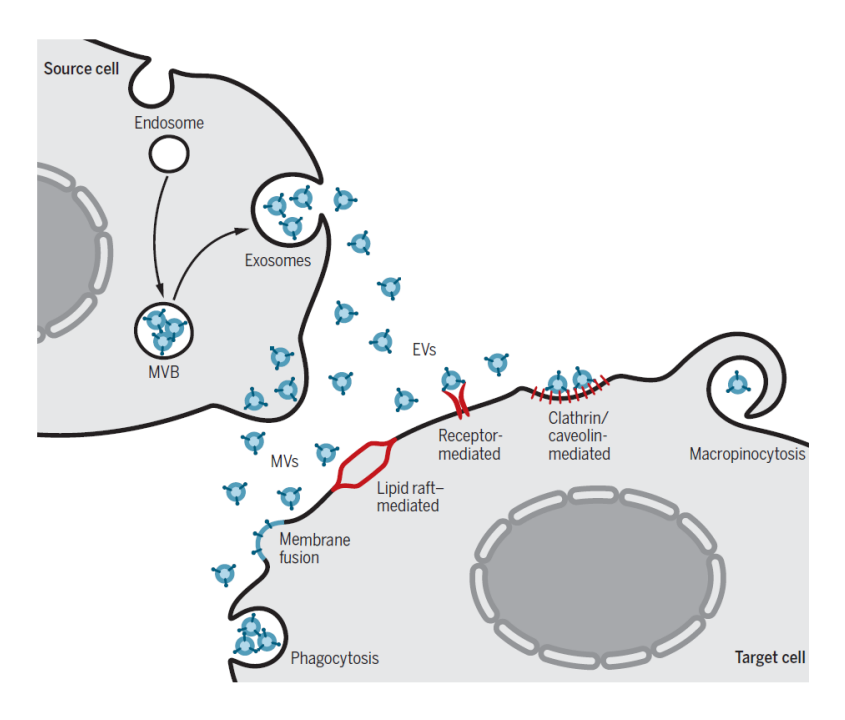


Figure 1.2: Uptake of EVs by recipient cells. EVs can be internalized into recipient cells and, therefore, release their cargo components, by membrane fusion or through endocytic routes including phagocytosis, receptor-mediated endocytosis, lipid raft—mediated endocytosis, clathrin-mediated endocytosis, caveolin-mediated endocytosis, and micropinocytosis. Adapted from [41].

1.3. Therapeutic potential of MSC-derived EVs

Since the pioneering breakthrough of Graça Raposo and her colleagues, in 1996, that demonstrated the capacity of EVs secreted from B lymphocytes to present antigens and, consequently, trigger T cell responses, investigation of EVs in biological processes and their possible therapeutic applications have received a lot of attention [41].

The functional impact of EVs is determined by the transfer of their cargo that trigger alterations on recipient cells. EVs specific cargos vary according to the intrinsic and extrinsic conditions experienced by their producing cells, particularly, the type, age and their functional state, as well as their culture environment [42,43]. Furthermore, EVs therapeutic potential have been studied through two different approaches. On one hand, it can rely on their intrinsic activity since they are able to replicate some of the therapeutic effects from their cells of origin (naïve EVs). As an alternative, given their ability to transport functional cargos, EVs can also be used as drug delivery systems (bioengineered EVs) [44].

Several studies have shown that EVs from different cell sources, including MSC-derived EVs, can be involved in the treatment of MI by providing cardioprotection and inducing regeneration in injured cardiac cells [45]. The intrinsic cardiac repair capacity of MSC-derived EVs was observed for the first time by Lai *et al.* in an animal model of MI in 2010, where the myocardial protection of MSCs and their secreted EVs was directly compared. The data showed that both MSC and their derived EVs could reduce inflammation, inhibit fibrosis and improve cardiac function, although MSC-derived EVs presented better results [46]. In recent years, many other studies have demonstrated the cardioprotective

mechanisms by which EVs act. For instance, angiogenesis, the growth of new vascular network, is a crucial mechanism for cardiac regeneration and healing [47]. MSC-derived EVs have shown pro-angiogenic activity *in vitro* through their impact on human umbilical vein endothelial cells (HUVECs) [48]. Furthermore, similar positive results have been obtained *in vivo*. Besides their pro-angiogenic function, EVs can also inhibit apoptosis, autophagy, and regulate inflammatory responses [46]. These cardioprotective effects of EVs result from the transfer of their specific cargos with pro-angiogenic, anti-apoptotic, anti-inflammatory and anti-cardiac remodeling effects, which shows a clear overlap with the proposed actions of MSC-derived CCM [32].

Specifically, among all EV functional cargo, miRNAs seem to be key elements. miRNAs are a class of noncoding small RNAs that affect mRNA stability and translation by binding to complementary target sites in 3'-UTRs of specific mRNA targets, playing crucial roles in gene expression of recipient cells [49]. Thus, miRNA could be responsible for the cardioprotective effects induced by EVs. In fact, MSC-derived EVs contain an extensive collection of miRNAs, such as miR-210, miR-126, miR-132, miR-21 and miR-145, that have all been demonstrated to play significant roles in angiogenesis [50]. For instance, Yu et al. showed, in a rat model of MI, that MSC-derived EVs highly expressing miR-19a restored cardiac contractile function and reduced infarct size, through downregulation of phosphatase and tensin homolog (PTEN) which resulted in the activation of Akt (protein kinase B) and ERK signaling pathways [51]. Of particular interest, miR-145 is another candidate that has been exploited in this context. This molecule is one of the downregulated miRNAs in several human cancers that acts trough the inhibition of several angiogenic factors, such as vascular endothelial growth factor (VEGF) and angiopoietin-2 (ANGPT2) [52,53]. In fact, it has been reported that delivery of EVs enriched with miR-145 could be a promising approach for cancer treatment, as they showed to possess anti-cancer properties, such as inhibitory effects on apoptosis induction and metastasis [54]. More recently, Arderiu et al. [55] demonstrated that downregulating the expression of miR-145 could promote the pro-angiogenic properties of MSCs, in vitro. Therefore, targeting miR-145 can also be a promising strategy to increase the therapeutic outcome of MSCs and their derived EVs for the treatment of ischemic diseases, although no studies have been conducted in this context using EVs.

A summary of several studies demonstrating MSC-derived EVs' beneficial effects both *in vitro* and *in vivo* and key elements involved in those effects is presented in Table 1.1. Noteworthy, despite the promising therapeutic potential of MSC-derived EVs, there are still considerable challenges preventing the progress of clinical research, mostly due to the low scalability of EV manufacturing, as static culture systems remain the most used and studied platforms.

Table 1.1: Summary of studies identifying beneficial effects of MSC-derived EVs.

| Cell Culture Platform | EV source | Molecular Signatures | Potency in vitro | Potency in vivo | Reference |
|----------------------------------|-----------------------|---|--|---|-----------|
| | Mouse BM- MSCs | Increase in miR-21a expression; downregu- lation of pro-apoptotic gene products | Reduced oxygen- glucose deprivation- induced cardiomyo- cyte apoptosis | Reduced infarct size | [56] |
| | Mouse BM- MSCs | Increase in miR-25 ex- pression; downregula- tion of pro-apoptotic gene products | Reduced oxygen- glucose deprivation- induced cardiomyo- cyte apoptosis and inflammatory re- sponses | Reduction in in- farct area | [57] |
| | Mouse BM- MSCs | miRNA-182 expression inhibits TLR4 signaling pathway | Macrophage polari- zation to M2 macro- phages | Reduced infarct size and inflam- mation | [58] |
| Static culture systems | Human BM-MSCs | None identified | Promoted prolifera- tion, migration and tube formation of HUVECs | Reduced infarct size and pro- moted myocar- dial repair | [59] |
| | Rat AT- MSCs | Overexpression of miR-126 | Promoted migration and tube formation of endothelial cells | Reduction in in- farct area; Im- proved cardiac function | [60] |
| | Rat BM- MSCs | Overexpression of hypoxia-inducible factor 1-alpha (HIF-1α); Upregulation of pro-angiogenic factors | Promoted prolifera- tion, migration and tube formation of HUVECs | Induced vascu- lar network for- mation; Re- duced fibrosis | [61] |
| | Human UCM- MSCs | Overexpression of miR-145; Decreased Smad3 expression | Inhibited cancer cell's proliferation and invasion; in- creased apoptosis and cell cycle arrest | Reduced tumor growth | [62] |
| Quantum bioreactor | Human UCM- MSCs | None identified | - | Improved car- diac function | [63] |
| Hollow- fiber bioreactor | Human BM-MSCs | High abundance of im- munoregulatory and angiogenic factors VEGF-A and IL-8 | - | - | [64] |
| Vertical- wheel bioreactor | Human BM-MSCs | Increase in miR-10, 19, 21, 132 and 377; up- regulation of metabolic, autophagy and ROS- related proteins | EVs derived from bioreactor culture promoted migration of human fibroblasts to an higher extent than EVs derived from static culture | - | [65] |

1.4. Manufacturing MSC-derived EVs for therapeutic use

MSC-derived EVs have demonstrated encouraging therapeutic effects in early research and, therefore, the development of a scalable and reproducible manufacturing process under good manufacturing practices (cGMP) for EV production and isolation is an imminent need. Importantly, EV products can vary depending on the cell source, but also by manufacturing conditions, such as culture platform used for cell expansion and EV generation, cell culture media and cell culture parameters, as well as downstream processing (DSP) protocols for EV isolation and concentration. Different technologies for EV isolation from CCM have been employed, mainly based on their density, size, or surface markers. Therefore, the choice of the isolation technique itself has also an important role in EV manufacturing, as it may lead to different EV populations being isolated and influencing EV yield, purity, physical properties and function [66].

Thus, to rationally design a large-scale manufacturing platform that could result in increased production as well as increased potency of therapeutic EVs, it is necessary to have a thorough understanding of the various ways in which these factors influence cellular responses and, consequently, EV production as well as their unique cargo components [67].

1.4.1. Clinical translation of MSC-derived EVs

Given the importance of controlling MSC-derived EVs manufacturing steps to facilitate the translation of EV-based products to the clinic, our discussion will now focus on different parameters that may be considered throughout process development.

Cell culture media used to expand cell banks and for the collection of EVs play a critical role in EV production, as it may alter their yields, content and function. For generation of therapeutic products, it is crucial to use a xeno- and EV-free culture media in order to avoid product variability and animal-associated contaminations [68,69].

MSCs have been expanded in vitro using different types of culture media, however, the majority of them rely on using fetal bovine serum (FBS) or human platelet lysate (hPL). Being a xeno- and serum-derived growth supplement, FBS poses several disadvantages related to the undefined serum composition that leads to batch-to-batch variations and high risk of contamination (bacteria, virus and mycoplasma) [70]. Xeno-free culture supplements, including hPL, have been created as an alternative to products originated from animals. The use of hPL presents a simpler regulatory path by avoiding the xenogeneic concerns, thus being preferred in terms of safety considerations. However, both FBS and hPL contain a large amount of EVs that can be co-isolated with the EVs secreted by cells, thus contaminating the end product [44]. Therefore, to avoid product contamination, new strategies for cell expansion and EV collection have been developed. For instance, one possible strategy is to use media that has been depleted of EVs by ultracentrifugation. However, the limited scalability of ultracentrifugation make this strategy challenging to implement in commercial-scale manufacturing [71]. Another strategy that has been explored is to use FBS or hPL supplemented media for cell expansion and, at the end of the cell expansion period, replace it with a supplement-free media without these components [44]. Finally, the use of a chemically-defined (CD) medium is currently the ideal option for the production of EV therapeutic products. CD medium consists of only well-established raw materials without any

direct animal or human origin. Consequently, it presents a greater lot-to-lot consistency, producing more reproducible cells and EV populations. Furthermore, it has been shown that cell expansion in CD medium promotes their proliferative potential [72,73].

The culture parameters/microenvironment can be manipulated in order to impact cells and, consequently, EVs production and bioactivity. For instance, low cell seeding densities have been linked with rapid proliferation of MSCs as well as high percentage of multipotent cells contrary to higher cell culture densities and, in turn, Patel *et al.* [74] have showed that proliferating MSCs can produce higher amounts of EVs. Furthermore, it is hypothesized that increased production of EVs may be an intercellular communication-related compensatory mechanism, as they also observed that often removal of EVs from CCM lead to increased total EV production. Further, their data also demonstrated that cell passage has an important impact in EV bioactivity, with EVs derived from lower cell passages promoting significantly higher cell migration *in vitro*. Some studies have also shown the importance of manipulating other parameters such as glucose, oxygen concentrations and pH levels [66], with the ultimate goal of maximizing cell proliferation and EV production while maintaining their clinical quality attributes throughout the entire manufacturing process.

1.4.2. Large-scale production of MSC-derived EVs in stirred-tank bioreactors

The clinical application of EV-based therapeutics derived from MSCs depends on large-scale production of EVs by viable cells kept under a well-established environment. The therapeutic doses required are variable and depend on the specific application. For example, in earlier pre-clinical trials, a dose of 10⁹–10¹¹ EVs were administered per mouse to achieve positive results [75].

Although, traditionally, MSCs are cultured in flask-based cultures, the limited ability to control critical culture parameters, the lack of homogeneity in the culture medium and the low EV numbers linked with this culture method, have made them unappealing for clinical and industrial applications [64]. For this reason, bioreactor systems have been used to replace standard flask-based cultures for *in vitro* cell expansion and EV production. In fact, several studies have linked bioreactor culture with higher EV yields [44,75]. Importantly, this yield increase is not entirely explained by the expanded cell density in bioreactors compared to flask-based cultures and may be related to increased secretion or decreased re-uptake by cells within the bioreactors [66].

Stirred systems offer a more homogeneous environment for cell culture, regarding nutrient delivery and oxygen transfer rates [76]. With built-in sensors, bioreactors allow for better microenvironmental monitoring and control of specific culture parameters, such as temperature, pH, dissolved oxygen and carbon dioxide. This, in contrast to flask culture, presents a more reproducible approach for *in vitro* cell expansion [66]. Currently, there are different bioreactor systems commercially available for the expansion of MSC, as stirred-tank bioreactors (STBR), wave-mixed bioreactors, vertical wheel pneumatically mixed bioreactors, hollow fiber perfusion bioreactors and packed bed bioreactors. Furthermore, in order to grow anchorage-dependent cells like MSCs in bioreactor systems, it is required to provide appropriate physical support, such as microcarriers, scaffolds/hydrogels or culturing MSCs as aggregates [23].

Expansion of MSCs immobilized on microcarriers has been widely studied in STBR [77,78]. STBR lowers maintenance expenses per production unit, which significantly lowers the costs associated with large-scale cultures. Other advantages come from its relatively simple scale-up and sampling and, furthermore, process validation is facilitated by the process monitoring [76,79].

Microcarriers are small particles, usually spherical, that provide surface matrices for cells to adhere and expand. For instance, cell growth can be maximized by increasing the number of microcarriers allowing for MSC transfer from bead to bead and thus facilitating process scale-up. Different types of microcarriers are currently available varying in their chemical composition (e.g. dextran, polystyrene, glass, porous silica, alginate), charge, surface coatings and porosity [80]. STBR have mechanical impellers, controlled by a mechanical shaft, that are responsible for maintaining microcarriers in suspension and allow medium homogenization [77]. Importantly, agitation impacts cellular physiology due to increased hydrodynamic shear stress. Thus, agitation speed needs to be adjusted in order to avoid MSC differentiation into shear-responsive mesenchymal lineages namely osteogenic or chondrogenic lineages [81,82]. Having all of this in mind, STBR seem to be a promising scale-up strategy for EV production, although not many studies have been conducted in this direction. Furthermore, as these systems enable better environmental control, mimic intercellular interactions displayed *in vivo*, and given that EVs composition and bioactivity reflects the physiologic state of their producing cells, these stirred systems may increase the translational value of secreted EVs in comparison to traditional flask-based cultures [64].

Different modes of operation, *i.e.*, feeding regimen, which represents a crucial factor for successful cell expansion [83], can be applied in these systems. In batch cultures, typically used in the biopharmaceutical industry, growth is limited due to nutrient depletion (such as glucose and glutamine) and metabolic by-products accumulation (such as lactate and ammonia) [84]. To overcome these limitations, fed-batch and perfusion operation modes have emerged as alternatives. In perfusion culture, media is continuously circulated through the culture, therefore there is a constant supply of nutrients and removal of undesired metabolic by-products. Although this strategy offers a continuous process and has been linked to increased cell proliferation in comparison to other feeding strategies, it requires large volumes of culture medium that, in turn, raises the expense of the procedure [85]. Finally, fedbatch culture has proven to be operationally simple, reliable and flexible. This strategy consists of partial culture medium exchange steps to remove metabolic waste from the bioreactor and replenish essential nutrients. However, as it has also been demonstrated that the paracrine and autocrine factors released by cells play a significant part in cell proliferation, extra caution must be taken to make sure that these advantageous factors are not totally eliminated or diluted to residual levels. Having this in mind, most studies have established medium exchange volumes that are \leq 50% of the working volume [77].

1.4.3. Downstream processing of MSC-derived EVs

Successful implementation of MSC-derived EV therapeutics requires DSP protocols to effectively isolate EVs with high yield and purity, while conserving their structure and their functional activity. Moreover, for clinical applications that require large amounts of EVs, it is crucial to have a cost-effective, scalable, compatible with a high-throughput production and standardized EV isolation process [86].

Differential centrifugation isolates EVs based on size and density through successive centrifugation steps with consecutive increase in centrifugal force. However, because not all EVs are equally distanced to the pellet and not all EVs present equal mass and density in relation to the medium, being distinctively sedimented, one common drawback of this technique is co-isolation. Moreover, this process is relatively time-consuming, requires a specialized ultracentrifuge and often leads to variable inconsistent results due to different rotor types and protocols used among researchers [87,88].

Density gradient ultracentrifugation isolates EVs according to their buoyant density, which implies EV migration until reaching the position of the gradient solution with their density (1.15 - 1.19 g/mL) [89]. This method enables to achieve high purity in comparison to other techniques, however, lower yields are obtained. Furthermore, this technique is not scalable, since the processing volume is limited by the thin loading zone, and is associated with high analytical time, complexity and costs [88,90]. Importantly, another drawback of this method is linked with the co-isolation of EVs with high-density lipoproteins, given their overlapped densities [91].

Precipitation methods have also been developed for EV isolation. By altering their solubility or dispersibility, EVs can be settled out of biological fluids [92]. Precipitation is usually induced with hydrophilic polymers, such as polyethylene glycol (PEG). These methods are user friendly, cost effective and straightforward to implement as a standard laboratory procedure. However, they may sediment several contaminants along with EVs. Furthermore, the final product can be contaminated with the precipitating reagent used, because it is not easily removed. Hence, although this technique is easy to apply, it might not be the method of preference to use for descriptive or functional assessment of EVs [89].

Immunoaffinity capture exploits the interaction of characteristic surface EV molecules to specifically capture them through interaction with ligands immobilized on a surface [93]. Although promising, this method is not widely used because there are still missing specific and fully discriminative EV markers [89].

EV isolation by other size-based methods, as size exclusion chromatography (SEC), have also been used. In SEC, a porous resin is utilized to sort particles out according to their size. Larger particles, as EVs, are not able to enter the pores and therefore flow around the resin, being eluted first. In opposition, smaller particles can penetrate the pores of the resin and are delayed in their passage through the column, being eluted in later fractions [93]. The column size cut-off is an important choice as, based on this, different chromatographic selectivity and resolutions are achieved. Importantly, one of the most compelling characteristics of SEC is its capacity to highly maintain EVs' integrity and functionality. Furthermore, the contact-free manner of SEC guarantees none or minimal sample loss and high yields [94]. Importantly, when considering the large volumes obtained from cell culture-derived EVs, an initial step might be needed for volume reduction prior to loading into the SEC column [95]. This can be performed with tangential flow filtration (TFF). In this technique, sample flow is directed in parallel to a semipermeable membrane, allowing for simultaneous sample concentration and removal of non-EV components [86]. Importantly, these two techniques (TFF and SEC) are GMP-compliant and scalable systems for EV isolation.

1.5. Strategies to improve the therapeutic outcome of MSC-derived EVs

Considering EV-based products as a promising approach for heart regeneration, improving yields and enhancing the therapeutic properties of manufactured EVs is imperative to achieve their full potential and progress toward clinical translation [96]. To tailor the production of more potent EVs, MSC could be either transiently preconditioned (following strategies such as cell transfection or by changing the microenvironment of MSC) or genetically modified to express factors involved in tissue regeneration.

When exposed to different stimuli in the cellular microenvironment both *in vivo* and *in vitro*, MSCs exhibit distinct secretion profiles and phenotypes [97]. Thus, several physical and biochemical preconditioning strategies have been shown to modulate EV yields and potency. However, it is not straightforward to assess the effects of these strategies, because the final EV yield is not only the result of release but it also implies EV recapture by cells [98].

One of the most prevalent features of tissue injury *in vivo* is the presence of an hypoxic environment. It is known that, in tissues characterized by a low oxygen environment, the hypoxia-inducible factor-1α (HIF-1α) is stabilized which, in turn, stimulates transcription of pro-angiogenic genes, such as VEGF and fibroblast growth factor-2 (FGF-2) [81]. This has drawn the attention of many groups to study the effects of hypoxic conditions *in vitro*, in particular, for EV manufacturing. In fact, it has been shown that MSCs cultured under hypoxic conditions (1-5%) exhibit increased EV release and modified cargo content (growth factors and miRNAs), displaying enhanced bioactivity towards cardiac regeneration [82,99,100]. Furthermore, CM subjected to glucose starvation, as a representation of physiological stress, showed an increase in EV secretion and, in addition, glucose starvation modified their cargo proteins and miRNAs. *In vitro* functional assays performed with HUVECs showed that incubation of these CM-derived EVs with HUVECs increased their transcriptional activity of pro-angiogenic genes and, moreover, induced HUVECs proliferation and pro-angiogenic potential [101]. In another study using STBR, MSC were expanded on microcarriers until becoming confluent, after which, to enhance EV production, cells were subjected to a high-speed stirring for 4 hours. This strategy induced local shear stress that resulted in an active release of EVs without compromising cell viability [102].

Additionally, EV release can be stimulated by the use of chemical agents. For instance, Ibáñez *et al.* demonstrated that microglial BV2 cells treated with ethanol showed an increase in EV secretion compared to non-treated cells. Ethanol upregulated mitochondria-associated endoplasmic reticulum membranes (MAM) activity and altered lipid metabolism by increasing cholesterol uptake, cholesterol esterification and SMase activity in microglia. In fact, both MAM and SMases have been linked with EV biogenesis and release [103].

As previously discussed in section 1.3, miRNAs are important cargo components of EVs, as they have been implicated as major contributors of MSC-derived EVs positive therapeutic outcomes in different diseases. Understanding the molecular pathways in which specific miRNAs are involved allows researchers to modulate their expression in accordance with the desired effect. Furthermore, because higher concentrations of these molecules in the cytosol of cells may result in increased loading in EVs, it is plausible to transfect miRNA of choice into cells to design EV therapeutic products [104]. Thus, transient cell transfection to overexpress/suppress specific miRNAs has been explored as a strategy to

enhance EVs therapeutic potential, in particular for cardiovascular repair. For miRNA delivery, lipofection has been widely used, particularly, using cationic liposomes. Lipofection is a chemical delivery method that uses liposomes (lipid complexes that have the same composition as the cell membrane) to deliver the desired molecule. Specifically, cationic liposomes, after being incubated with the cells, are able to bind to cell surfaces and can be endocytosed or directly fuse with the cell membrane to release their content [105]. Zhang et al. [106] endowed BM-MSC-derived EVs with pro-angiogenic capacity by lipofecting BM-MSCs with miR-126, which promoted the proliferation, migration and angiogenesis of HUVECs. In this study, BM-MSC-derived EVs administration in a mouse skin defect model accelerated revascularization and wound healing in vivo. miR-145 is expressed in blood vessels by vascular smooth muscle cells (VSMCs). This miRNA targets genes related to VSMCs phenotype, differentiation and interaction with endothelial cells to modulate vessel stabilization. Recently, it was shown that transfecting MSCs with a miR-145 inhibitor could enhance their pro-angiogenic activity both in vitro and in vivo [55]. This suggests how miRNA-enriched EVs can be used as future therapies for MI patients. However, several miRNAs are pleiotropic and can trigger undesirable side effects. For instance, intramyocardial introduction of EVs overexpressing miR-21 inhibited cell death and improved cardiac function, however, this molecule is also known to have pro-fibrogenic effects. So, it is of utmost importance to have in consideration that the design of an EV therapeutic product might need an optimized combination of miRNAs or other molecules to avoid possible harmful effects, producing only its cardioprotective effects [104].

On the other hand, to achieve a long-term and stable transgene expression, MSCs can be genetically modified (gmMSC) to enhance their therapeutic properties. For instance, Gnecchi *et al.* [107] demonstrated that injection of CCM derived from gmMSC overexpressing Akt gene in the heart reduced MI size and improved ventricular function in a rodent model of AMI. Potential mediators of these effects were assessed through RNA analysis that showed overexpression of several genes, coding for factors with pro-angiogenic and cardioprotective effects, in particular VEGF and FGF-2. In another study, intramyocardial transplantation of EVs derived from BM-MSCs genetically modified to overexpress GATA-4 transcription factor restored cardiac contractile function and reduced infarct size in a mouse model. Such EVs were enriched in anti-apoptotic miRs, in particular miR-19a [51]. Other studies have shown that lentiviral vectors expressing cardioprotective and pro-angiogenic factors could be used to improve heart function when administrated by intramyocardial injection into a mouse model of MI [108]. A summary of several strategies to improve EV therapeutic outcome is presented in Table 1.2.

Overall, EV production involves a substantial number of input parameters that can be modulated in order to produce an effect on the desired final therapeutic product, whether on its physical and chemical assets (size, number), cargo components, purity, stability or on its bioactivity [98].

Table 1.2: Strategies to enhance the therapeutic outcome of MSC-derived EVs.

| Stimulation | Cells | Main mechanism | Outcome | Reference |
|-------------------------------------|--------------|--|--|-----------|
| Hypoxia | MCF7 | Increase in miRNA-210 expression | Increase in EV Secretion | [82] |
| | Mouse BM-MSC | Increase in nSMase2 expression | Reduced infarct expansion and im- proved ejection fraction post-MI | [99] |
| Low pH | HEK293 | None identified | Increase in EV secretion | [109] |
| Glucose Starvation | H9C2 | Increase in miRNA-17, 19a, 19b, 20a, 30c and 126 expression | Increase in EV secre- tion; Promoted angio- genesis in HUVECs | [101] |
| Shear Stress | Murine MSC | None identified | Increase in EV secre- tion | [102] |
| Ethanol | BV2 | Upregulation of MAM and SMase | Increase in EV secre- tion; Increase in pro-in- flammatory molecules in EVs | [103] |
| PDGF | hMSC | Increase in c-KIT and SCD expression levels | Increase in EV secre- tion; Promoted angio- genesis in HMECs | [110] |
| Transfection with miR-126 | hBM-MSC | Upregulation of VEGF and Ang-1 genes; acti- vation of PI3K/Akt sig- nalling pathway | Promoted angiogenesis in HUVECs and wound healing in vivo | [106] |
| Transfection with miR-21 | Rat MSC | Upregulation of HIF-1α, VEGF, SDF-1, p-Akt, p- ERK1/2; Downregula- tion of PTEN | Promoted angiogenesis in HUVECs | [111] |
| Transfection with miR-145 inhibitor | Human AT-MSC | Upregulation of the an- giogenic transcription factor ETS1 | Enhanced MSC's pro- angiogenic activity in vitro and in vivo | [55] |
| Genetical modification | Human BM-MSC | Overexpression of VEGF | Promoted HUVEC migration; Enhanced blow flow restoration <i>in vivo</i> | [112] |
| Genetical modification | Rat BM-MSC | Overexpression of IL- 33 | Reduced fibrosis and inflammation of the heart tissue <i>in vivo</i> | [87] |

2. Aim of the thesis

Several cell types, including MSCs, have been explored in clinical settings addressing cardiac regeneration. MSCs role in tissue repair predominantly relies on paracrine mechanisms, including EV-mediated responses in the damaged tissue. However, the clinical translation of MSC-derived EVs is currently limited by their manufacturing scalability.

The main goal of this thesis was to explore different strategies to improve the outcome of hAT-MSC-derived EVs based therapies, aiming to maximize EV secretion yields and enhancing their therapeutic potential:

- MSC preconditioning with low concentration levels of glucose, as a representation of physiological stress;
- MSC preconditioning with miR-145-5p inhibitor, in order to promote an augmented angiogenic response in hAT-MSC-derived EVs;
- III. Culture of gmMSC with lentivirus co-expressing factors involved in cell response to ischemic cardiomyopathy (Apelin and FGF-2).

For this purpose, hAT-MSC were cultured using a microcarrier-based culture system in STBR under hypoxic, chemically-defined and cGMP-compatible conditions. hAT-MSC-derived EVs were concentrated and isolated from CCM using TFF followed by SEC and then characterized in terms of yield, particle size distribution, immunophenotype and morphology. Finally, the therapeutic potential of the manufactured hAT-MSC-derived EVs was assessed *in vitro*.

Overall, through stimulation of MSCs with biophysical and biochemical cues, together with the implementation of a robust manufacturing process for hAT-MSCs-derived EVs, we hope to provide a positive contribution to the future clinical translation of EV-based therapeutic products.

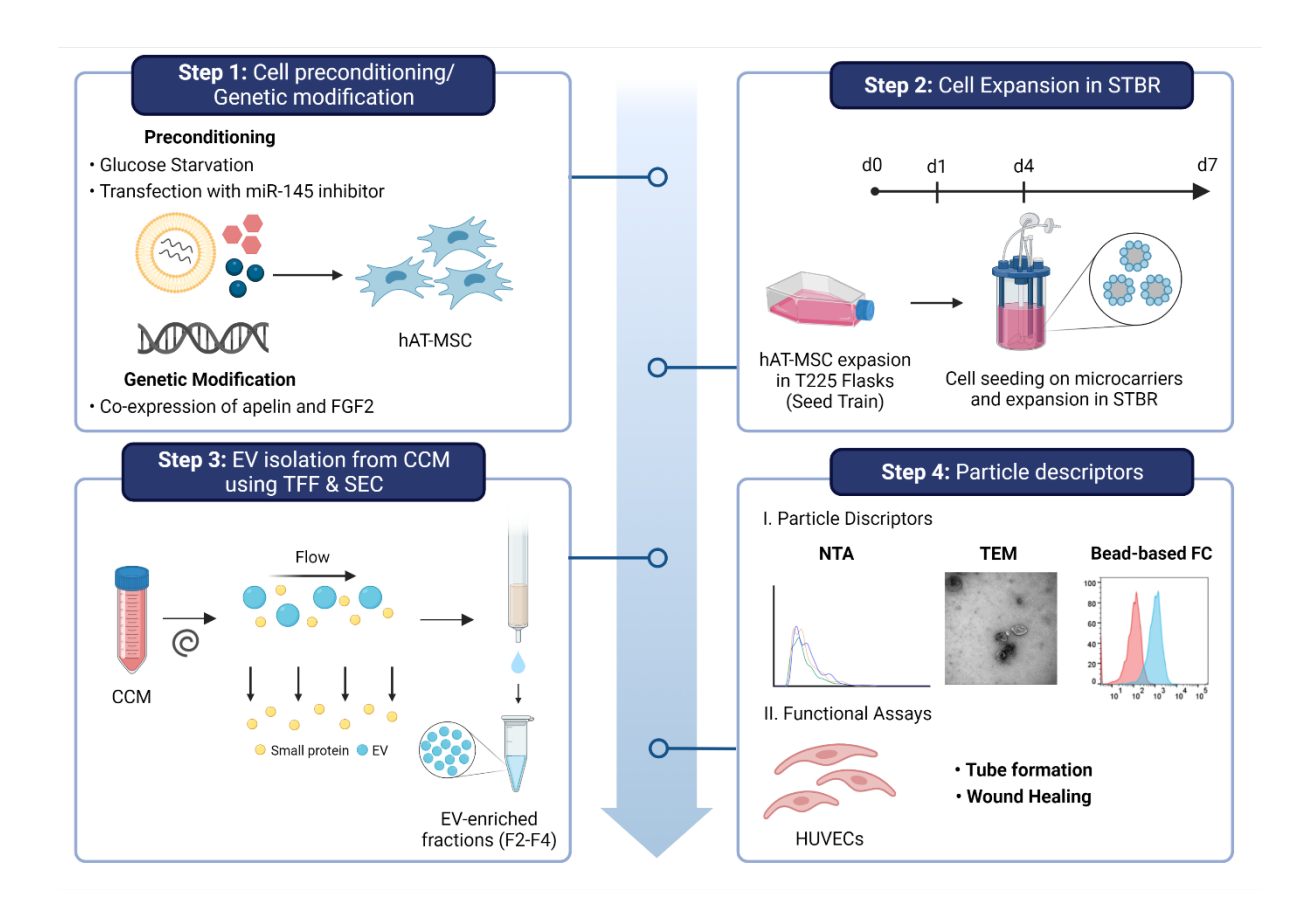


Figure 2.1: Schematic overview of the workflow of the thesis. The main aim of this thesis was to explore different strategies in STBR systems for manufacturing MSC-derived EVs with increased cardiac regenerative capacity while maximizing EV production. hAT-MSC-derived EVs were concentrated and isolated from the CCM relying on a size-based separation protocol using TFF followed by SEC. Particle characterization was assessed to ensure purity and characteristic attributes of EV samples and functional assays were performed to assess the therapeutic potential of EVs.

3. Materials and Methods

3.1 hAT-MSC culture

3.1.1 hAT-MSC sources

Two distinct donors of human AT-MSC (hAT-MSC) were provided to our group by Navarra University (UNAV), while gmMSC, transduced with a lentivector co-expressing apelin and FGF-2, were provided by Institut National de la Santé et de la Recherche Médicale (INSERM), under the scope of the international project CardioPatch.

3.1.2 hAT-MSC expansion in static culture systems

In order to reach the required number of cells to inoculate the STBR, hAT-MSCs were routinely propagated in static culture systems, T225 flasks (Thermo Scientific™). The flasks were coated with Animal Component-Free Attachment Substrate (STEMCELL Technologies™) diluted at a ratio of 1 to 300 in Dulbecco's phosphate buffered saline (DPBS) for 1 h at room temperature (RT). Afterwards, the T225 flasks were washed with DPBS. Cells were thawed and plated at a cell density of 1800-2000 cell/cm², cultured in a CD medium MesenCult™ (STEMCELL Technologies™) supplemented with 1% (v/v) of GlutaMAX™ (Gibco®, Thermo Fisher Scientific) and 0.2% (v/v) of MesenCult™-ACF Plus supplement (STEMCELL Technologies™) (MesenCult). hAT-MSC were kept at 37°C and 5% CO₂ in a humidified atmosphere and a complete medium exchange was performed every 3-4 days.

Upon reaching 80-90% confluency, MSC were washed with DPBS and then detached from the flasks using the xeno-free cell detachment solution TrypLE™ Select (1x) (Gibco, Life Technologies) for 10 min at 37°C. The enzymatic action is stopped by dilution, with the addition of fresh culture medium with the equivalent volume of TrypLE™ used before. The cell suspension was then centrifuged at 300 g for 10 min at RT, the supernatant was discarded and the remaining cell pellet was re-suspended in an appropriate volume of culture medium. After cell concentration and viability analysis using the NucleoCounter® NC-202™ automated cell counter (ChemoMetec), MSCs were either re-seeded into a T-flask (static control) or inoculated in STBR (as described in the following section). Whenever required, cells were cryopreserved in a freezing solution (90% FBS and 10% dimethyl sul-foxide (DMSO)).

3.1.3 hAT-MSC expansion in STBR

BioBLU 0.3c Single-Use Vessels (Eppendorf[™]), equipped with a pitched-blade 45° impeller, were used for the stirred culture of hAT-MSCs. Low Concentration (LC) Synthemax® II Corning® microcarriers (Sigma-Aldrich) were used at a final concentration of 16 g/L (correspondent to a surface area of 1152 cm²).

Prior to cell inoculation, microcarriers were conditioned with cell culture medium for at least 1 h. Afterwards, hAT-MSCs, previously expanded in T225 flasks, were inoculated at a cell density of 4x10³ cell/cm² in a total volume of 100 mL of MesenCult. For the first 24h, an intermittent agitation regime was performed in order to promote cell attachment to the microcarriers surface. This regime is composed of agitation cycles of 1 min of agitation at 60 rpm and 59 min with agitation off. From this point

onwards, the bioreactors were continuously agitated between 60-70 rpm (agitation rate was adjusted depending on the culture status to limit cell aggregation) and 100 mL of culture medium was added to reach a final working volume of 200 mL. In addition to the controlled stirring, the dissolved oxygen (DO), temperature and pH were controlled throughout the entire culture. The desired oxygen concentration, 14.3% DO (*i.e.*, 3% pO₂), corresponding to physiological oxygen levels, was controlled through overlay gassing (1.2 sL/h; 0.1 vvm).

Samples of 2 mL were taken daily for analysis of cell numbers and viability. A 50% culture medium exchange on day 4 of cell culture. In addition to this feeding strategy, daily glucose supplementation (Gibco®, Thermo Fisher Scientific), along with a 50% culture medium exchange on day 4, was evaluated. Supplementation was done so that glucose levels were maintained close to the glucose concentration present in the fresh medium (5.5 mM). In all experiments, cells were cultivated for 7 days.

At the end of the cell culture, the bioreactor agitation was stopped to allow microcarrier deposition and initiate cell harvest. After microcarrier and cell deposition, the culture medium was collected for EV isolation, the cells were washed with DPBS and then detached from the microcarriers surface using TrypLE™ Select (1x) (Gibco, Life Technologies) at 37°C with the following cycles of agitation: 5 min at 135 rpm followed by a pulse of 5 sec at 180 rpm, for a total incubation time of 15-20 min. The enzymatic action was stopped by dilution, with the addition of Mesencult with the equivalent volume of TrypLE™ used before. The cell/microcarrier suspension was recovered from the bioreactor and filtrated through a cell strainer (sterile nylon mesh) with pore size of 70 µm (Falcon) into a 225 mL conical centrifuge tube (Falcon). The cell suspension was then centrifuged at 300 g for 10 min at RT, the supernatant was discarded, and the remaining cell pellet was re-suspended in an appropriate volume of culture medium. After cell concentration and viability analysis using the NucleoCounter® NC-202™ automated cell counter (ChemoMetec), cells were cryopreserved as mentioned before.

3.2 hAT-MSC transfection with miR-145-5p inhibitor

hAT-MSCs were cultured in static culture systems as previously described. Prior to transfection, cells were seeded in T225 flasks at a cell density of 40 000 cell/cm 2 . After 24 h, the cells were transfected with 50 μ M miR-145-5p inhibitor (Thermo Fisher), using Lipofectamine RNAiMAX (Thermo Fisher) according to the manufacturer's instructions. Transfected cells were incubated at 37°C for 6 h. Afterwards, the cells were harvested and inoculated in STBR, as described in section 3.1.3. The efficiency of miRNA transfection was confirmed via RT-PCR, as described in section 3.3.6.

3.3 Analytical Techniques for characterization of hAT-MSC

3.3.1 Cell concentration and viability

In 2D planar culture systems, cell growth was assessed only at day 7 of culture, while in STBR cell proliferation was daily assessed. To this purpose, two samples of 2 mL (technical replicates) were taken daily from the BioBLU vessels. In 1.5 mL eppendorf[™] tubes, the cells attached to the microcarriers surface were allowed to settle on the bottom of the eppendorf[™] tube for 1-2 min. After performing a washing step with DPBS, 300-450 µL of TrypLE solution were added, to detach the cells from the

microcarriers surface, and the mixture was then incubated for 10-15 min at 37°C. After that, the same volume of culture medium was added to dilute the solution.

In both culture systems, cell concentration and viability were assessed using a NucleoCounter® NC-202™ automated cell counter (ChemoMetec).

3.3.2 Qualitative assessment of cell viability

Cell viability was evaluated following incubation with two fluorescent probes diluted in DPBS: fluorescein diacetate (FDA, 5 mg/mL in H₂O, Sigma-Aldrich) and propidium iodide (PI, 1 mg/mL in H₂O, Sigma-Aldrich). Fluorescence images were captured with a fluorescence microscopy (DMI6000, Leica) and further analyzed with ImageJ open source software.

3.3.3 Analysis of extracellular metabolite concentration

The cell culture supernatant from both STBR and static controls was centrifuged for 5 min at 500 g at RT to remove cell debris. The resultant supernatant was stored at -20°C until further metabolite analysis using Cedex Bio Analyzer (Roche) in order to quantify the concentrations of glucose (Glc), lactate (Lac), ammonia (NH₃) and glutaMAX (L-alanine-L-glutamine).

3.3.4 Flow cytometry of hAT-MSC surface markers

In accordance with the criteria established by ISCT [26], immunophenotypic analysis of hAT-MSCs specific surface markers and hematopoietic contaminants was performed by flow cytometry before and after expansion in both 2D planar systems and STBR. To this purpose, a panel of monoclonal antibodies were used: CD29-PE, CD73-PE, CD90-FITC, CD105-PE (Biolegend®), CD34-PE, CD45-PE (BD Biosciences®) and HLA-DR-PE (Biolegend®). Isotype controls were also prepared (PE and FITC mouse IgG1 and PE mouse IgG2 (Biolegend®)).

Briefly, samples with a cell concentration of $1x10^6$ - $3x10^6$ cell/mL prepared in 100 μ L of DPBS supplemented with 1% FBS were incubated with the labeled antibodies at RT for 20-30 min in the dark. Following incubation, cells were washed twice with DPBS 1% FBS, to remove any excess antibody. Afterwards, cells were resuspended in 300 μ L of DPBS 1% FBS. Samples were acquired using the BD FACS Celesta (BD Biosciences) and a minimum of 10 000 events per sample were recorded. The analysis of the acquired data was performed using FlowJo software (Becton, Dickinson Company).

3.3.5 Trilineage differentiation of hAT-MSCs

Following the criteria established by ISCT to characterize MSC [26], the ability of hAT-MSC to differentiate into the adipogenic, osteogenic and chondrogenic lineages (trilineage differentiation potential) was evaluated.

Regarding the osteogenic and adipogenic differentiation, hAT-MSC were cultured in 24-well plates (Corning®), seeded at 1x10⁴ cell/cm² per well in 1 mL of MesenCult medium. When cells reached approximately 90% of confluency, cell culture medium was exchanged to osteogenic or adipogenic differentiation medium (PromoCell), both supplemented according to the manufacturer's instructions, except on control wells where cell culture medium used was MesenCult (non-differentiated cell conditions). hAT-MSCs were then incubated for 14 days at 37°C and a complete medium exchange was

performed every 3-4 days. After 14 days, cells were washed with DPBS and fixed with paraformaldehyde (PFA) 4% (w/v) for 30 min at RT and subsequently stained with Alizarin Red S solution 2% (v/v) for the presence of osteocytes and stained with Oil Red O 0.3% (v/v) to identify the presence of adipocytes, both for 1 h. Finally, after being washed at least three times with dH₂O or with DPBS, to detect the presence of osteocytes or adipocytes, respectively, the staining images were captured in a computer-assisted light microscope (MC170 HD, Leica Microsystems GmbH).

The ability of hAT-MSCs to differentiate into the chondrogenic lineage was assessed in three dimensional cultures of cells in aggregates. To this purpose, a cell pellet of 1x10⁶ cells was prepared in a total volume of approximately 100-200 µL of MesenCult medium and the pellet was added, drop by drop, into a 24 ultra-low attachment well plate (Corning®) to promote cell aggregation for 20 min, after which MesenCult medium was added to the well. On the following day, the medium was exchanged to chondrogenic differentiation medium (PromoCell), supplemented according to the manufacturer's instructions, except on control wells where the cell culture medium was MesenCult (non-differentiated cell conditions). hAT-MSCs were then incubated for 21 days at 37°C and a complete medium exchange was performed every 3-4 days. After 21 days, cells were washed with DPBS and fixed with PFA 4% (w/v) for 30 min at RT. Subsequently, cells were stained with Alcian-Blue 8GX for 1 h. Finally, the cell aggregates were washed at least three times with dH₂O, and the staining images were captured in a computer-assisted light microscope (MC170 HD, Leica Microsystems GmbH).

3.3.6 RT-PCR

Total RNA was extracted from both STBR and static controls using the MirVana ™ miRNA Isolation Kit, with Phenol (Thermo Fisher). Reverse transcription was performed with TaqMan™ Advanced miRNA cDNA Synthesis Kit (Thermo Fisher), following manufacturer instructions, and quantified in the NanoDrop™ 2000c (Thermo Scientific™).

TaqMan® Advanced miRNA Assays (Applied Biosystems) were used for the relative quantification of miRNA, according to the manufacturer's protocol, using hsa-miR-145-5p and normalized to the internal control hsa-miR-186-5p (both from Thermo Fisher). Briefly, each PCR was performed in 10 μ L reactions containing 2.5 μ L of cDNA, 5 μ L of TaqMan® Fast Advanced Master Mix (2X), 0.5 μ L of TaqMan® Advanced miRNA Assay (20X) and 2 μ L RNase-free water. Samples were thermocycled using the LightCycler 480 Instrument II 384-well block (Roche) with program cycles as follow: pre-incubation for 10 min at 95°C; 45 cycles of amplification with denaturation at 95°C for 15 sec and annealing/extension at 60°C for 60 sec.

The Cycle threshold (Ct) was determined using LightCycler 480 Software version 1.5 (Roche). The results were analyzed using the 2 -ΔΔCT method for relative gene expression analysis. The gene expression data was normalized using the housekeeping reference hsa-miR-186-5p, and represented relatively to a control sample.

3.3.7 Droplet digital PCR (ddPCR)

ddPCR was used to evaluate the lentiviral transgene expression levels of gmMSC. Total RNA was extracted from both STBR and static controls using the RNeasy Mini kit (Quiagen). cDNA was synthesized by Transcriptor High Fidelity cDNA Synthesis Kit, following manufacturer instructions and quantified in the NanoDrop™ 2000c (Thermo Scientific™).

All ddPCR assays were performed using the QX200 ddPCR system according to the manufacturer's instructions (Bio-Rad). The primers used are listed in Table 3.1. Briefly, the PCR samples were prepared using 11 µL of a 2x ddPCR™ EvaGreen Supermix, 1.1 µL of each primer (900 nM final concentration), 2.2 µL of cDNA (30 ng/µL final concentration) and 19.8 µL of RNase-free water. Afterwards, 20 µL of the PCR samples were placed in a droplet generator cartridge (DG8TM, Bio-Rad Technologies), 70 µL of droplet generator oil (Bio-Rad Technologies) was added, and the cartridge was placed into a droplet generator. Droplets were then thermocycled at 95°C for 10 min, followed by 40 cycles of 94°C for 30 sec, 53°C for 1 min, and a final extension for 10 min at 98°C. Following amplification, samples were placed in the Bio-Rad QX200TM Droplet Reader (Bio-Rad Technologies). Results were analyzed with QuantaSoft™ analysis software (Bio-Rad Technologies). The ddPCR data were used when more than 15,000 droplets per well were read.

Table 3.1: List of all primers used in ddPCR.

| | Forward primer | Reverse primer |
|--------------------------|------------------------------|------------------------------|
| Lentiviral transgene | 5'- TTAAGACCAATGACTTACAAG-3' | 5'- GGAGTGAATTAGCCCTTC-3' |
| Housekeeping gene (HPRT) | 5'- TGCTTTCCTTGGTCAGGCAGT-3' | 5'- CTTCGTGGGGTCCTTTTCACC-3' |

3.4 Concentration and isolation of MSC-derived EVs

CCM from days 4 and 7 of cell culture obtained from 2D planar cultures or STBR was recovered to isolate EVs. The isolation method consisted of TFF followed by SEC.

Briefly, the conditioned medium was submitted to two low-speed centrifugation steps: 300 g for 10 min followed by 2000 g for 10 min (5804 centrifuge, Eppendorf®) (both at 4°C). The resultant supernatant was stored at 4°C for a maximum of 3 days until further EV concentration and isolation.

To purify EVs from large volumes of conditioned medium, a pre-concentration step is required for volume reduction prior to loading into the SEC column. Therefore, following the centrifugation steps, the conditioned medium was concentrated into a volume of 2 mL using a MicroKros Hollow Fiber Filter Module with 500 kDa cut-off filters (Spectrum® MicroKros). Flow was supplied using either syringes or a peristaltic pump (SARTOFLOW® Slice 200) with a flow rate of 30 mL/min. In the final step, the CCM was exchanged with DPBS, by continuously feeding the system with DPBS to concentrate the conditioned medium back to 2 mL.

Afterwards, EV isolation was performed by SEC using a qEV SEC column (Izon) with a 70 nm pore size to separate particles based on their size. The column was first primed with DPBS after which 0.5 mL of the TFF concentrated solution was loaded into the column and eluted with DPBS. After sample

addition, the first 3 mL collected were discarded. Immediately after, 20 fractions of 0.5 mL were collected, and the column was washed with DPBS containing 0.1% sodium azide (w/v) and stored with this solution until further use.

Samples obtained from STBR – Glucose and STBR – gmMSC experiments, as well as samples obtained from their respective static controls, were immediately stored at -80°C until further analysis. Samples obtained from STBR – Transfected experiments (fractions 2-4), as well as samples obtained from their respective static controls, were pooled together and an additional concentration step was performed using Amicon-2 10 kDa centrifugal filter units (Merck Milipore), where samples were centrifuged at 4000 g for 20 min followed by a spin down for 2 min at 1000 g (both at 4°C). All samples were then stored at -80°C.

3.5 MSC-derived EV characterization

3.5.1 Nanoparticle tracking analysis (NTA)

EV concentration and size distribution profiles were measured by nanoparticle tracking analysis (NTA) using NanoSight NS300 (Malvern Panalytical, UK) equipped with a 405 nm laser and NTA software version 3.3.

Samples of 1 mL were prepared by diluting the EV solution with DPBS to obtain a final concentration in the range of 10⁶-10⁹ particles/mL. For each sample, three videos of 30 sec were recorded, using fresh sample for each acquisition. The videos were obtained with identical software settings: camera level of 13-15, screen gain 10 and detection threshold 2-4.

3.5.2 Protein quantification

Total protein contents were assessed in EV samples using the Thermo Scientific™ BCA Protein Assay Kit. Both EV samples (diluted in DPBS to obtain a final concentration in the range of 0.5-20 µg/mL) and standard protein solutions were prepared (n=3 technical replicates) and incubated with the microBCA Working Reagent for 2 h at 37°C. Afterwards, the absorbance was measured at 562 nm on a plate reader (Infinite M200 Pro, Tecan) and a standard curve was prepared by plotting the average Blank-corrected 562 nm reading for each protein standard vs its concentration in µg/mL and further used to determine protein concentration in each sample.

3.5.3 Bead-based flow cytometry

EV specific surface markers such as CD81, CD63 and CD9 were assessed by bead-based flow cytometry. For that purpose, the exosome-Human CD81 Flow Detection Reagent (Invitrogen™, ThermoFisher) was used.

Briefly, superparamagnetic beads coated with a primary monoclonal antibody specific for CD81 membrane antigen were first washed with DPBS using a DynaMag[™]-2 Magnet (Thermo Fisher). EV samples were incubated with 5x10⁴ beads overnight at 4°C in 1.5 mL low protein binding collection tubes (Thermo Fisher Scientific[™]) on a oscillator mixer at a ratio of 3.0x10⁴ - 3.3x10⁴ particle to bead. After being centrifuged at 900 g for 1 min at RT, the beads were washed twice with DPBS (using a magnetic rack to retain the bead-bound EV samples), resuspended in DPBS and incubated with 5 µL

(diluted in 100 μL of DPBS) of the panel of antibodies of interest – CD9-PE, CD63-PE or CD81-PE (Biolegend®) – for 30 min at 4°C protected from light. Samples were once again washed and resuspended in DPBS and, finally, analyzed in a flow cytometer (BD FACS Celesta (BD Biosciences)). The results were obtained by plotting the percentage of positive EVs for the surface markers CD9, CD63 and CD81. Analysis of the data was done using FlowJo software.

3.5.4 Transmission Electron Microscopy (TEM)

EV morphology was assessed by Transmission Electron Microscopy (TEM). First, 100 mesh copper grids formvar/carbon were precoated and glow discharged. Samples were mixed (1:1) with formaldehyde 4% (w/v) in 0.1 M phosphate buffer solution for 5 min and then incubated for another 5 min at RT to allow them to adhere to the grids. Grids were washed with 10 drops of dH₂O and stained with 1 drop of 2% (w/v) uranyl acetate for 5 min at RT protected from light.

Imaging was done on a Tecnai G2 Spirit BioTWIN Transmission Electron Microscope (FEI Company™) operating at 120 kV and data collected with Olympus-SIS Veleta CCD Camera. This analysis was performed at the Electron Microscopy Facility in Instituto Gulbenkian de Ciência.

3.6 Functional Assays

3.6.1 Tube formation assay

The angiogenic capacity of hAT-MSC-derived EVs was tested *in vitro*, using HUVECs, from Lonza®. Cells were propagated in T25/T75 flasks (Thermo Fisher Scientific™) in Endothelial Cell Growth Medium supplemented according to manufacturer's instructions (complete EGM™-2, Lonza®) and kept at 37°C and 5% CO₂ in a humidified atmosphere. Culture medium was exchanged every 3 days and cells were passaged upon reaching 80-90% of confluency.

15 hours before starting the assay a complete medium exchange was performed with Endothelial Cell Growth Medium without any supplementation (basal EGM[™]-2). Afterwards, 50 µL of Matrigel® Growth Factor Reduced Basement Membrane Matrix (Corning®) was added to a 96-well culture plate (Corning®) and then incubated at 37°C for 1 h to solidify the gel. HUVECs were seeded onto the plate so that each well contained 1.2-1.5x10⁴ cells. Subsequently, cells were treated with hAT-MSC-derived EV at a ratio of 6x10³ particle/cell, appropriately diluted in basal EGM[™]-2. Negative and positive control wells were treated with basal EGM[™]-2 and complete EGM[™]-2, respectively. Each well contained a total volume of 200 µL. Cells were incubated at 37°C for 8 h.

Images of the tube formation were obtained using the IncuCyte[™] software instrument (Essen Bio-Science) and were afterwards analyzed using the Angiogenesis Analyzer toolset in ImageJ (Carpentier).

3.6.2 Wound healing assay

To study the effect of the hAT-MSC-derived EVs in cell migration *in vitro*, the wound healing assay was performed using HUVECs. Cells were expanded in the same conditions mentioned in section 3.6.1. After reaching 80-90% confluency, HUVECs were seeded (3x10⁴ cells per well) in a 96-well ImageLock™ tissue culture plate (Essen BioScience) in complete EGM™-2 and kept at 37°C and 5% CO₂

in a humidified atmosphere for 8 h. Afterwards, a complete medium exchange was performed with basal EGMTM-2 supplemented with 0.1% FBS (v/v) and cells were incubated for 15 h. Subsequently, 200 μ L of EV samples were diluted in basal EGMTM-2 supplemented with 0.1% FBS (v/v) in order to obtain a particle/cell ratio of 6x10³. Cells were treated with these samples for 24 h. Basal EGMTM-2 supplemented with 0.1% FBS (v/v), diluted with a volume of DPBS equivalent to the volume of the prepared EV samples, was used as negative control, whereas complete EGMTM-2 was used as a positive control. Lastly, 24 h later, the samples were retrieved from each well, 100 μ L of DPBS was added and, by using a 96-pin WoundMakerTM, the wounds were created in each well of the 96-well plate. The wells were then washed twice with DPBS to remove the detached cells and the EV samples were returned to each well.

Images of the wounds were automatically obtained and registered every 2 h using the IncuCyte[™] software instrument (Essen BioScience) for a total of 24 h. The images obtained were analyzed using the ImageJ Wound Healing Size Analyzer toolset, which allowed to calculate the percentage of wound closure relative to time-point 0 h according to Equation 3.1.

Wound Closure (%) =
$$\frac{A_0 - A_t}{A_0} \times 100\%$$
 3.1

where A_0 is the initial wound area and A_t is the wound area at t hours after the initial scratch being performed.

3.7 Statistical analysis

Data are shown as mean ± standard deviation. Statistical significance was determined by one-way analysis of variance (ANOVA) with Tukey's multiple comparison test using the GraphPad Prism 7 software. * p<0.05, ** p<0.01, *** p<0.001, **** p<0.0001 were considered significant.

4. Results and Discussion

Considering the growing interest in MSC-derived EVs as therapeutic entities in cardiac regenerative medicine, development of robust and standardized scalable manufacturing processes is an imminent need. EV manufacture comprises both upstream and downstream processing that needs to be optimized in order to accelerate clinical translation of safe and effective EV-based therapeutics. Improving MSC-derived EV yields and enhancing their therapeutic potential is critical to favour their application. Cell preconditioning with either physical or biochemical approaches could constitute suitable strategies to improve the pro-angiogenic activity of MSC. In this work, we explored two different strategies to increase EV production as well as their pro-angiogenic function – MSC preconditioning with miR-145-5p inhibitor or with low concentration levels of glucose (section 4.1) and culture of genetically modified MSC with a lentivirus co-expressing Apelin and FGF-2 (section 4.2).

Expansion of hAT-MSC in STBR and hAT-MSC-derived EV concentration and isolation were performed based on previous protocols established by our group [113]. Briefly, cell culture was supported by microcarriers (LC Synthemax II) in DASbox® mini STBR under hypoxic conditions (3% O₂) with a working volume of 200 mL. Prior to cell inoculation in STBR, cells were cultured in static culture systems, as described in section 3.1.2. Subsequently, bioreactor vessels were inoculated at 4x10³ cell/cm² of LC Synthemax® II microcarriers (at a concentration of 16 g/L). Following a 24h attachment phase, cells were cultured for 7 days, while the agitation rate was kept between 60-70 rpm throughout culture time. The increase in the agitation rate was due to visible microcarrier aggregation and deposition in the bottom of the culture vessel, which might impair cell growth [114]. In parallel, hAT-MSCs were also cultured in planar systems (T-flasks) under hypoxic conditions to compare EV productivity and bioactivity in both cell culture systems.

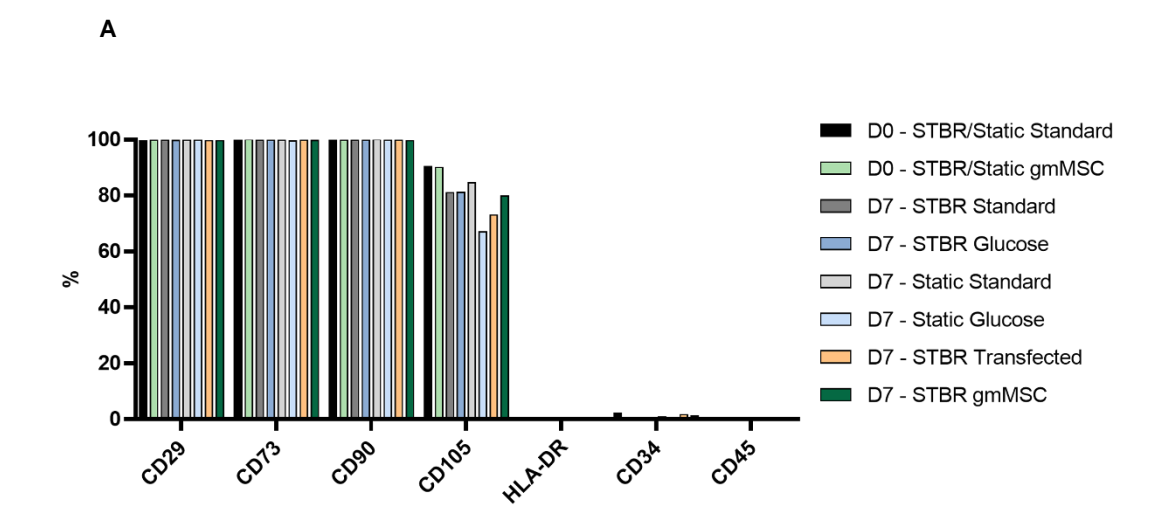
Cell expansion in STBR possesses several advantages over expansion in planar systems, such as easier scale up, enhanced process monitoring, flexible modes of operation, and lower cost for production [115]. Furthermore, cell expansion under hypoxic conditions (1-5% O₂) replicates oxygen concentration *in vivo* and it has been reported that cells cultured in these conditions exhibit a greater expansion potential, decreased senescence and apoptosis [116]. The cell culture media is another important parameter to consider when establishing cell culture conditions. The most commonly utilized medium relies on using supplements such as FBS or hPL, which poses several disadvantages, including batch-to-batch variability and contamination concerns [44,70]. Furthermore, such supplements contain large amount of EVs that can be co-isolated with EVs secreted by cells, thus contaminating the end products. Therefore, to avoid lol-to-lot variations and produce more reproducible cell and EV populations, in this work, we used a CD medium, MesenCult [66].

To ensure that the quality attributes of hAT-MSCs, transfected hAT-MSC and genetically modified hAT-MSC were maintained following expansion in STBR and static culture systems, both cell immunophenotype and trilineage differentiation potential were determined before and after cell expansion (Figure 4.1), in accordance with the criteria established by ISCT [27].

For all experimental conditions used in this study, more than 99% of the cell populations were positive for CD29, CD73, CD90 and CD105 whilst for CD34, CD45 and HLA-DR less than 2% of the

cell populations were positive for these markers (Figure 4.1A). These results confirm that cells maintained their immunophenotype. However, lower and more variable percentages for positive CD105 cells were obtained (67-90.3%). In fact, it has been reported that changes in cell culture methods have an impact in CD105 expression, for instance the use of serum-free medium during cell culture [117,118]. Furthermore, CD105 expression is more susceptible in comparison to CD29, CD73 and CD90 to DSP steps used to dissociate the cells, in particular to dissociation reagents, such as TrypLE [119]. Gálvez *et al.* has also described changes in CD105 expression due to different passage number and cell confluency [120].

The cells' ability to differentiate towards the adipogenic, osteogenic and chondrogenic lineages corroborates that, in all experimental conditions, hAT-MSC retained their multipotency (Figure 4.1B).



D0- STBR/Static Standard D7 - STBR Glucose D7- STBR Standard D0- gmMSC

D7- Static Standard D7- Static Glucose D7- STBR Transfected D7- STBR gmMSC

В

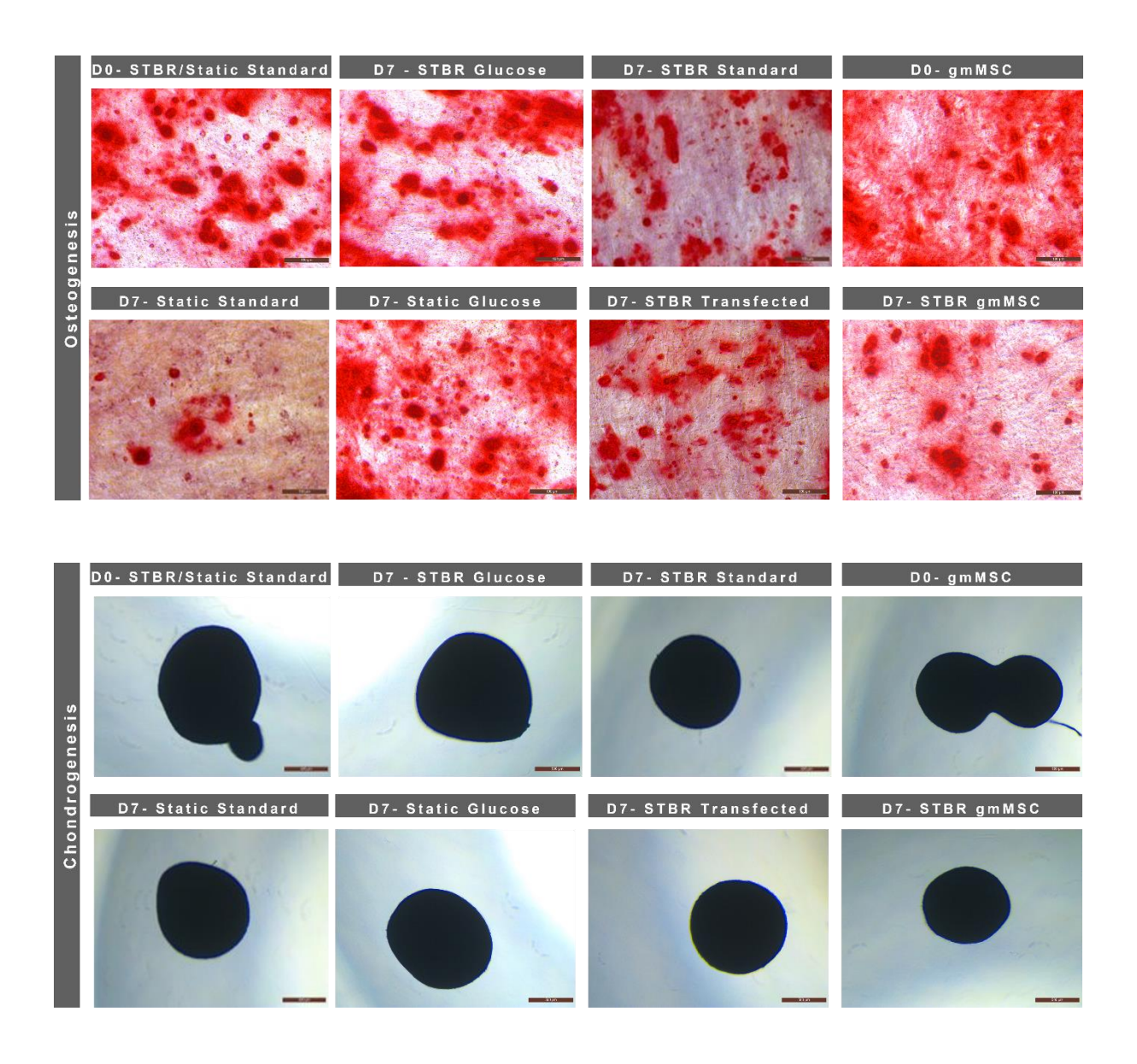


Figure 4.1: hAT-MSCs, transfected hAT-MSC and hAT-gmMSC characterization. (A) Flow cytometry analysis of hAT-MSCs surface markers. (B) Representative images of the ability of hAT-MSCs to differentiate into adipogenic, osteogenic and chondrogenic mesoderm lineages. Scale bar = $200 \mu m$.

4.1 Production of metabolic and miRNA pre-conditioned hAT-MSC and their derived EVs in microcarrier-supported stirred-tank bioreactors

EV yields and their cargo components vary depending on the status of the cells from which they are derived. Consequently, subjecting MSCs to distinct external cues using biophysical or biochemical strategies could potentially contribute to tailor EV production towards a desired function [121]. For instance, it has been shown in several studies that hypoxia preconditioning can result not only in increased number of released EVs but also impact EV's cargo composition, enhancing their pro-angiogenic and cardioprotective properties which, ultimately, can result in improved myocardial repair [99,100,122,123]. Furthermore, Garcia et al. [101] showed that glucose starvation in cardiomyocytes can also trigger EV secretion and promote EVs' pro-angiogenic effects. Mounting evidence shows that EVs mediate the therapeutical effects of their parental cells trough miRNA delivery [55–57]. Therefore, in a different approach, MSCs can be transfected to promote the expression of specific miRNAs and thus enhance their therapeutic outcome as well as of their derived EVs for the treatment of ischemic diseases. Moreover, the cell culture platform itself can constitute another strategy to modulate EV production. Traditionally, for MSC-derived EV production, flask-based culture systems have often been used. However, several studies have now been linking bioreactor culture with higher EV yields [44,75]. Particularly, a recent study by Jeske et al. [65] showed that shear stress and establishing a 3D microenvironment in bioreactor systems, particularly in vertical-wheel bioreactors, not only promotes EV secretion from MSCs compared to flask-based culture systems, but also modulates their miRNA and protein cargo molecules. Specifically, they reported upregulation of several miRNAs that have implications in angiogenesis and wound healing in bioreactor culture.

In the first task of this Thesis, we explored the effects of two different cell preconditioning strategies. This approach involved preconditioning hAT-MSC cultured in STBR through i) tailoring glucose concentration throughout culture time and ii) transfection with miR-145-5p inhibitor to promote an augmented angiogenic response.

4.1.1 Metabolic preconditioning of hAT-MSC and production of their derived EVs

The first task of this work focused on assessing the impact of glucose starvation on the ability of hAT-MSC to secret EVs. Therefore, two different feeding strategies were implemented. As represented in Figure 4.2, in one bioreactor, a 50% (v/v) culture medium exchange was performed on day 4 of cell culture (STBR - Standard) and, in the other cell culture strategy, in addition to the 50% (v/v) culture medium exchange on day 4, glucose was added daily, from day 2 onward, to maintain similar concentration levels to the glucose concentration present in the fresh cell culture medium (5.5 mM) (STBR - Glucose). The same feeding strategies were implemented in static controls (Static - Standard and Static - Glucose).

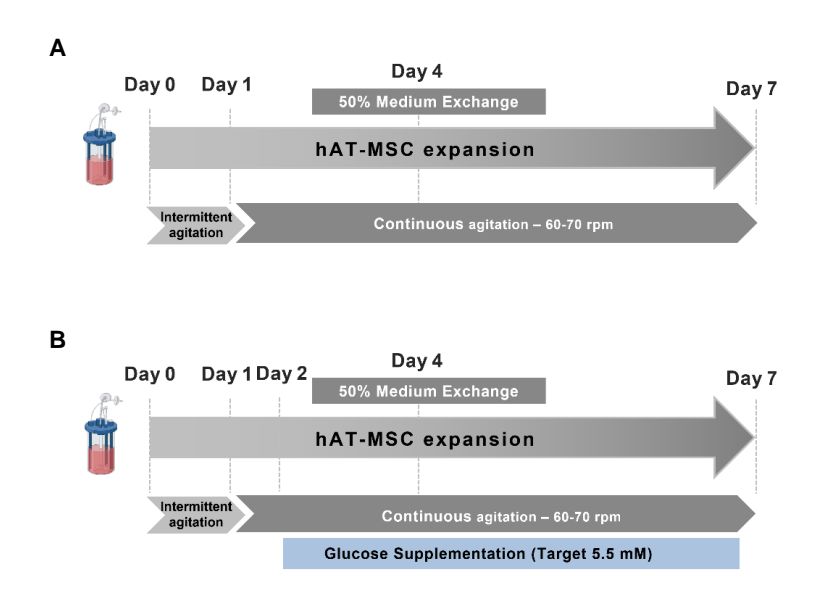
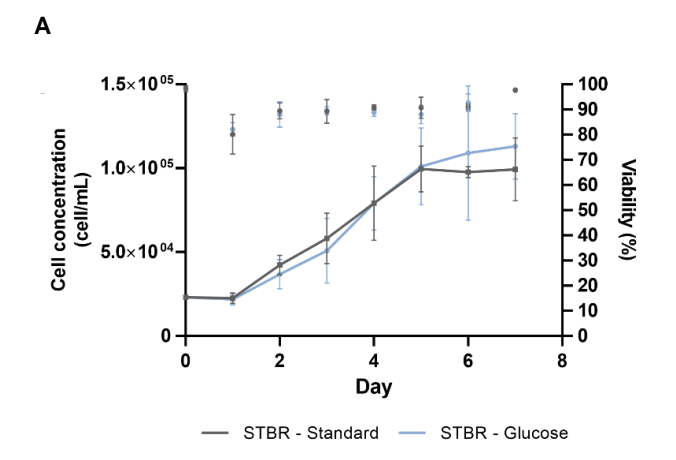


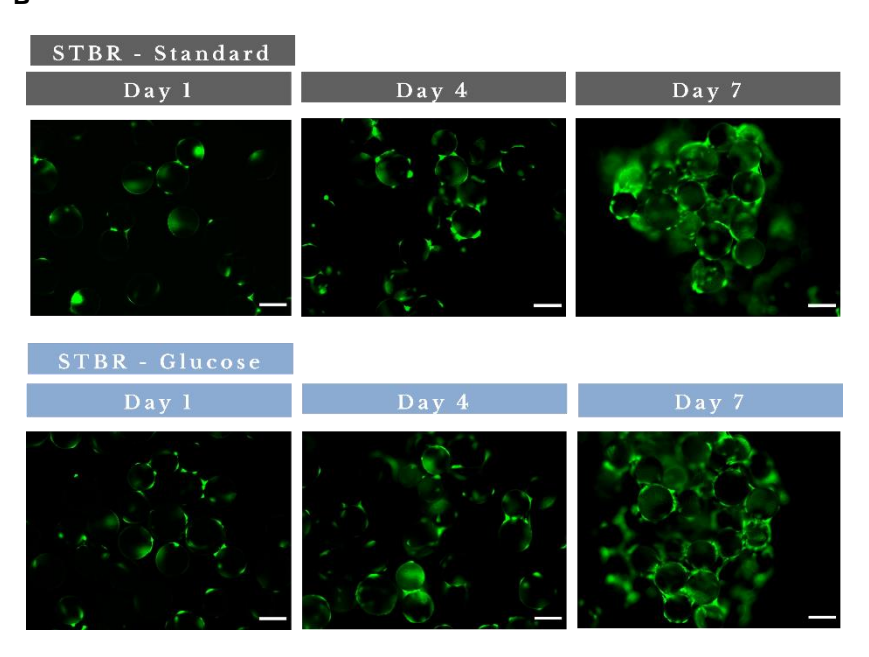
Figure 4.2: Schematic representation of the feeding strategies implemented during hAT-MSC culture in STBR – Standard and STBR - Glucose. (A) STBR – Standard: 50% medium exchange on day 4 of culture; (B) STBR - Glucose: 50% medium exchange on day 4 of culture and daily glucose supplementation.

Cells were successfully expanded in both strategies, with identical growth profiles, suggesting that the progressive decrease of glucose concentration in the condition STBR – Standard did not impact the ability of cells to proliferate on the microcarrier available surface area (Fig. 4.3A). Importantly, high cell viability was maintained throughout the entire culture time (\geq 90%) (measured with the NucleoCounter® NC-202TM) (Figure 4.3A), confirming the high cell viability qualitatively assessed through cell membrane integrity analysis (Figure 4.3B). Cell adhesion efficiency of hAT-MSC to microcarriers, assessed 24h after inoculation, was 98 ± 14% and 94 ± 14% in the conditions STBR - Standard and STBR - Glucose, respectively. At the end of culture, cell concentration in STBR - Standard was (9.9 ± 1.9)x10⁴ cell/mL (expansion ratio: 4.3 ± 0.8) and (1.1 ± 0.2)x10⁵ cell/mL (expansion ratio: 4.9 ± 0.9) in STBR - Glucose.

Looking into metabolite concentration profiles (Figure 4.3C), it is possible to observe the effect of the 50% (v/v) culture medium exchange on day 4 of culture, which led to an increase in both glucose and GlutaMAX (Ala-Gln) concentration, along with a decrease in lactate and ammonia concentration. In STBR - Standard, on the last days of culture, decrease of glucose concentration levels below 1 mM were observed while in the condition STBR - Glucose, glucose supplementation resulted in slightly different metabolic patterns, avoiding glucose depletion across the whole cell expansion process. Importantly, in both strategies, lactate and ammonia concentrations were maintained below inhibitory values (lactate: 35.4 mM, ammonia: 2.4 mM - inhibitory levels reported for human BM-MSCs [124]) throughout the entire culture period.



В



С

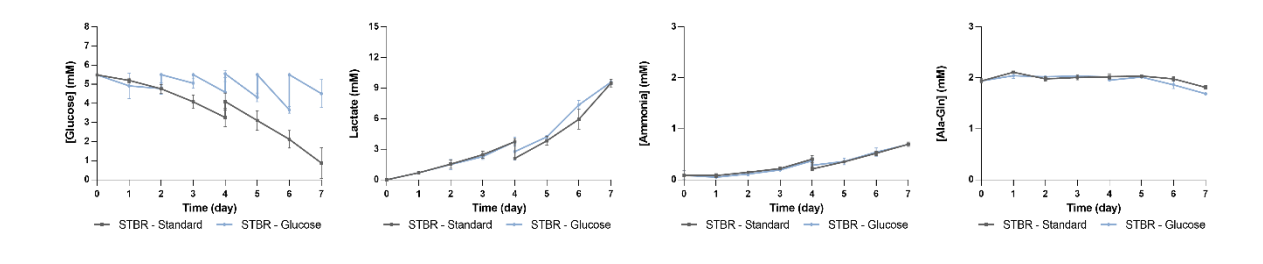
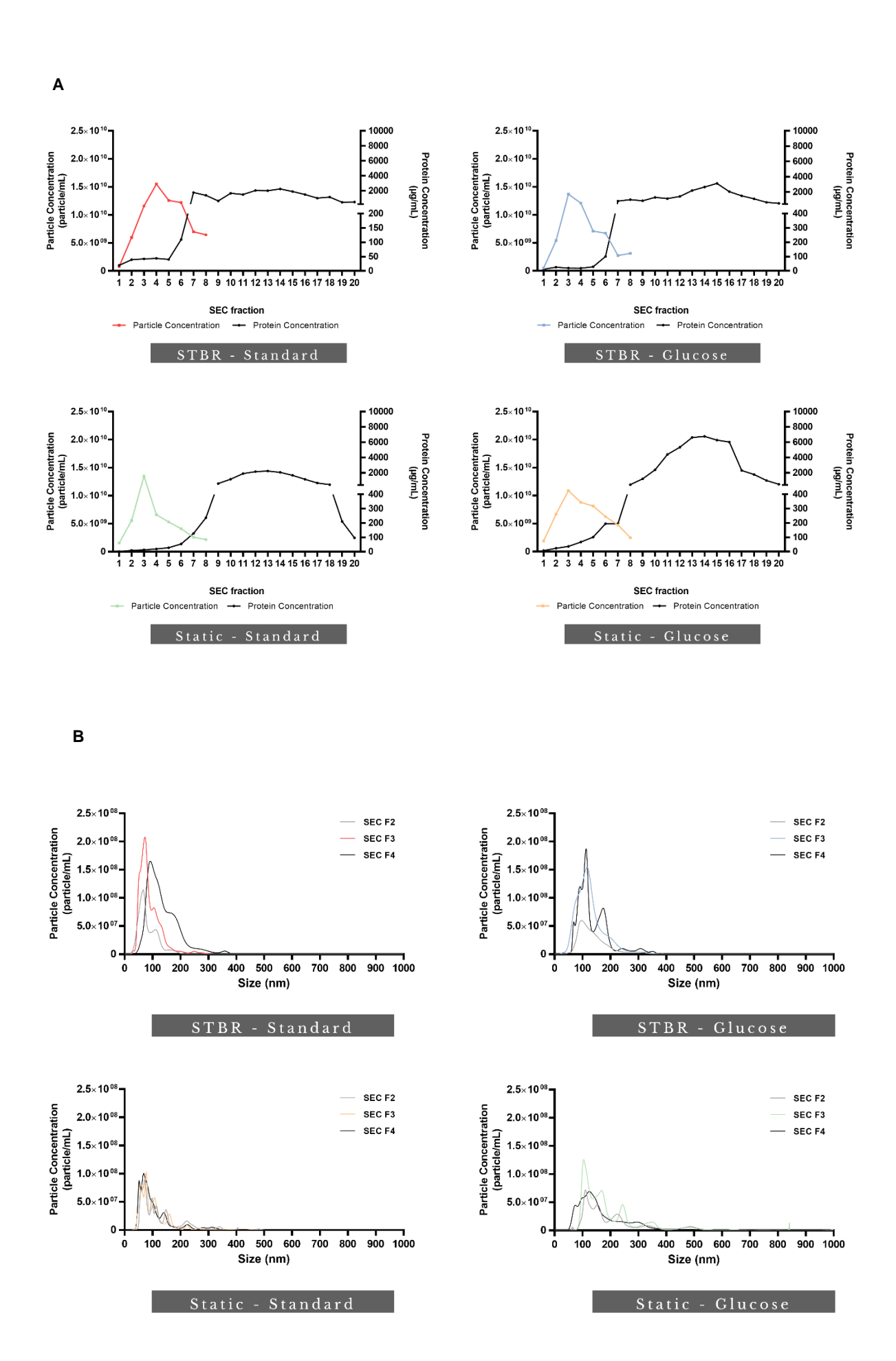


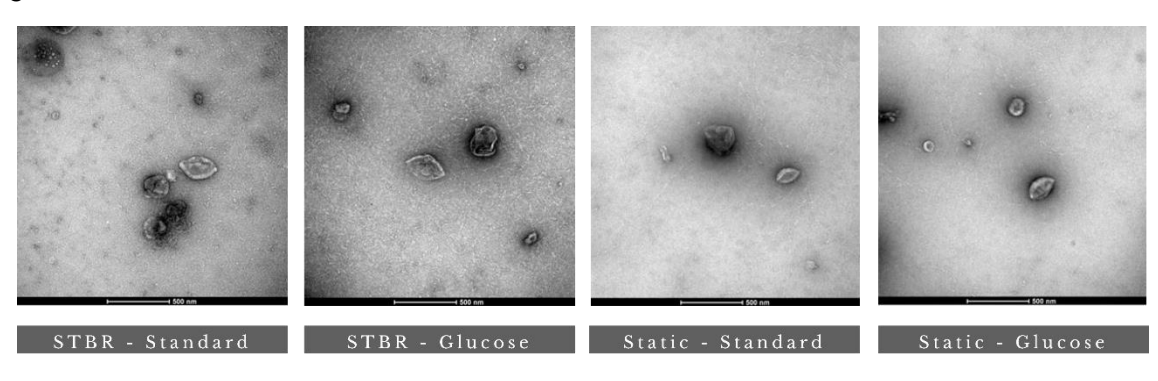
Figure 4.3: hAT-MSC culture characterization after expansion in STBR – Standard and STBR - Glucose. (A) Growth curves and viability of hAT-MSCs during culture in STBR. (B) Representative images of FDA (live cells, green)/ PI (dead cells, red)-stained cells at days 1, 4 and 7 of hAT-MSC culture in STBR. Scale bar = 200 μ m. (C) Metabolite concentration profiles during hAT-MSC culture in STBR. Mean and standard deviation are based on 4 independent runs for STBR - Standard and 3 independent runs for STBR - Glucose.

For the development of a robust and standardized manufacturing process of hAT-MSC-derived EVs, the downstream processing also plays an important role, as efficient, scalable and cGMP-compliant methods are required for clinical applications [125]. In order to concentrate and isolate MSC-derived EVs, the CCM was processed relying on a size-based separation protocol using TFF followed by SEC. For that purpose, the CCM was collected following the 50% medium exchange at day 4 and, upon hAT-MSC expansion, on the cell harvest day (day 7). Finally, after EV isolation, SEC fractions 2-4 were used to assess EV yields and potency. Of notice, since the aim of this first task was to evaluate the impact of glucose starvation, only CCM collected on day 7 of culture, when glucose levels below 1 mM were observed for the condition STBR - Standard, was considered to evaluate these parameters.

NTA was conducted across SEC fractions 1-8 to evaluate particle concentration and size distribution. The level of contaminating protein, quantified by microBCA assay, was assessed per isolated SEC fraction of each condition (Figure 4.4A). Figure 4.4A shows that higher particles concentrations are obtained in SEC fraction 2-4, while proteins are eluted in later SEC fractions. Similar size distribution profiles were observed between all samples, being enriched in the 100-300 nm size range (Figure 4.4B), with overall mean size of 103.3 ± 23.6 nm, 136.4 ± 5.2 nm, 100.5 ± 21.6 nm and 193.0 ± 13.2 nm for STBR – Standard, STBR – Glucose, Static – Standard and Static – Glucose, respectively. Furthermore, TEM characterization of these samples confirmed typical EV morphology, as shown by their cup-shaped morphology [126] (Figure 4.4C). Additionally, in the TEM images, it is possible to observe a background without granularity that may corroborate the low co-isolation of proteins [127]. Finally, EV specific surface markers CD81, CD63 and CD9 were assessed by bead-based flow cytometry. Overall, high expression of these characteristic markers was detected (80.1%, 89.3% and 71.9%, for CD81, CD63 and CD9, respectively) (Figure 4.4D).



С



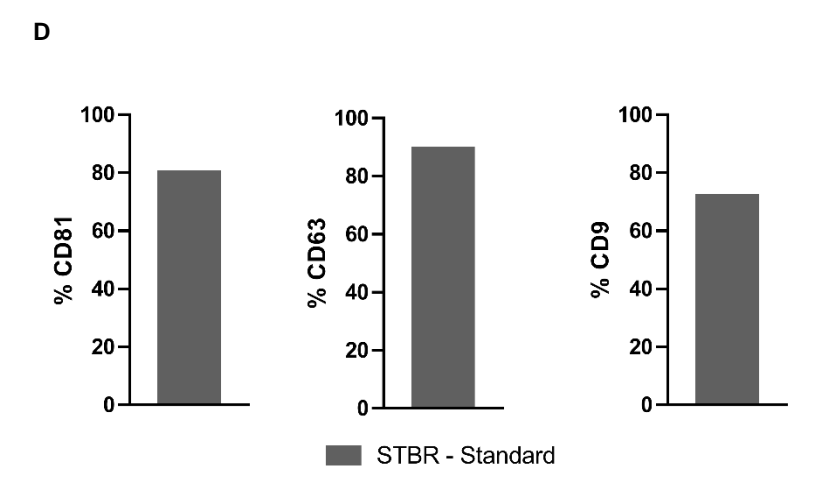


Figure 4.4: Characterization of hAT-MSC-derived EVs obtained from STBR - Standard, Static - Standard, STBR - Glucose and Static - Glucose at day 7 of culture. (A) Representative particle and protein concentration in SEC fractions. (B) Representative size distribution profiles of hAT-MSC-derived EVs in SEC fractions 2-4 analyzed by NTA. (C) Representative TEM images of hAT-MSC-derived EV samples. Scale bar = 500 nm. (D) Bead-based flow cytometric analysis of EV surface markers CD81, CD63 and CD9 following EV production in STBR - Standard.

Total particle counts determined by NTA were used to compare EV recovery yields from the different culture conditions, considering the total number of producing cells (EV productivity) and total volume of CCM (EV concentration) (Figure 4.5). While 5.9 (\pm 0.1) x108 particle/mL and 5.5 (\pm 0.8) x109 particle/106 cell were obtained in the condition STBR - Glucose, increased EV concentration (7.3 (\pm 1.2) x108 particle/mL) and productivity (7.7 (\pm 2.0) x109 particle/106 cell) was observed for the condition STBR – Standard, which show an overall increase associated with the glucose starvation strategy (1.2-and 1.4-fold increase in EV concentration and productivity, respectively). In fact, a previous study by Garcia *et al.* has reported that glucose starvation in cardiomyocytes increased their EV secretion [101]. Since in the last days of cell culture in the STBR - Standard condition, glucose concentration in the medium was below 1 mM, this could explain the higher EV yields, therefore highlighting the efficacy of the preconditioning strategy herein explored.

Lower EV yields were obtained for the static controls with the Static - Standard condition rendering $4.7 (\pm 1.3) \times 10^8 \, \text{particle/mL}$ and $3.3 (\pm 1.4) \times 10^9 \, \text{particle/} 10^6 \, \text{cell}$, while Static - Glucose condition

yielded 5.6 (\pm 1.6) x10⁸ particle/mL and 4.9 (\pm 2.1) x10⁹ particle/10⁶ cell. In this case, although glucose concentration in the medium were also below 1 mM (Supplementary information Figure 7.1), EV concentration and productivities are higher in the Static - Glucose condition. Nevertheless, no statistical differences were observed in any of the conditions under evaluation.

Overall, it is possible to observe an increase in EV production associated with cell culture in STBR, with 2.3-fold increase in EV productivity when AT-MSC are cultured following the standard condition. Indeed, previous studies have also reported higher EV yields when cell expansion is performed in bioreactor systems, which could be potentially related with the fluid shear and consequent mechanical stimulation that cells are exposed to when cultured in these conditions [44,65,75].

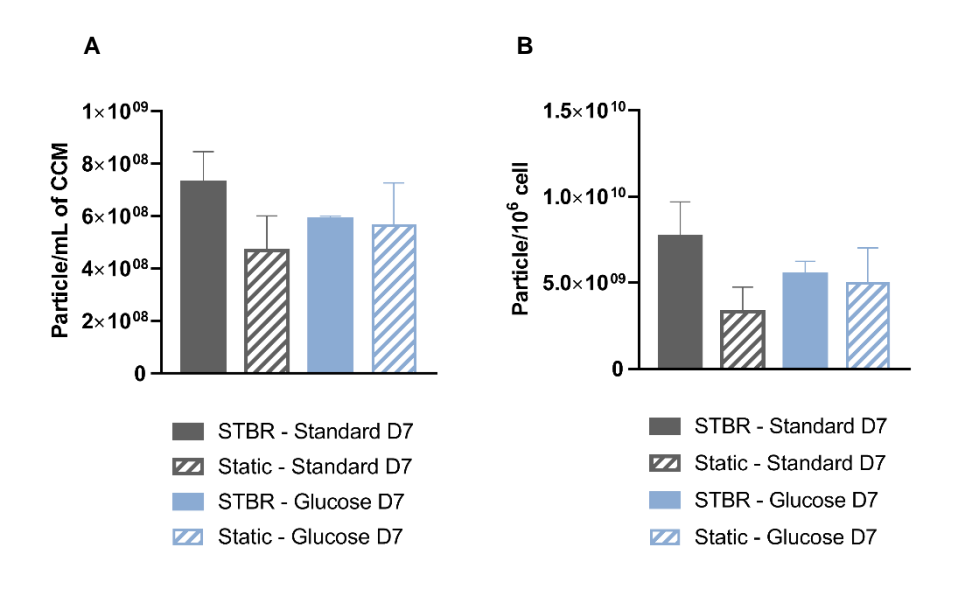


Figure 4.5: EV production yields obtained in STBR - Standard, Static - Standard, STBR - Glucose and Static - Glucose at day 7 of culture. (A) EV concentration (particle/mL of CCM). **(B)** EV productivity (particle/10⁶ cell). Mean and standard deviation are based on 3 independent runs for STBR - Standard and Static - Standard and 2 independent runs for STBR Glucose and Static - Glucose, using 2 biological donors.

To assess the biological function of hAT-MSC-derived EVs and their pro-angiogenic potential, two functional assays were performed: tube formation and wound healing assays which, respectively, evaluate the ability of HUVECs to form tubular structures [128] and migrate [129] in response to EV signaling.

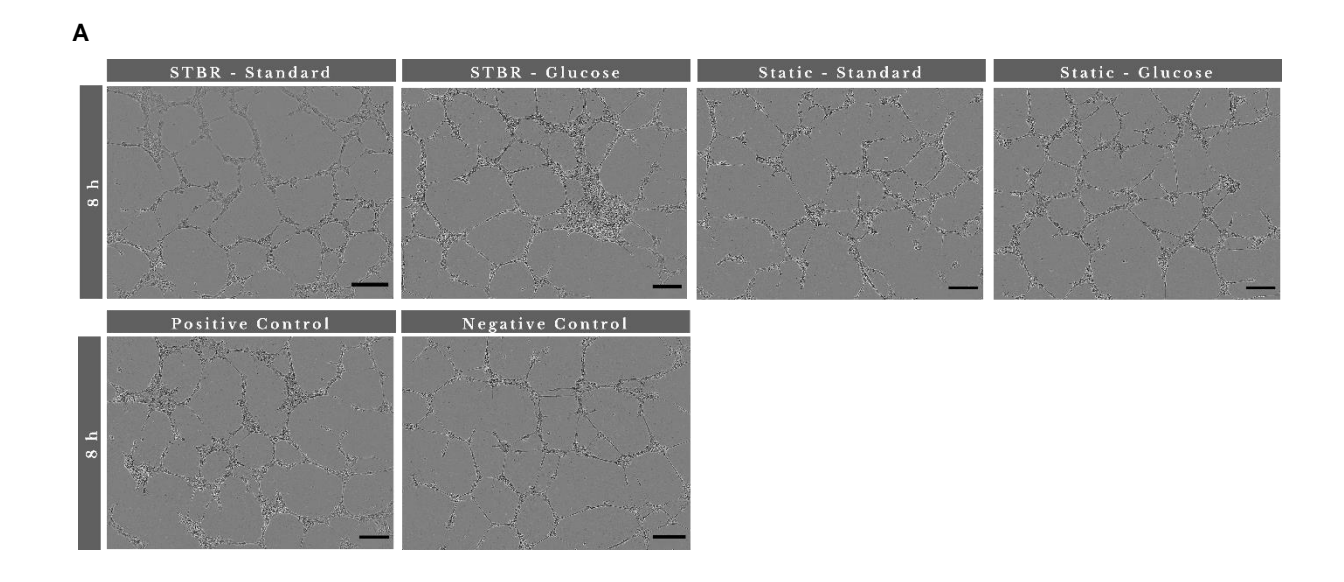
Regarding the tube formation assay, HUVECs were seeded on top of Matrigel and the capacity of hAT-MSC-derived EVs to promote the formation of tubular structures was quantified at 8h using the ImageJ Angiogenesis Analyzer toolset. Results are presented in Figure 4.6A and 4.6B. The number of nodes (*i.e.* intersections of 3 segments) increased from 195 \pm 47 in Negative Control (Basal EGM $^{\text{TM}}$ -2) up to 347 \pm 31 and 328 \pm 33 in STBR - Standard and STBR - Glucose conditions, respectively, and up to 284 \pm 21 and 287 \pm 77 in Static - Standard and Static – Glucose conditions, respectively. Regarding the total master segment length (*i.e.* sum of the length of the detected master segments in the analyzed area), data showed an increase from 7103 \pm 1413 in Negative Control (Basal EGM $^{\text{TM}}$ -2) up to 10688 \pm 742 and 9860 \pm 647 in STBR - Standard and STBR - Glucose, respectively, and up to 8642 \pm 844 and

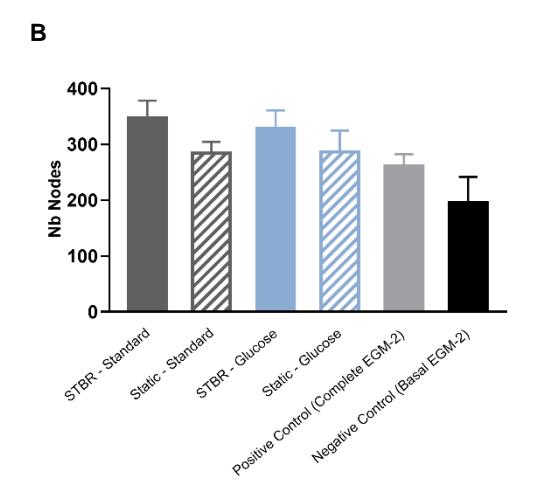
 9299 ± 962 in Static - Standard and Static - Glucose conditions, respectively. These results show an increase in capillary-like tube formation associated with production in STBR - Standard.

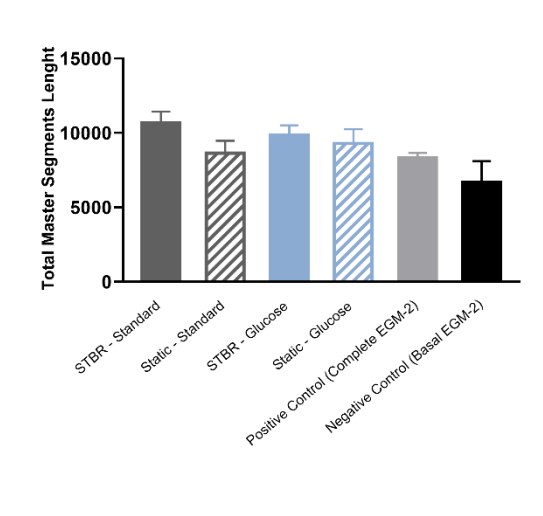
Experimental results following the *in vitro* scratch wound healing assay (Figure 4.6C-E) (percentage of wound closure 20h post scratch: $57.5 \pm 2.8\%$, $43.3 \pm 0.9\%$, $38.5 \pm 1.1\%$ and $38.7 \pm 7.1\%$ for STBR - Standard, STBR - Glucose, Static - Standard and Static - Glucose, respectively) are in line with the enhanced angiogenic potential of the STBR – Standard condition relatively to the glucose supplemented cell cultures. Moreover, our results demonstrate that hAT-MSC-derived EVs produced in STBR can promote an increase in both capillary-like tube formation and migration capacity of HUVECs to a greater extent when comparing to the ones derived from static culture conditions. Overall, these data are in agreement with previous studies that showed that EVs derived from stirred culture conditions have enhanced bioactivity in wound healing assays [65,130].

EV's angiogenic potential rely mainly on their capacity to release bioactive molecules, such as growth factors, that modulate molecular pathways in recipient cells. Particularly, previous studies have reported that MSC-derived EVs contain and transfer several growth factors, such as VEGF, plateletderived growth factor (PDGF), and transforming growth factor-β (TGF-β), that have been shown to promote modulation of the angiogenic phenotype of endothelial cells [131,132]. VEGF is a well-established initiator of angiogenesis, which is known to bind to tyrosine kinase receptors on the surface of HUVECs and mediate their recruitment. TGF-β stimulates PDGF synthesis and, in turn, PDGF induces endothelial cell proliferation and migration [132,133]. In addition, MSC-derived EVs also contain several pro-angiogenic miRNAs that can change gene expression and bioactivity of the recipient cells. Several miRNAs, such as miR-210, miR-126 and miR-21, were found to be enriched in MSC-derived EVs and to have an effect in proliferation, migration and tube formation capacity of HUVECs, via targeting the expression of specific molecules and growth factors with pro-angiogenic activities as the ones mentioned above [50]. Garcia et. al. [101] showed that cardiomyocytes, in the presence of low concentration of glucose, not only produced a higher amount of EVs but also showed that glucose starvation modulates EV cargo molecules. Of particular interest, these EVs overexpressed several miRNAs (miRNA-17, miRNA-19, miRNA-20, miRNA-126) that are capable of stimulating phenotypical and functional changes in endothelial cells and, therefore, promote angiogenesis [134].

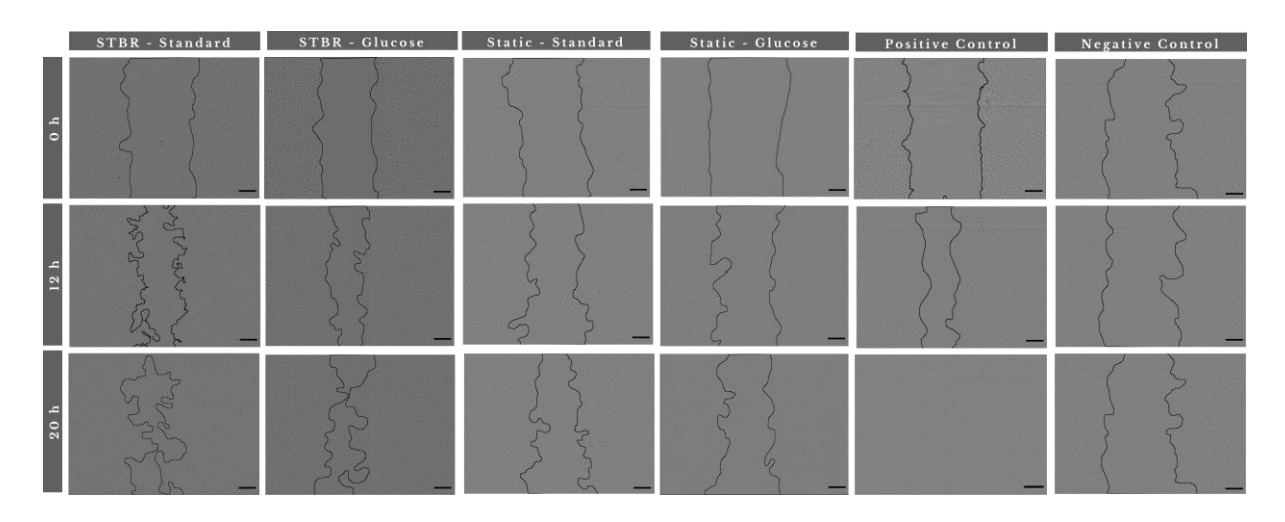
Nevertheless, subsequent experiments should focus on dissecting the transcriptome and proteome of EVs subjected to distinct stimuli and further understand their mechanism of action. Overall, given the added benefits provided by EVs manufactured following the STBR - Standard condition, this strategy was selected and implemented throughout this work.







С



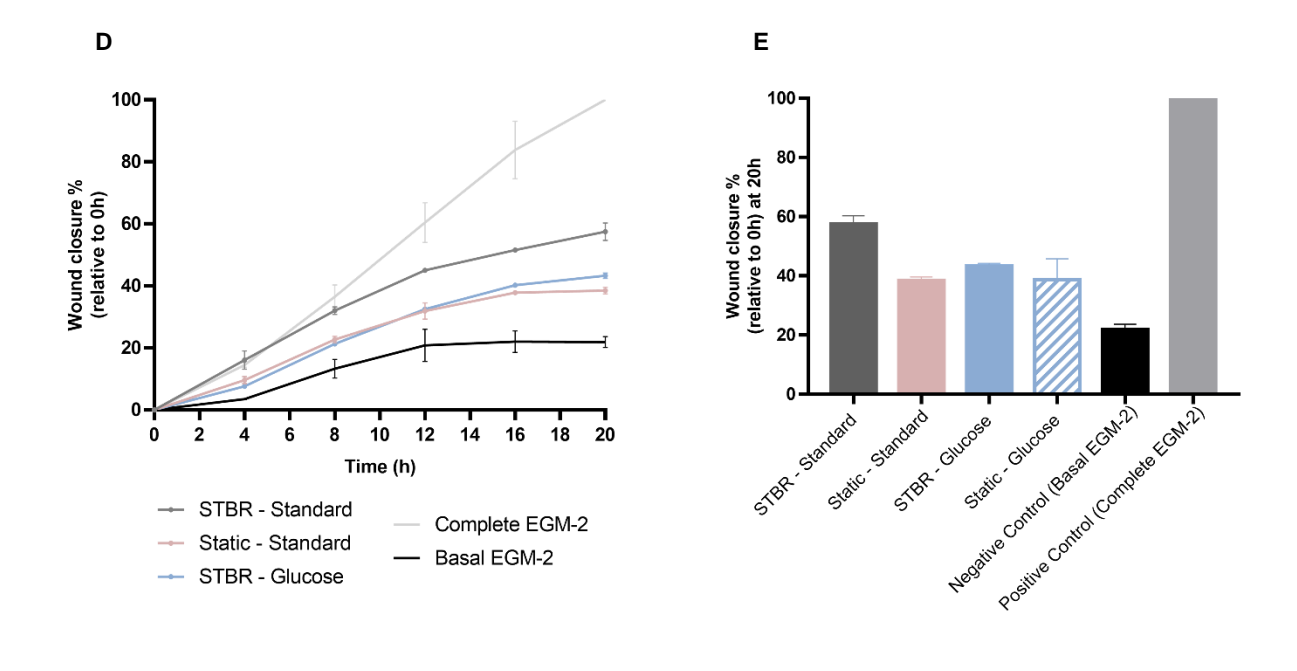


Figure 4.6: Functional analysis of EV biological activity after expansion in STBR – Standard, Static – Standard, STBR – Glucose and Static – Glucose, assessed by tube formation and wound healing assays. (A) Representative images of tube formation assay at 8h post seeding onto Matrigel. Scale bar = $200 \, \mu m$. (B) Quantification of tube formation assay parameters (number of nodes and total master segment length) with the ImageJ Angiogenesis Analyzer toolset. (C) Representative images of wound healing assay at 0h, 12h and 20h post-scratch. Scale bar = $200 \, \mu m$. (D) Percentage of wound closure increase throughout the 20h assay relative to initial wound area at 0h. (E) Percentage of wound closure at 20h post-scratch. Mean and standard deviation are based on 1 independent run.

4.1.2 Preconditioning hAT-MSC with miR-145-5p inhibitor and production of their derived EVs

miRNAs, a class of small RNAs, can interact with target mRNAs and affect their stability and translation, and thus can modulate gene expression of recipient cells. Their activity has been implicated in many diseases, including cardiovascular diseases [135,136]. Particularly, miR-145-5p is known as a tumor suppressor in several human cancers. MiR-145 is downregulated in these tumors and it has been reported that its overexpression inhibits tumor angiogenesis and growth, by mediating the expression of pro-angiogenic factors, such as VEGF and ANGPT2 [53,137]. These findings suggested that a possible regulatory pathway may exist in the pathological progress of myocardial infarction as well. Particularly, Arderiu *et al.* [55] reported that the angiogenic potential of MSCs could be modulated through control of miR-145 expression. In fact, downregulation of miR-145 promoted migration and tube-like formation of MSCs both *in vitro* and *in vivo*. Therefore, targeting miR-145 may be a promising strategy to increase the therapeutic efficiency of MSCs for the treatment of ischemic diseases. Thus, in the second part of this work, hAT-MSC were transfected with miR-145-5p inhibitor, in order to promote an augmented angiogenic response in hAT-MSC-derived EVs.

Prior to experiments in STBR, a 2D assay, in T75 flasks, was performed to assess the efficacy of the transfection protocol. hAT-MSC were seeded at a cell density of 40 000 cell/cm² and, 24h later, cells were transfected with 50 μ M miR-145-5p inhibitor, using Lipofectamine RNAiMAX. Cells were harvested 6h later and seeded in T-flasks. Subsequently, to evaluate cell concentration and viability, as well as miR-145-5p expression, T-flasks were harvested on days 1, 2, 4 and 7 of culture. Cell concentration and viability (Figure 4.7A), evaluated throughout culture, indicated that transfected cells were successfully expanded, showing an identical growth profile to the control cells (non-transfected), and high cell viability was maintained (\approx 90%). The efficiency of miRNA transfection was confirmed by RT-PCR on days 0 and 2 following transfection. Figure 4.7B shows that miR-145-5p inhibitor was successfully transfected into hAT-MSC, given the low expression of miR-145-5p in comparison to non-transfected cells.

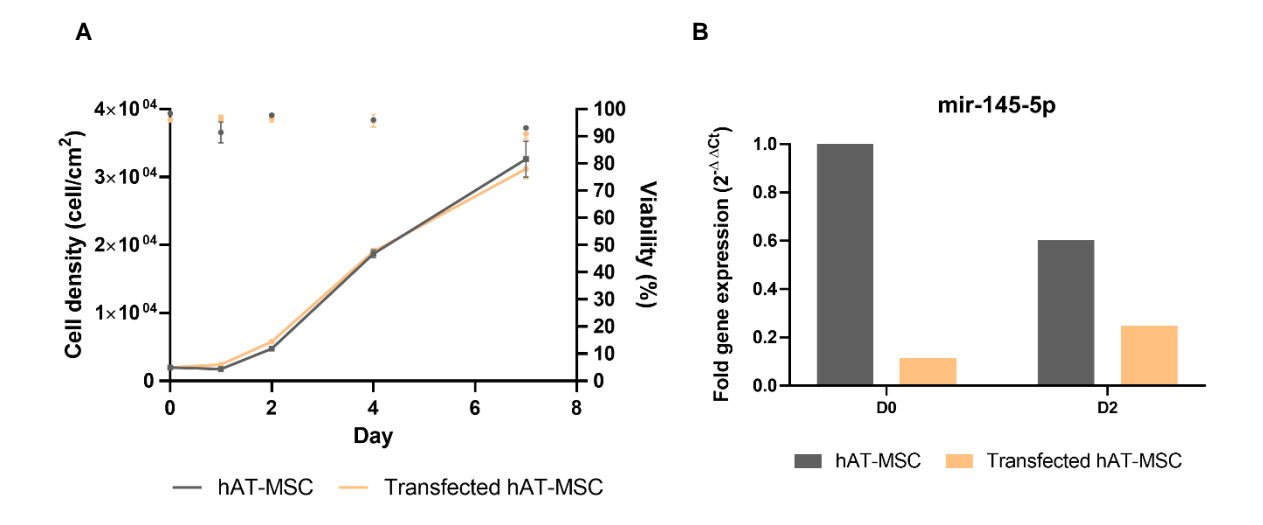
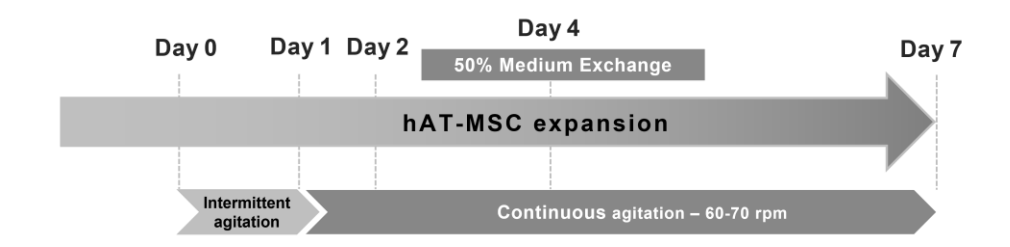
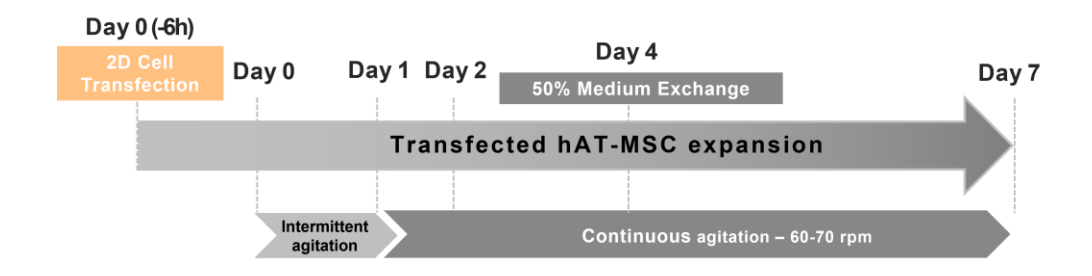


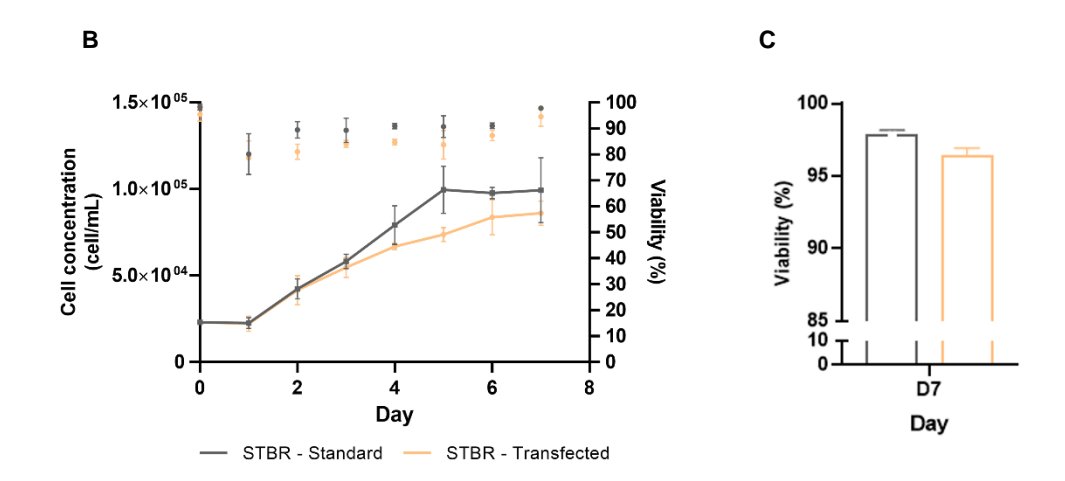
Figure 4.7: hAT-MSC and transfected hAT-MSC culture characterization after expansion in static conditions. (A) Growth curves and viability of hAT-MSCs and transfected hAT-MSCs during culture in T75 flasks. (B) Gene expression of mir-145-5p at day 0 and day 2 of cell expansion. Gene expression was quantified using the 2 -ΔΔCT method relatively to day 0 of culture (relative to non-transfected hAT-MSC).

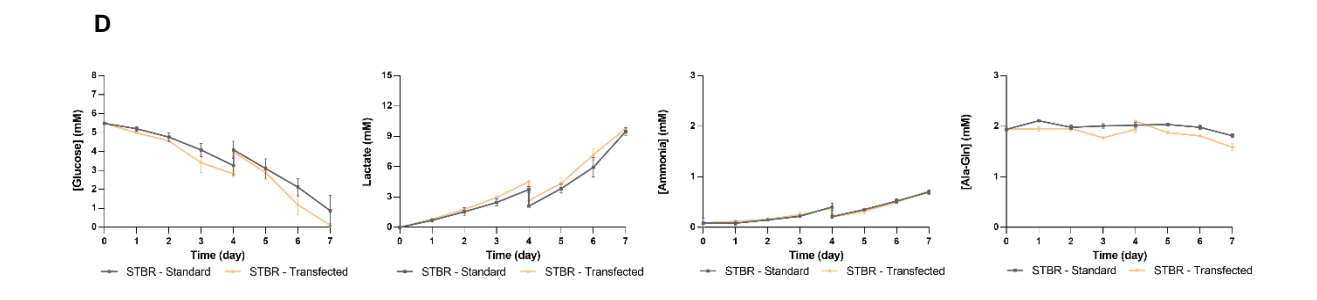
Once confirmed the efficiency of the transfection protocol, hAT-MSC and transfected hAT-MSC were inoculated in DASbox® mini stirred tank bioreactors (Figure 4.8A), as previously described. In Figure 4.8B, it is possible to observe that cells were able to successfully grow, reaching a final concentration of $(9.9 \pm 1.8) \times 10^4$ cell/mL for the non-transfected cells (STBR – Standard) and $(8.6 \pm 0.7) \times 10^4$ cell/mL for the transfected cells (STBR – Transfected). Although growth curves exhibit a slightly different profile, similar cell concentration and viability were obtained on day 7 of culture (Figure 4.8C). Additionally, the metabolite concentration profiles (Figure 4.8D), where both strategies exhibit similar consumption/production patterns, corroborate the efficiency of the cell expansion strategy implemented following transfection with miR-145-5p inhibitor. Importantly, in both cases, lactate and ammonia levels were kept below inhibitory values (lactate: 35.4 mM, ammonia: 2.4 mM - inhibitory levels reported for human BM-MSCs) [124]) throughout the entire culture in both bioreactors.











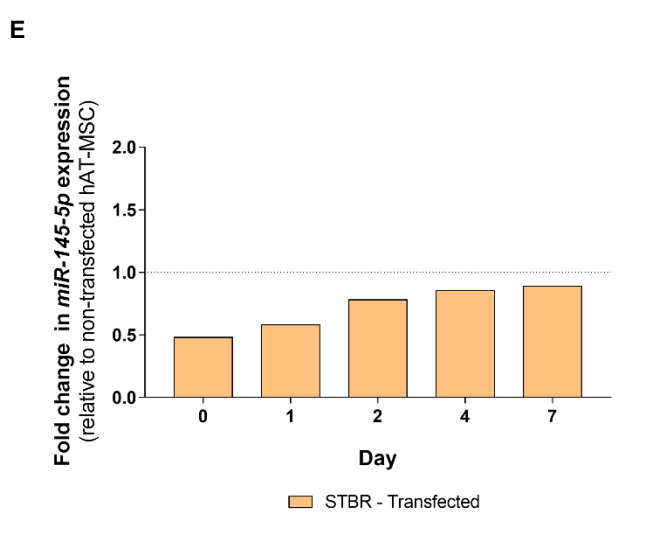
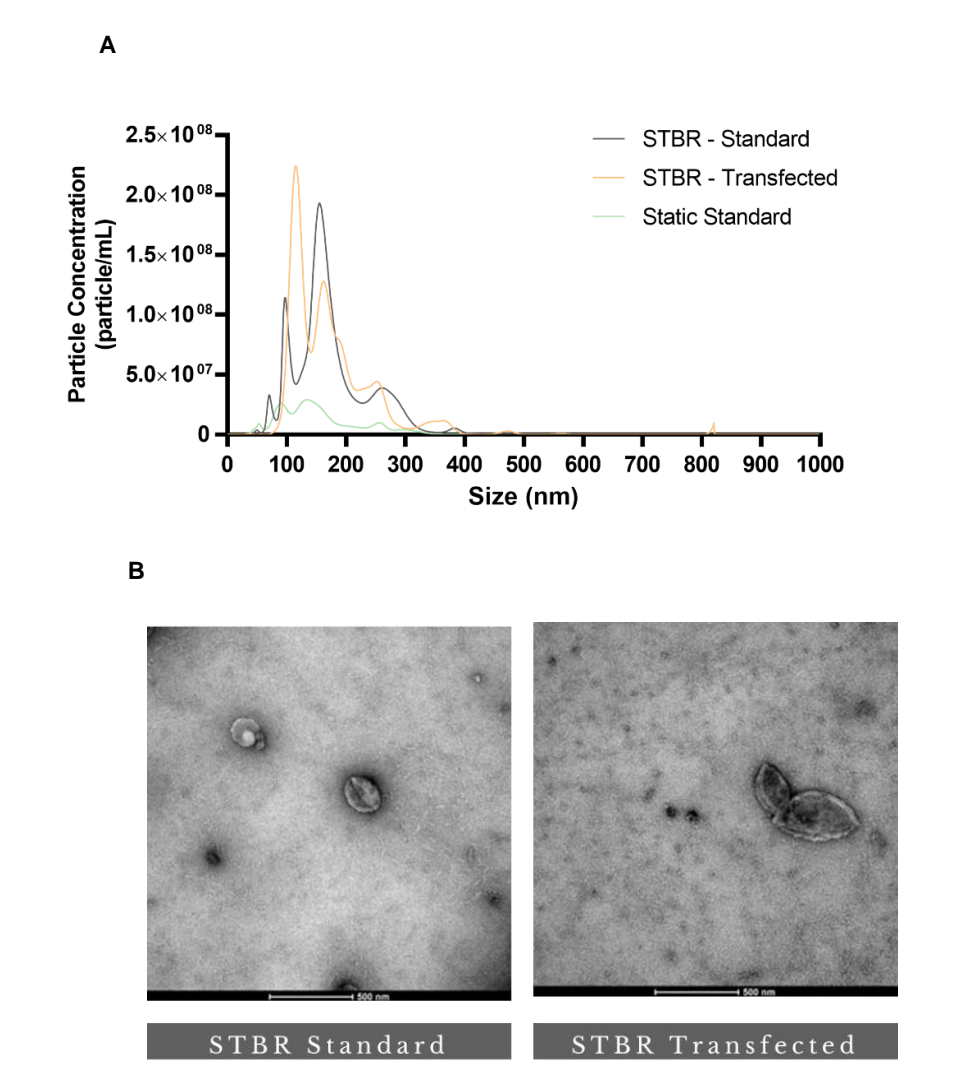


Figure 4.8: hAT-MSC and transfected hAT-MSC culture characterization after STBR expansion. (A) Schematic representation of the expansion protocol in STBR – Standard and STBR - Transfected. (B) Growth curves and viability. (C) Cell viability on the harvest day (day 7). (D) Metabolite concentration profiles throughout STBR culture. (E) Gene expression of mir-145-5p throughout 7 days of culture. Gene expression was quantified using the 2 - AACT method relatively to the respective day of culture (relative to non-transfected hAT-MSC). Mean and standard deviation are based on 4 independent runs.

Due to the fast loss of miR-145-5p inhibitory effect in transfected cells (Figure 4.8E), only CCM collected on day 4 of culture was considered to evaluate EV yields and potency. For that purpose, CCM was processed using TFF followed by SEC. SEC fractions 2-4 were pooled and submitted to an additional concentration step using Amicon-2 10kDa centrifugal filter units, where samples were centrifuged at 4000 g for 20 minutes followed by a spin down step for 2 minutes at 1000 g. Size distribution profiles were similar to the ones obtained with non-pooled fractions as reported in section 4.1.1 (Figure 4.9A) and no substantial differences were observed in mean particle size (170.4 \pm 15.6 nm, 162.9 \pm 32.89 nm and 157.2 \pm 19.9 nm for STBR - Standard, STBR - Transfected and Static - Standard, respectively). Additionally, TEM results indicate that EVs retained their typical morphology (Figure 4.9B). Results regarding the expression of EV specific surface markers (analyzed by bead-based flow cytometry) showed an overall high expression of CD81, CD63 and CD9 (values ranging from 58.6-97.2%) (Figure 4.9C).



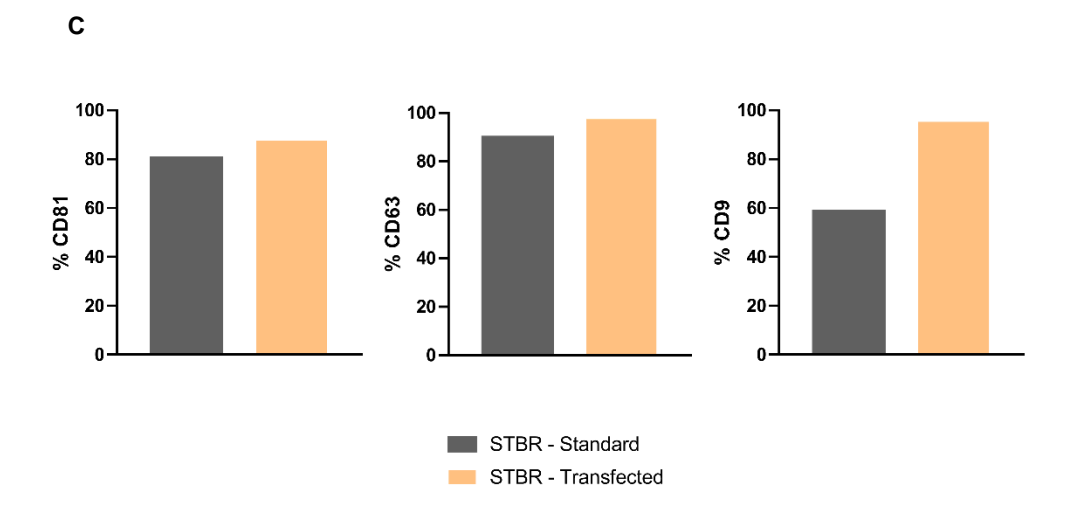


Figure 4.9: Characterization of hAT-MSC-derived EVs obtained from STBR - Standard, Static - Standard and STBR - Transfected at day 4 of culture. (A) Representative size distribution profiles of hAT-MSC-derived EVs in pooled SEC fraction analyzed by NTA. (B) Representative TEM images of hAT-MSC-derived EV samples. Scale bar = 500 nm. (C) Bead-based flow cytometric analysis of EV surface markers CD81, CD63 and CD9 following EV production in STBR - Standard and STBR - Transfected conditions.

Looking across the calculated EV yields (Figure 4.10), results on EV concentration were 6.9 (±0.1) x10⁸ particle/mL, 8.8 (±0.6) x10⁸ particle/mL and 3.0 (±1.8) x10⁸ particle/mL for STBR – Standard, STBR – Transfected and Static – Standard, respectively. Regarding EV productivity, 1.2 (±0.2) x10¹⁰ particle/10⁶ cell for STBR – Standard and 1.52 (±0.3) x10¹⁰ particle/10⁶ cell for STBR – Transfected were obtained. A side-by-side comparison between transfected and non-transfected cells shows an overall increase in EV productivity and concentration in STBR culture (~1.3-fold increase) and in static culture (~3.0-fold increase; *p*=0.0046). Since miRNAs have multiple target genes, it is possible that miR-145 could target mRNA molecules that affect EV biogenesis leading to a decrease in EV release. In fact, it has been reported that miR-145 has tumor metastasis suppression effects by direct destabilization of Rab27a mRNA [52,138]. Rab27a is part of a family of Ras-related small GTPases and it is involved in intracellular transport pathways, *i.e.*, EV production or release. Indeed, it has been reported that silencing Rab27a reduces the amount of EVs released [139]. However, in order to confirm this hypothesis further gene expression assays need to be performed.

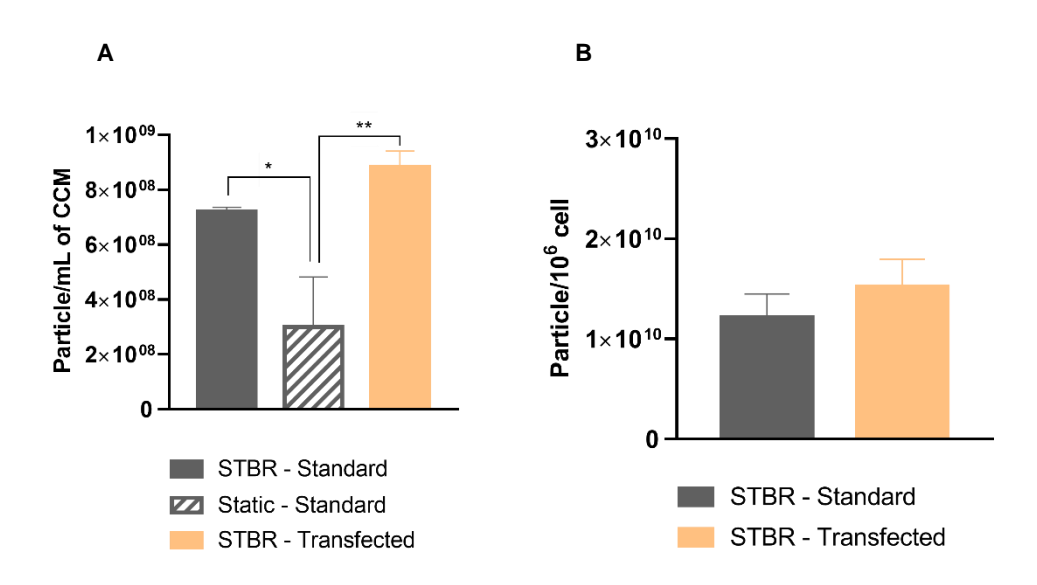


Figure 4.10: EV production yields obtained in STBR - Standard, Static - Standard and STBR - Transfected at day 4 of culture. (A) EV concentration (particle/mL of CCM). (B) EV productivity (particle/10⁶ cell). Mean and standard deviation are based on 2 independent runs for STBR - Standard and Static - Standard and 3 independent runs for STBR - Transfected. * p<0.05, ** p<0.01, determined by two-way ANOVA followed by Tukey's test.

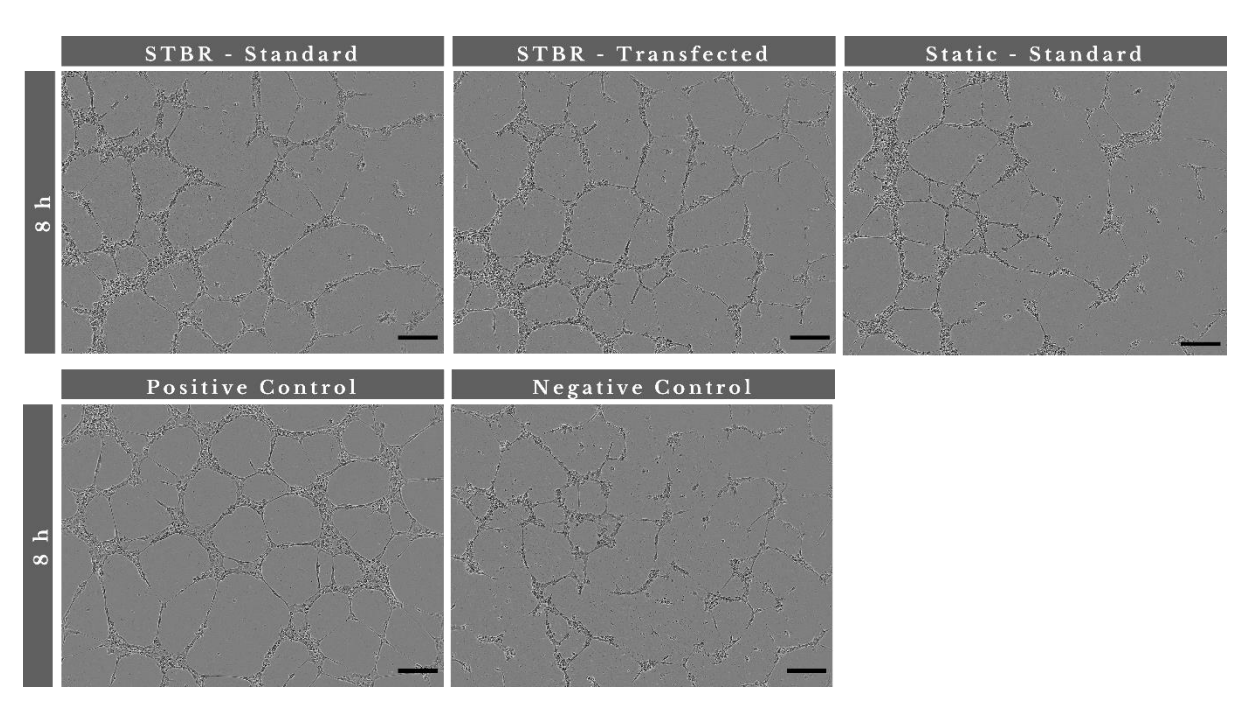
The main goal of this task was to evaluate whether miR-145-5p inhibitor transfection could have an effect on hAT-MSC-derived EV's pro-angiogenic activity. Therefore, the capacity of HUVECs to form a network of tube-like structures following exposure to EVs derived from transfected and non-transfected hAT-MSC was evaluated by tube formation assay. Additionally, the effect of EVs on HUVECs migration capacity was quantified by wound healing assay.

Analysis of the ability of hAT-MSC-derived EVs to promote capillary-like tube formation showed that the number of nodes increased from 269 \pm 22 in STBR - Standard and 297 \pm 6 in Static - Standard up to 344 \pm 25 in STBR - Transfected while the total master segment length increased from 8051 \pm 630 in STBR - Standard and 7924 \pm 609 in Static - Standard up to 10461 \pm 1469 in STBR - Transfected (Figure 4.11A-B). These data are in line with the results obtained for the wound healing assay (Figure

4.11C-E). In fact, cell's ability to migrate into the scratch wound was enhanced after treatment with transfected hAT-MSC-derived EVs when comparing to cells treated with non-transfected hAT-MSC-derived EVs, with a wound closure percentage at 20h of 49.3 ± 9.4%.

Overall, our results showed that transfection with miR-145-5p inhibitor promoted an augmented angiogenic response of hAT-MSC-derived EVs, although without statistical differences. In fact, miR-145 has been previously shown to have an inhibitory role in tumor angiogenesis and growth, through targeting the expression of angiogenic factors, such as VEGF [53]. A previous study by Climent *et al.* [140] reported that miR-145 is capable of regulating angiogenesis by reducing the ability of HUVECs to form capillary-like structures and decreasing their proliferation index, through direct targeting of hexokinase II (HKII) and integrin β8 genes. Moreover, Arderiu *et al.* [55] reported for the first time that the angiogenic potential of MSCs could be modulated through control of miR-145 expression. They identified ETS1 (v-ets avian erythroblastosis virus E26 oncogene homolog 1) as direct target of miR-145 in MSCs. ETS1 expression is induced in endothelial cells by pro-angiogenic growth factors (such as FGF-2 and VEGF) and it has been described as a principal regulator that converts endothelial cells to their angiogenic phenotype, by regulating the expression of matrix metalloproteinases (MMP-1, MMP-3, and MMP-9) and integrin β3 [141].

Α



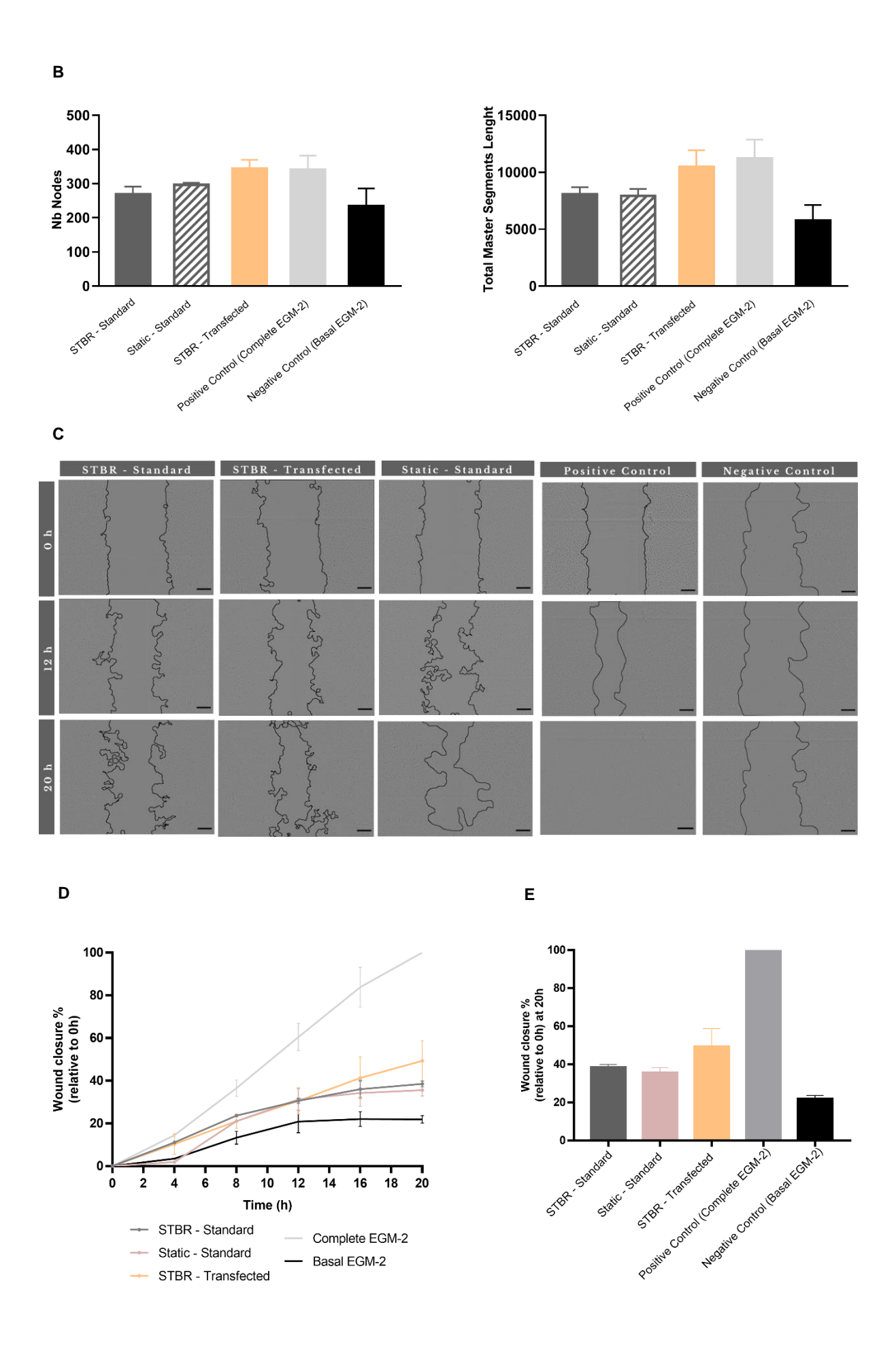


Figure 4.11: Functional analysis of EV biological activity after expansion for 4 days in STBR – Standard, Static – Standard and STBR – Transfected, assessed by tube formation and wound healing assays. (A) Representative images of tube formation assay at 8h post seeding onto Matrigel. Scale bar = $200 \mu m$. (B) Quantification of tube formation assay parameters (number of nodes and total master segment length) with the ImageJ Angiogenesis Analyzer toolset. (C) Representative images of wound healing assay at 0h, 12h and 20h post-scratch. Scale bar = $200 \mu m$. (D) Percentage of wound closure increase throughout the 20h assay relative to initial wound area at 0h. (E) Percentage of wound closure at 20h post-scratch. Mean and standard deviation presented are based on 1 independent run.

4.2 Production of gmMSC and gmMSC-derived EVs in microcarrier-supported stirred-tank bioreactors

In addition to metabolic and miRNA preconditioning strategies, the therapeutic properties of MSCs and their derived EVs may be enhanced through long-term and stable expression of specific factors following cell genetic modification. Based on the beneficial effects reported in MI models, several authors have been introducing different factors in MSC, such as Akt, bFGF (basic fibroblast growth factor), VEGF, GATA-4 (GATA binding protein 4) and HGF (hepatocyte growth factor) [51,107,112,142].

In this work, we used MSCs genetically modified with a lentiviral vector expressing factors involved in cell response to ischemic cardiomyopathy, in particular FGF-2 and apelin. Apelin is a ligand for the G-protein-coupled receptor, APJ, that is expressed by myocardial cells and some vascular smooth cells. The apelin and APJ constitute a signaling pathway that has been reported to have multiple cardiac and vascular functions. Particularly, several authors have demonstrated that apelin-induced effects include reduced infarct size [143] and ameliorated myocardial contractile function [144]. On the other hand, FGF-2 is known to regulate numerous cellular functions, such as cell proliferation, survival, migration and apoptosis, and processes such as wound healing, tumorigenesis, angiogenesis, vasculogenesis and blood vessel remodeling [145]. Its role in myocardial infarct repair has also been studied. Particularly, overexpression of FGF-2 in mice have resulted in increased fibroblast proliferation and collagen deposition, increased endothelial proliferation, and enhanced cardiomyocyte hypertrophy, ultimately limiting infarct expansion and preserving left ventricular function [146].

gmMSC were expanded in DASbox® mini stirred tank bioreactors (Figure 4.12A-B), using the same protocol described in section 4.1, with final cell concentrations at day 7 of (8.2 ± 0.3) x10⁴ cell/mL for STBR - Standard and (5.2 ± 0.6) x10⁴ cell/mL for STBR - gmMSC. Throughout cell culture in STBR, although gmMSC generally presented lower cell viability levels compared to non-gmMSC, following cell harvest, both conditions presented similar cell viability ($\approx 97\%$). Metabolite concentration profiles correlate with the growth curves as increased cell numbers resulted in higher concentrations of lactate and ammonia and increased glucose consumption during the 7 days of cell culture and supports the lower cell concentrations obtained in STBR – gmMSC in comparison to STBR – Standard. Neither ammonia nor lactate concentration have reached cell growth inhibitory levels (Figure 4.12C).

The lentiviral transgene mRNA expression levels of gmMSC were evaluated by ddPCR. To achieve ddPCR data with well-defined positive droplets, an optimization assay for adjustment of the annealing/extension temperature was performed. A temperature gradient from 50 to 59.3°C was tested and the optimal annealing/extension temperature was obtained at 53°C (Figure 4.12D). After this, lentiviral transgene mRNA expression levels were assessed on the inoculation day (D0) and following 7 days of cell expansion (D7), evidencing that gmMSC maintained the lentiviral transgene mRNA expression (Figure 4.12E).

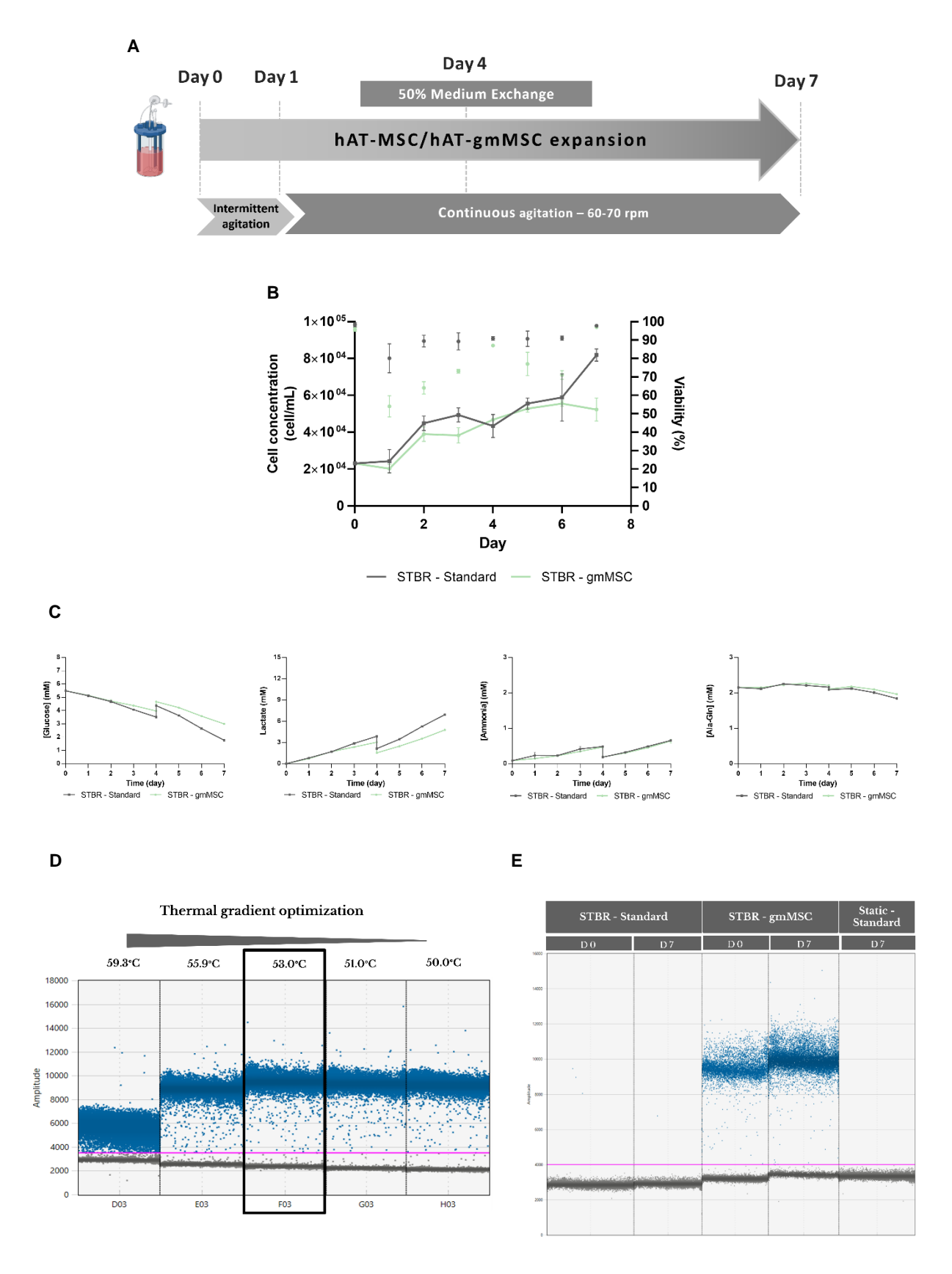


Figure 4.11: hAT-MSC and gmMSC culture characterization after STBR expansion. (A) Schematic representation of the expansion protocol. **(B)** Growth curves and viability. **(C)** Metabolite concentration profiles throughout STBR culture. **(D)** ddPCR thermal gradient optimization to select optimal annealing temperature - 53°C. **(E)** Lentiviral transgene mRNA expression levels at days 0 and 7 of culture. Mean and standard deviation are based on 1 independent run.

To further evaluate EV production and bioactivity, the CCM collected on day 7 of culture from both 2D and STBR culture systems was processed by TFF followed by SEC. NTA was conducted across the three SEC selected fractions to evaluate particle concentration and size distribution. Average particle size (Figure 4.13A) showed similar mean sizes between each condition and within the 100-300 nm size range. Furthermore, TEM images showed that EVs retained their typical cup-shaped morphology (Figure 4.13B). Finally, EV specific surface markers such as CD81, CD63 and CD9 were assessed by bead-based flow cytometry (Figure 4.13C). Overall, high expression of these characteristic markers was detected (values ranging from 58.6-99.7%).

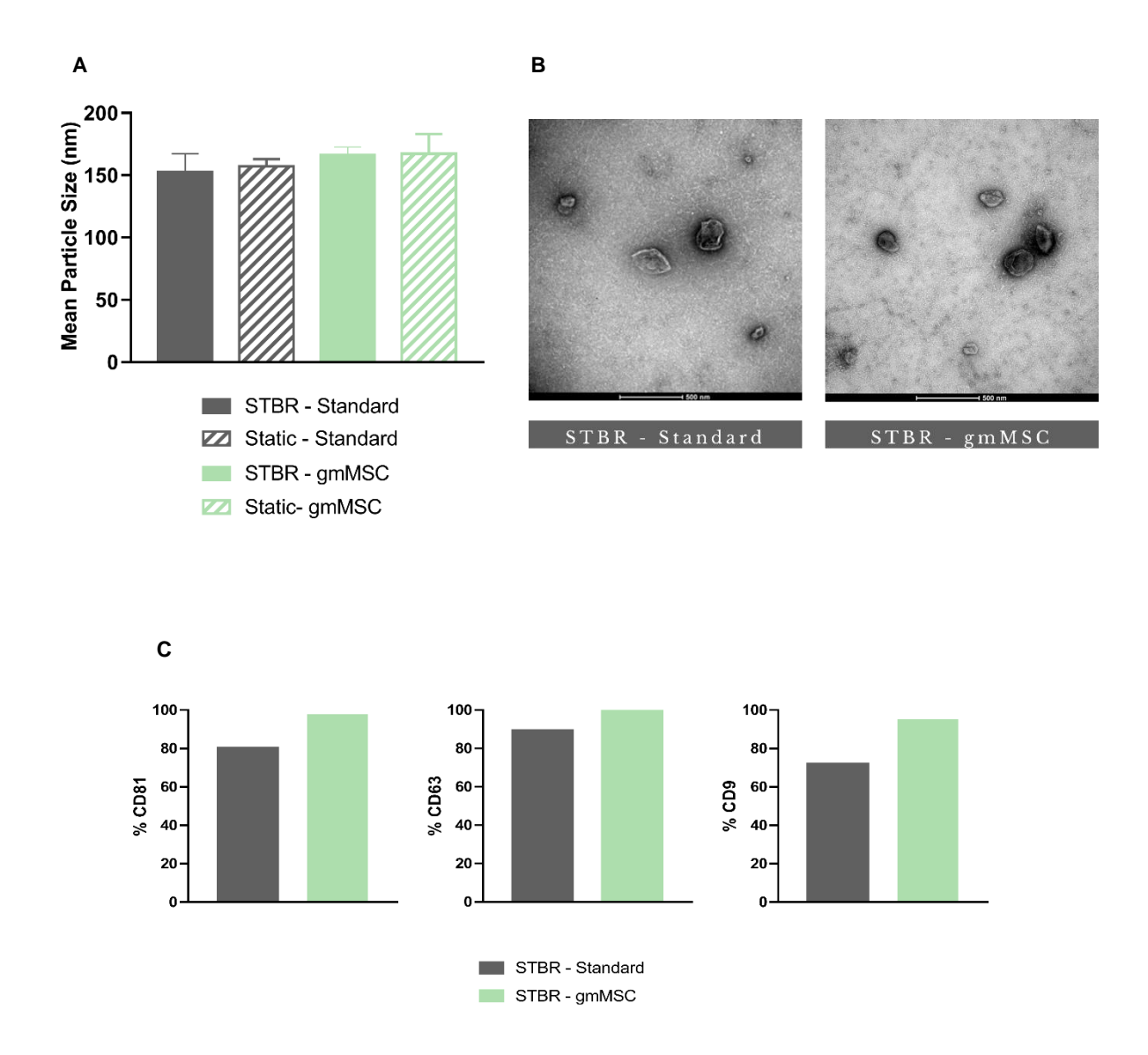


Figure 4.13: Characterization of hAT-MSC-derived EVs obtained from STBR - Standard, Static - Standard, STBR - gmMSC and Static - gmMSC at day 7 of culture. (A) Mean sizes of hAT-MSC-derived EVs in SEC fractions 2-4 analyzed by NTA. (B) TEM images of hAT-MSC-derived EV samples. Scale bar = 500 nm. (C) Beadbased flow cytometric analysis of EV surface markers CD81, CD63 and CD9 following EV production in STBR - Standard and STBR - gmMSC.

Total particle counts determined by NTA were used to calculate EV recovery yields (Figure 4.14A and B). Results show an overall increase in EV concentration and productivity in STBR – gmMSC relatively to STBR – Standard (1.2- and 1.8-fold increase, respectively). Although the mechanisms behind this increase were not studied, one possible hypothesis might be associated with the overexpression of FGF-2. Although its effects rely mainly on its pro-angiogenic activity, FGF-2 can also have an impact on EV biogenesis/release. Particularly, a recent study showed that neuronal cells treated with FGF showed increased release of EVs, by affecting the molecular machinery required for vesicle fusion to the plasma membrane [147]. Specifically, proteomic analysis of FGF-treated neuronal EVs demonstrated an increase in SNARE proteins concentration. Furthermore, in other study, Javidi-Sharifi *et al.* [148] showed that activation of FGF2-FGFR1 signaling (FGF-2 and its receptor) promoted BM-MSC's EV release. However, the same tendency was not observed in Static conditions (results on Static – Standard were 5.9x10⁸ particle/mL and 3.6x10⁹ particle/10⁶ cell, and 4.8x10⁸ particle/mL and 2.9x10⁹ particle/10⁶ cell on Static – gmMSC).

To assess if gmMSC-derived EVs present the ability to induce angiogenesis, HUVECs were treated with gmMSC-derived EVs from both static and STBR culture systems. Regarding the tube formation assay (Figure 4.15A and B), the number of nodes increased from 202 ± 35 in the Negative Control (Basal EGM™-2) up to 245 ± 42 and 219 ± 64 in STBR - gmMSC and Static - gmMSC conditions, respectively. Regarding the total master segment length data, an increase from 5889 ± 755 in Negative Control (Basal EGM™-2) up to 7631 ± 153 and 5669 ± 2333 in STBR - gmMSC and Static gmMSC conditions, respectively, was observed. We subsequently investigated whether the gmMSCderived EVs could promote the migratory activity of HUVECs following HUVECs treatment with 6000 particles/cell. As seen in Figure 4.15C and 4.15D, after 20h of treatment, gmMSC-derived EVs have promoted wound closure of 44.9 ± 1.1% and 50.3 ± 3.3% for STBR - gmMSC and Static - gmMSC. respectively. In fact, previous studies have reported that both FGF-2 and apelin have pro-angiogenic functions. A study demonstrated that FGF-2 induces VEGF expression in endothelial cells [149]. In turn, VEGF binds to tyrosine kinase receptors on the surface of endothelial cells and promotes their proliferation and migration, initiating the angiogenesis process. Moreover, in another study, FGF-2 geneticallymodified MSCs showed increased expression and secretion of angiogenesis-related factors, such as VEGF, FGF-2, and TGF-β. CCM derived from expansion of these cells promoted migration of HUVECs and increased their vascular network formation capacity [150]. On the other hand, apelin can also promote proliferation, migration and tube formation in endothelial cells. For instance, Kunduzova et al. demonstrated that apelin dose-dependently induces a pro-angiogenic response in HUVECs, through activation of APJ pathway [151]. Thus, we can propose that FGF-2 and apelin can contribute to the promigratory effect of gmMSC-derived EVs on HUVECs. However, further experiments should focus on dissecting the transcriptome and proteome of released EVs in order to compare them across the different conditions and further understand their effects, while performing comparative assays with non-genetically modified hAT-MSCs.

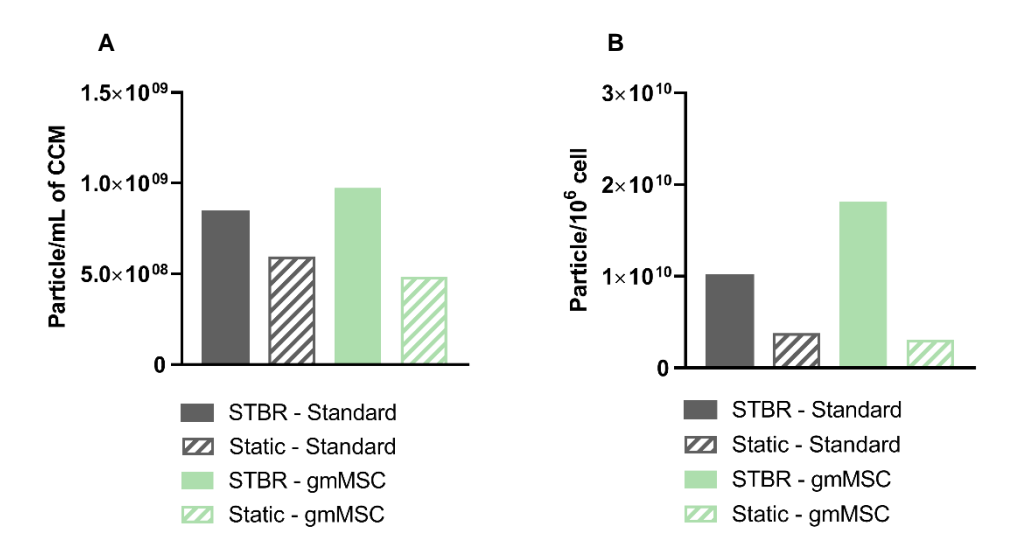
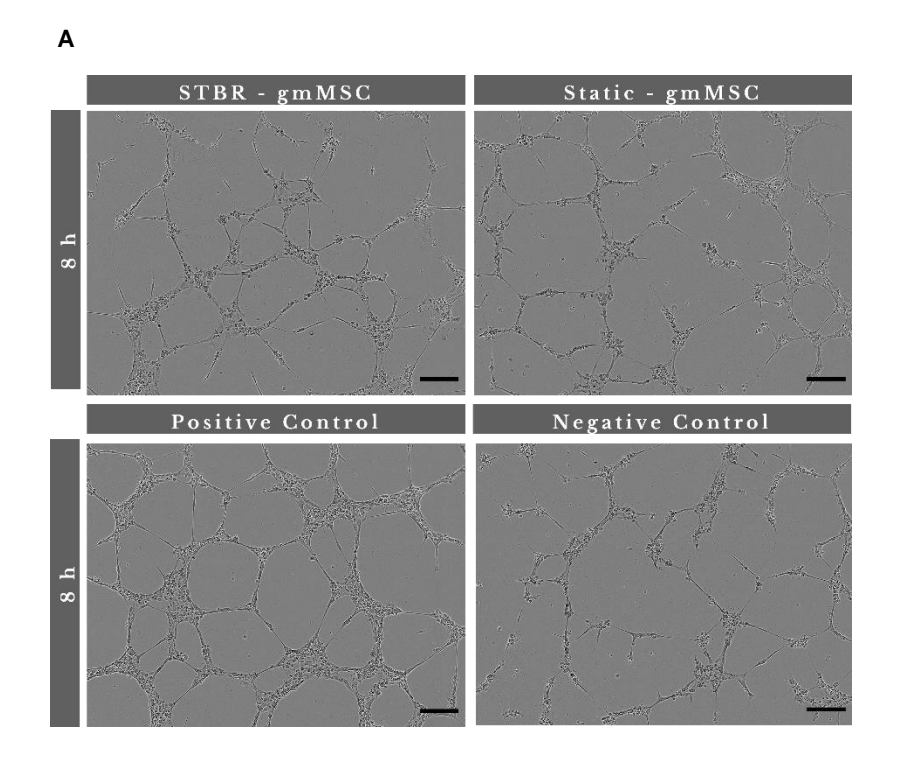
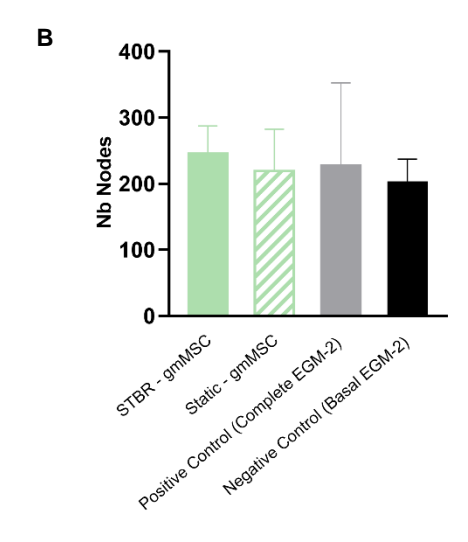
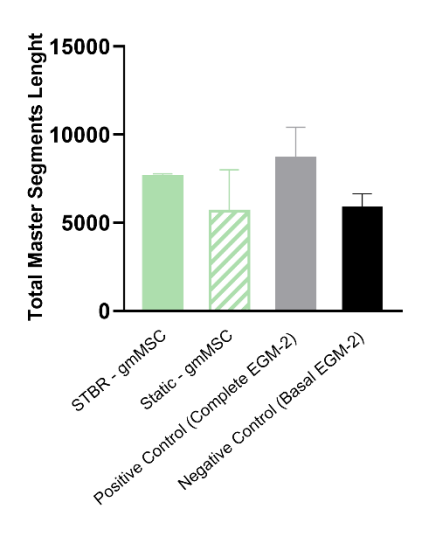


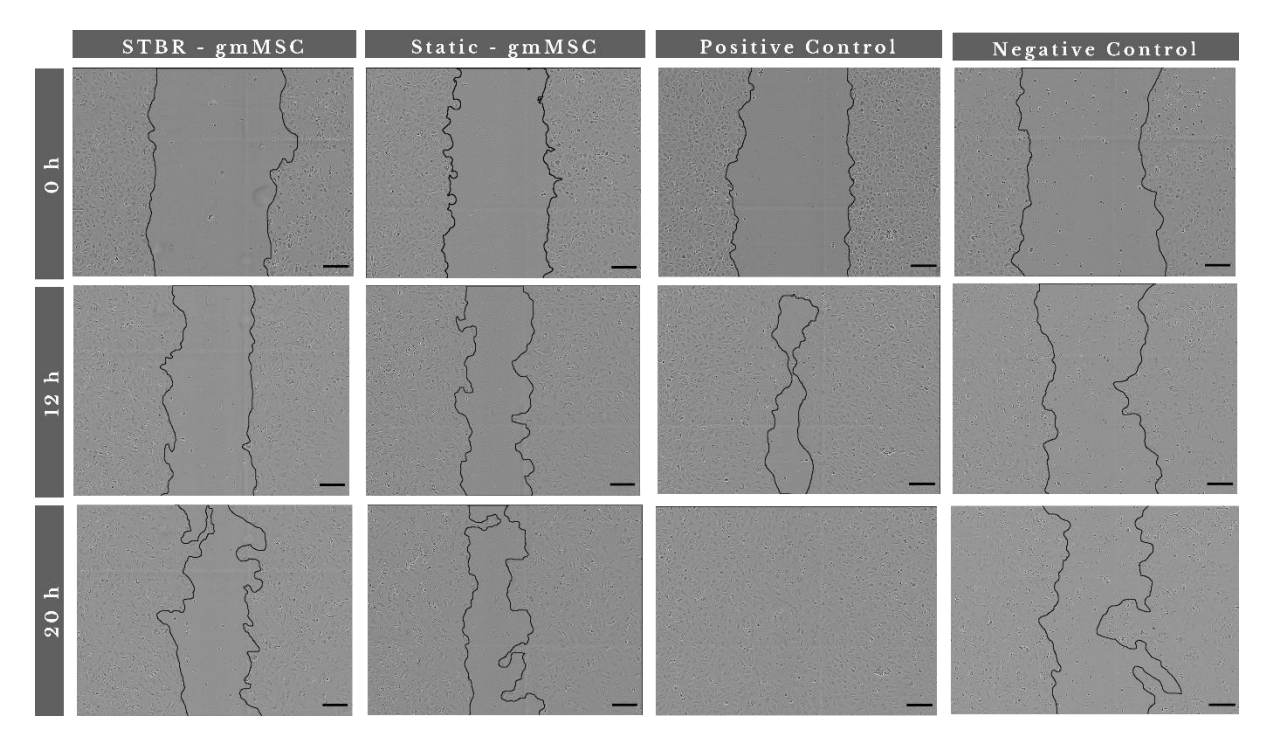
Figure 4.14: EV production yields obtained in STBR - Standard, Static Standard, STBR - gmMSC and Static - gmMSC at day 7 of culture. (A) EV concentration (particle/mL of CCM). (B) EV productivity (particle/10⁶ cell).







С



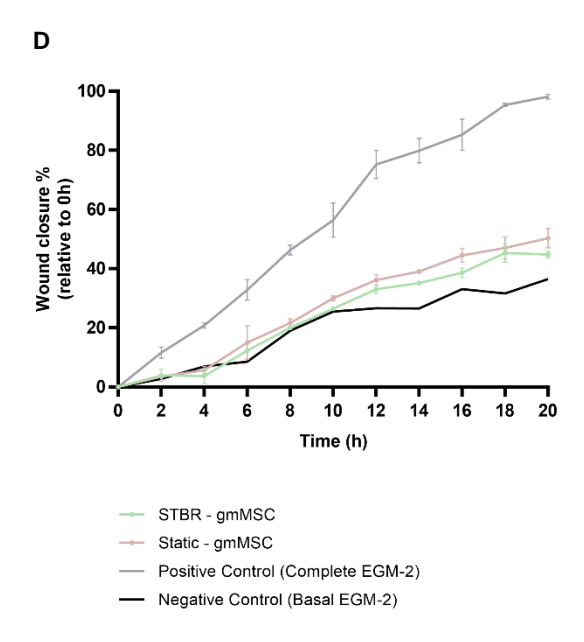


Figure 4.15: Functional analysis of EV biological activity after expansion in STBR – gmMSC and Static – gmMSC, assessed by tube formation and wound healing assays. (A) Representative images of tube formation assay at 8h post seeding onto Matrigel. Scale bar = $200 \mu m$. (B) Quantification of tube formation assay parameters (number of nodes and total master segment length) with the ImageJ Angiogenesis Analyzer toolset. (C) Representative images of wound healing assay at 0h, 12h and 20h post-scratch. Scale bar = $200 \mu m$ (D) Percentage of wound closure increase throughout the 20h assay relative to initial wound area at 0h. Mean and standard deviation present are based on 1 independent run.

5. Conclusions and Future Work

In this thesis, different strategies for manufacturing MSC-derived EVs with increased cardiac regenerative potential while maximizing EV secretion yields were explored, particularly, MSC metabolic and miRNA preconditioning and genetic modification, while implementing a scalable bioprocess for hAT-MSC-derived EV manufacturing.

Growing evidence suggests that cell secretion of paracrine factors, namely EVs, have a relevant role in the clinically-relevant properties attributed to cell-based therapies for cardiac regeneration. Becoming aware of EV's paracrine-mediated effects, along with the drawbacks associated with cell-based therapies, has led to a shift in clinical focus from cell-based to cell-free approaches. Furthermore, different strategies involving cell preconditioning and genetic modification for the modulation of EV's cardiac therapeutic potential and/or enhancing EV secretion yields have been experimentally tested in numerous studies with promising results [82,101,106,107,110].

A chemically-defined culture system for expansion of hAT-MSCs and manufacture of their derived EVs in microcarrier-supported STBR was implemented under hypoxic conditions. Cells cultured in STBR following different strategies (standard condition, daily glucose supplementation, transfected cells and genetically modified MSC) were successfully expanded, exhibiting high cell viability (\geq 95%) on the harvest day. Identical growth profiles and expansion ratios (\simeq 4-5-fold) were obtained, except for the STBR – gmMSC strategy (\simeq 2-fold). Furthermore, both cell immunophenotype and trilineage differentiation potential were determined before and after cell expansion confirming that hAT-MSCs, transfected hAT-MSC and gmMSC maintained their quality attributes.

EVs were isolated by TFF followed by SEC, two cGMP-compatible technologies that allow to achieve high EV yields and purity levels [125]. Particle characterization by NTA provided information regarding EV production capacity for each strategy and further characterization by bead-based flow cytometry, microBCA and TEM showed that EVs maintained their characteristic attributes and absence of protein contamination.

The ability of hAT-MSCs to secrete EVs showed an increase in both EV productivity (1.4-fold increase) and EV concentration (1.2-fold increase) when MSCs are cultured at low glucose concentration levels in STBR, showing the importance of standardizing cell culture conditions and, particularly, controlling metabolites concentration to develop more robust platforms for EV production. Nevertheless, in the future, to further maximize cell growth and EV production, another strategy could be explored. For instance, glucose supplementation pulses could be added daily and, after cells reach stationary growth and the maximum cell concentration is achieved, a complete medium exchange could be performed with a glucose-deprived cultured medium to boost EV release.

Additionally, we have shown that transfection with miR-145-5p inhibitor can also constitute an approach to achieve higher EV yields (1.3-fold increase). Finally, EV isolation from gmMSC transduced with a lentivector co-expressing apelin and FGF2 (gmMSC) rendered increased EV productivity and concentration levels (1.8- and 1.2-fold increase, respectively), although additional biological replicates should be included to corroborate these findings.

Taken into consideration the clinical translation of EVs as possible therapies, maximizing EV production is of extreme importance because, similarly to the context of cell therapies, where great cell numbers per dose are required, predictors indicate that large quantities of EVs will be needed for clinical use, with estimated numbers per patient ranging from 10¹⁰ to 10¹⁴ particles per dose [152]. Although dose required is highly variable, depending on both the therapeutic target and the delivery method.

Furthermore, since the clinical applicability of these EVs depends on their bioactivity, their therapeutic potential was assessed through *in vitro* functional assays using HUVECs, to study their tube formation and wound healing capacity. Overall, EV samples from the different strategies showed tube formation and wound healing ability, highlighting their promising cardiac therapeutic potential. In particular, EVs obtained from MSCs cultured in STBR under glucose starvation and from MSC transfected with miR-145-5p inhibitor promoted cell migration and stimulated angiogenesis to a higher extent in comparison with EVs obtained from glucose supplemented and non-transfected MSCs. Future work should focus on implementing cellular uptake assays of EVs to better investigate the mechanism of action of the EV populations. Moreover, comparative proteomic and RNA-seq analyses must be performed in order to gain insight into the specific signals directed to the cells that are responsible for the angiogenic potential of the EVs manufactured following the different strategies. In addition, to evaluate other cardioprotective effects of EVs rather than angiogenesis and cell migration, other cell-based functional assays may be performed to determine their effects on cell proliferation, apoptosis, inflammatory regulation and fibrosis.

EV storage is another parameter that may affect EV's characteristics, including its stability, number, aggregation and functionality [153]. Currently, EVs are stored for long periods of time at -80°C and at 4°C for short periods of time. However, the impact of storage conditions is not consensual in the scientific community. Ultimately, these knowledge gaps may hold back the widespread applicability of EVs [154] and highlight the importance of standardizing EV bioprocessing parameters to facilitate their clinical translation. So, in the future, the impact of storing at different temperatures, such as 4°C, -20°C and -80°C, should be assessed by quantifying particle numbers, protein and miRNA content, and their potency at different times during storage.

Lastly, bioengineering approaches can also be explored to accelerate clinical translation of safe and effective EV-based therapeutics. Particularly, several groups have been developing efficient systems to enable non-invasive implantation and a sustained release and gradual delivery to maximize their regenerative capacity [155–157]. Modifications of EV and their producing cells have also been explored in order to control biodistribution and specific cell targeting [152].

6. Bibliography

- 1. Mensah, G. A., Roth, G. A. & Fuster, V. The Global Burden of Cardiovascular Diseases and Risk Factors: 2020 and Beyond. *J. Am. Coll. Cardiol.* **74**, 2529–2532 (2019).
- 2. Heidenreich, P. A. *et al.* Forecasting the future of cardiovascular disease in the United States: a policy statement from the American Heart Association. *Circulation* **123**, 933–944 (2011).
- 3. Buttar, H. S., Li, T. & Ravi, N. Prevention of cardiovascular diseases: Role of exercise, dietary interventions, obesity and smoking cessation. *Exp. Clin. Cardiol.* **10**, 229–249 (2005).
- 4. Gupta, R. & Losordo, D. W. Challenges in the translation of cardiovascular cell therapy. *J. Nucl. Med.* **51**, 122–127 (2010).
- 5. Sebastião, M. J. *et al.* Bioreactor-based 3D human myocardial ischemia/reperfusion in vitro model: a novel tool to unveil key paracrine factors upon acute myocardial infarction. *Transl. Res.* **215**, 57–74 (2020).
- 6. Le, T. & Chong, J. Cardiac progenitor cells for heart repair. Cell Death Discov. 2, 2–5 (2016).
- 7. Cohn, J. N., Ferrari, R. & Sharpe, N. Cardiac remodeling-concepts and clinical implications: A consensus paper from an International Forum on Cardiac Remodeling. *J. Am. Coll. Cardiol.* **35**, 569–582 (2000).
- 8. Hashimoto, H., Olson, E. N. & Bassel-Duby, R. Therapeutic approaches for cardiac regeneration and repair. *Nat. Rev. Cardiol.* **15**, 585–600 (2018).
- 9. Menasché, P. Cell therapy trials for heart regeneration lessons learned and future directions. *Nat. Rev. Cardiol.* **15**, 659–671 (2018).
- Hassan, N., Tchao, J. & Tobita, K. Concise Review: Skeletal Muscle Stem Cells and Cardiac Lineage: Potential for Heart Repair. Stem Cells Transl. Med. 3, 183–193 (2014).
- 11. Jain, M. *et al.* Cell therapy attenuates deleterious ventricular remodeling and improves cardiac performance after myocardial infarction. *Circulation* **103**, 1920–1927 (2001).
- 12. Menasché, P. *et al.* The myoblast autologous grafting in ischemic cardiomyopathy (MAGIC) trial: First randomized placebo-controlled study of myoblast transplantation. *Circulation* **117**, 1189–1200 (2008).
- 13. Bolli, R. *et al.* Cardiac stem cells in patients with ischaemic cardiomyopathy (SCIPIO): Initial results of a randomised phase 1 trial. *Lancet* **378**, 1847–1857 (2011).
- 14. Van Berlo, J. H. *et al.* C-kit+ cells minimally contribute cardiomyocytes to the heart. *Nature* **509**, 337–341 (2014).
- Bolli, R., Tang, X. L., Guo, Y. & Li, Q. After the storm: An objective appraisal of the efficacy of c-kit+ cardiac progenitor cells in preclinical models of heart disease. *Can. J. Physiol. Pharmacol.* 99, 129–139 (2021).
- 16. Malliaras, K. et al. Intracoronary cardiosphere-derived cells after myocardial infarction: Evidence of therapeutic regeneration in the final 1-year results of the CADUCEUS trial (Cardiosphere-derived aUtologous stem CElls to reverse ventricular dysfunction). J. Am. Coll. Cardiol. 63, 110–122 (2014).
- 17. Ghiroldi, A. et al. Cell-based therapies for cardiac regeneration: A comprehensive review of past

- and ongoing strategies. Int. J. Mol. Sci. 19, (2018).
- 18. Wysoczynski, M. & Bolli, R. A realistic appraisal of the use of embryonic stem cell-based therapies for cardiac repair. *Eur. Heart J.* **41**, 2397–2404 (2020).
- 19. Menasché, P. *et al.* Human embryonic stem cell-derived cardiac progenitors for severe heart failure treatment: first clinical case report. *Eur. Heart J.* **36**, 2011–2017 (2015).
- 20. Tulloch, N. L. *et al.* Growth of Engineered Human Myocardium with Mechanical Loading and Vascular Co-culture. *Circ. Res.* **109**, 47–59 (2012).
- 21. Kawamura, M., Miyagawa, S., Miki, K. & Saito, A. Feasibility, Safety, and Therapeutic Efficacy of Human Induced Pluripotent Stem Cell-Derived Cardiomyocyte Sheets in a Porcine Ischemic Cardiomyopathy Model. *Circulation* **126**, 29–37 (2012).
- 22. Murphy, M. B., Moncivais, K. & Caplan, A. I. Mesenchymal stem cells: environmentally responsive therapeutics for regenerative medicine. *Exp. Mol. Med.* **45**, (2013).
- 23. Serra, M., Cunha, B., Peixoto, C., Gomes-Alves, P. & Alves, P. M. Advancing manufacture of human mesenchymal stem cells therapies: technological challenges in cell bioprocessing and characterization. *Curr. Opin. Chem. Eng.* **22**, 226–235 (2018).
- 24. U.S. National Library of Medicine. www.clinicaltrials.gov. Accessed 17 Aug. 2022.
- 25. Kern, S., Eichler, H., Stoeve, J., Kluter, H. & Bieback, K. Comparative Analysis of Mesenchymal Stem Cells from Bone Marro , Umbilical Cord Blood, or Adipose Tissue. *Stem Cells* **24**, 1294–1301 (2006).
- 26. Dominici, M. *et al.* Minimal criteria for defining multipotent mesenchymal stromal cells . The International Society for Cellular Therapy position statement. *Cytotherapy* **8**, 315–317 (2006).
- 27. Fu, Y. et al. Trophic Effects of Mesenchymal Stem Cells. *Tissue Eng. Part B* 23, 515–528 (2017).
- 28. Baglio, S. R., Pegtel, D. M. & Baldini, N. Mesenchymal stem cell secreted vesicles provide novel opportunities in (stem) cell-free therapy. *Front. Physiol.* **3**, 359 (2012).
- 29. L, P. K., Kandoi, S., Misra, R., Vijayalakshmi, S. & Rajagopal, K. The mesenchymal stem cell secretome: A new paradigm towards cell-free therapeutic mode in regenerative medicine. *Cytokine Growth Factor Rev.* **46**, 1–9 (2019).
- 30. Abels, E. R. & Breakefield, X. O. Introduction to Extracellular Vesicles: Biogenesis, RNA Cargo Selection, Content, Release, and Uptake. *Cell. Mol. Neurobiol.* **36**, 301–312 (2016).
- 31. Yue, B. *et al.* Exosome biogenesis, secretion and function of exosomal miRNAs in skeletal muscle myogenesis. *Cell Prolif.* **53**, (2020).
- 32. Fu, Y. *et al.* Trophic Effects of Mesenchymal Stem Cells in Tissue Regeneration. *Tissue Eng. - Part B Rev.* **23**, 515–528 (2017).
- 33. Keshtkar, S., Azarpira, N. & Ghahremani, M. H. Mesenchymal stem cell-derived extracellular vesicles: novel frontiers in regenerative medicine. *Stem Cell Res. Ther.* **9**, 63 (2018).
- 34. Murphy, D. E. *et al.* Extracellular vesicle-based therapeutics: natural versus engineered targeting and trafficking. *Exp. Mol. Med.* **51**, 1–12 (2019).
- 35. Ostrowski, M. *et al.* Rab27a and Rab27b control different steps of the exosome secretion pathway. *Nat. Cell Biol.* **12**, 19–30 (2010).

- 36. Cocucci, E. & Meldolesi, J. Ectosomes and exosomes: shedding the confusion between extracellular vesicles. *Trends Cell Biol.* **25**, 364–372 (2015).
- 37. Doyle, L. M. & Wang, M. Z. Overview of Extracellular Vesicles, Their Origin, Composition, Purpose, and Methods for Exosome Isolation and Analysis. *Cells* **8**, 727 (2019).
- 38. Qiu, G. *et al.* Functional proteins of mesenchymal stem cell-derived extracellular vesicles. *Stem Cell Res. Ther.* **10**, 359 (2019).
- 39. Holm, M. M., Kaiser, J. & Schwab, M. E. Extracellular Vesicles: Multimodal Envoys in Neural Maintenance and Repair. *Trends Neurosci.* **41**, 360–372 (2018).
- 40. Wiklander, O. P. B., Brennan, M. Á., Lötvall, J., Breakefield, X. O. & Andaloussi, S. E. L. Advances in therapeutic applications of extracellular vesicles. *Sci. Transl. Med.* **11**, (2019).
- 41. Lu, M. *et al.* Recent advances on extracellular vesicles in therapeutic delivery: challenges, solutions, and opportunities. *Eur. J. Pharm. Biopharm.* **119**, 381–395 (2017).
- 42. Murali, V. P. & Holmes, C. A. Mesenchymal stromal cell-derived extracellular vesicles for bone regeneration therapy. *Bone Reports* **14**, 101093 (2021).
- 43. Fattore, A. Del *et al.* Differential effects of extracellular vesicles secreted by mesenchymal stem cells from different sources on glioblastoma cells. *Expert Opin. Biol. Ther.* **15**, 495–504 (2015).
- 44. Fuzeta, M. de A., Bernardes, N., Oliveira, F. D. & Al., E. Scalable Production of Human Mesenchymal Stromal Cell-Derived Extracellular Vesicles Under Serum- / Xeno-Free Conditions in a Microcarrier-Based Bioreactor Culture System. *Front. Cell Dev. Biol.* **8**, 553444 (2020).
- 45. Chong, S. Y. *et al.* Extracellular vesicles in cardiovascular diseases: Alternative biomarker sources, therapeutic agents, and drug delivery carriers. *Int. J. Mol. Sci.* **20**, (2019).
- 46. Zhang, B., Tian, X., Hao, J., Xu, G. & Zhang, W. Mesenchymal Stem Cell-Derived Extracellular Vesicles in Tissue Regeneration. *Cell Transplant.* **29**, (2020).
- 47. Chung, A. S., Lee, J. & Ferrara, N. Targeting the tumour vasculature: insights from physiological angiogenesis. *Nat. Rev. Cancer* **10**, 505–514 (2010).
- 48. Bian, S., Zhang, L., Duan, L. & Wang, X. Extracellular vesicles derived from human bone marrow mesenchymal stem cells promote angiogenesis in a rat myocardial infarction model. *J. Mol. Med.* **92**, 387–397 (2014).
- 49. Brien, J. O., Hayder, H., Zayed, Y. & Peng, C. Overview of MicroRNA Biogenesis, Mechanisms of Actions, and Circulation. *Front. Endocrinol. (Lausanne).* **9**, 402 (2018).
- 50. Merino-gonzález, C. *et al.* Mesenchymal Stem Cell-Derived Extracellular Vesicles Promote Angiogenesis: Potencial Clinical Application. *Front. Nutr.* **7**, 24 (2016).
- 51. Yu, B. *et al.* Exosomes Secreted from GATA-4 Overexpressing Mesenchymal Stem Cells Serve as a Reservoir of Anti-Apoptotic microRNAs for Cardioprotection. *Int. J. Cardiol.* **182**, 349–360 (2015).
- 52. Tang, L., Wei, D. & Yan, F. MicroRNA-145 functions as a tumor suppressor by targeting matrix metalloproteinase 11 and Rab GTPase family 27a in triple-negative breast cancer. *Cancer Gene Ther.* **23**, 258–265 (2016).
- 53. Zou, C. et al. MiR-145 inhibits tumor angiogenesis and growth by N-RAS and VEGF. Cell Cycle

- **11**, 2137–2145 (2012).
- 54. Sheykhhasan, M. *et al.* Exosomes of Mesenchymal Stem Cells as a Proper Vehicle for Transfecting miR-145 into the Breast Cancer Cell Line and Its Effect on Metastasis. *Biomed Res. Int.* **5516078**, (2021).
- 55. Arderiu, G. *et al.* MicroRNA-145 regulates the differentiation of adipose stem cells toward microvascular endothelial cells and promotes angiogenesis. *Circ. Res.* **125**, 74–89 (2019).
- 56. Luther, K. M. *et al.* Exosomal miR-21a-5p mediates cardioprotection by mesenchymal stem cells. *J. Mol. Cell. Cardiol.* **119**, 125–137 (2018).
- 57. Peng, Y., Zhao, J., Peng, Z., Xu, W. & Yu, G. Exosomal miR-25-3p from mesenchymal stem cells alleviates myocardial infarction by targeting pro-apoptotic proteins and EZH2. *Cell Death Dis.* **11**, 317 (2020).
- 58. Zhao, J. *et al.* Mesenchymal stromal cell-derived exosomes attenuate myocardial ischaemia-reperfusion injury through miR-182-regulated macrophage polarization. *Cardiovasc. Res.* **115**, 1205–1216 (2019).
- 59. Bian, S. *et al.* Extracellular vesicles derived from human bone marrow mesenchymal stem cells promote angiogenesis in a rat myocardial infarction model. *J. Mol. Med.* **92**, 387–397 (2014).
- 60. Luo, Q. & Chen, G. Exosomes from MiR-126-Overexpressing Adscs Are Therapeutic in Relieving Acute Myocardial Ischaemic Injury. *Cell. Physiol. Biochem.* **44**, 2105–2116 (2017).
- 61. Sun, J. *et al.* HIF-1 α overexpression in mesenchymal stem cell-derived exosomes mediates cardioprotection in myocardial infarction by enhanced angiogenesis. *Stem Cell Res. Ther.* **11**, 373 (2020).
- Ding, Y. et al. Exosomes derived from human umbilical cord mesenchymal stromal cells deliver exogenous miR-145-5p to inhibit pancreatic ductal adenocarcinoma progression. Cancer Lett. 442, 351–361 (2019).
- 63. Bellio, M. A. *et al.* Systemic delivery of large-scale manufactured Wharton's Jelly mesenchymal stem cell-derived extracellular vesicles improves cardiac function after myocardial infarction. *J. Cardiovasc. Aging* **2**, 9 (2022).
- 64. f extracellular vesicles from human bone marrow mesenchymal stromal cells yields nanGobin,
 J. et al. Hollow-fiber bioreactor production nanovesicles that mirrors the immuno- modulatory antigenic signature of the producer cell. Stem Cell Res. Ther. 12, 127 (2021).
- 65. Jeske, R. *et al.* Upscaling human mesenchymal stromal cell production in a novel vertical-wheel bioreactor enhances extracellular vesicle secretion and cargo profile. *Bioact. Mater.* (2022).
- 66. Adlerz, K., Patel, D., Rowley, J., Ng, K. & Ahsan, T. Strategies for scalable manufacturing and translation of MSC-derived extracellular vesicles. *Stem Cell Res.* **48**, 101978 (2020).
- 67. Patel, D. B., Santoro, M., Born, L. J., Fisher, J. P. & Jay, S. M. Towards rationally designed biomanufacturing of therapeutic extracellular vesicles: impact of the bioproduction microenvironment. *Biotechnol. Adv.* **36**, 2051–2059 (2018).
- 68. Agnes, R. *et al.* Serum Deprivation of Mesenchymal Stem Cells Improves Exosome Activity and Alters Lipid and Protein Composition Serum Deprivation of Mesenchymal Stem Cells Improves Exosome Activity and Alters Lipid and Protein Composition. *iScience* **16**, 230–241 (2019).

- 69. Maumus, M. *et al.* Mesenchymal Stem Cell-Derived Extracellular Vesicles: Opportunities and Challenges for Clinical Translation. *Front. Bioeng. Biotechnol.* **8**, (2020).
- 70. Gottipamula, S., Muttigi, M. S., Kolkundkar, U. & Seetharam, R. N. Serum-free media for the production of human mesenchymal stromal cells: a review. *Cell Prolif.* **46**, 608–627 (2013).
- 71. Théry, C., Amigorena, S., Raposo, G. & Clayton, A. Isolation and Characterization of Exosomes from Cell Culture Supernatants and Biological Fluids. *Curr. Protoc. Cell Biol.* **3**, (2006).
- 72. Lee, M. *et al.* Enhanced Cell Growth of Adipocyte-Derived Mesenchymal Stem Cells Using Chemically-Defined Serum-Free Media. *Int. J. Mol. Sci.* **18**, 1779 (2017).
- 73. Bobis-wozowicz, S. *et al.* Diverse impact of xeno-free conditions on biological and regenerative properties of hUC-MSCs and their extracellular vesicles. *J. Mol. Med.* **95**, 205–220 (2017).
- 74. Patel, D. B. *et al.* Impact of cell culture parameters on production and vascularization bioactivity of mesenchymal stem cell-derived extracellular vesicles. *Bioeng. Transl. Med.* **2**, 170–179 (2017).
- 75. Haraszti, R. A. *et al.* Exosomes Produced from 3D Cultures of MSCs by Tangential Flow Filtration Show Higher Yield and Improved Activity. *Mol. Ther.* **26**, 2838–2847 (2018).
- 76. Kehoe, D. E., Jing, D., Lock, L. T., Tzanakakis, E. S. & Ph, D. Scalable Stirred-Suspension Bioreactor Culture of Human Pluripotent Stem Cells. *Tissue Eng. Part A* **16**, 405–421 (2010).
- 77. Soure, A. M. De, Fernandes-platzgummer, A., Silva, C. L. & Cabral, J. M. S. Scalable microcarrier-based manufacturing of mesenchymal stem/stromal cells. *J. Biotechnol.* **236**, 88–109 (2016).
- 78. Fuzeta, M. D. A., Dargen, A., Branco, D. M., Fernandes-platzgummer, A. & Lobato, C. Addressing the Manufacturing Challenges of Cell-Based Therapies. *Adv. Biochem. Eng.* **171**, 225–278 (2020).
- 79. May, A., Grolms, M., Olmer, R., Martin, U. & Zweigerdt, R. Facilitating scale up: controlled stem cell cultivation in stirred suspension bioreactors. *Biotech Int.* 19–21 (2011).
- 80. Koh, B. *et al.* Three dimensional microcarrier system in mesenchymal stem cell culture: a systematic review. *Cell Biosci.* **10**, 75 (2020).
- 81. Madrigal, M., Rao, K. S. & Riordan, N. H. A review of therapeutic effects of mesenchymal stem cell secretions and induction of secretory modification by different culture methods. *J. Transl. Med.* **12**, (2014).
- 82. King, H. W., Michael, M. Z. & Gleadle, J. M. Hypoxic enhancement of exosome release by breast cancer cells. *BMC Cancer* **12**, 421 (2012).
- 83. Eibes, G. *et al.* Maximizing the ex vivo expansion of human mesenchymal stem cells using a microcarrier-based stirred culture system. *J. Biotechnol.* **146**, 194–197 (2010).
- 84. Butler, M. Animal cell cultures: recent achievements and perspectives in the production of biopharmaceuticals. *Appl. Microbiol. Biotechnol.* **68**, 283–291 (2005).
- 85. Lembong, J. *et al.* Bioreactor Parameters for Microcarrier-Based Human MSC Expansion under Xeno-Free Conditions in a Vertical-Wheel System. *Bioengineering* **7**, 73 (2020).
- 86. Paganini, C. *et al.* Scalable Production and Isolation of Extracellular Vesicles: Available Sources and Lessons from Current Industrial Bioprocesses. *Biotechnol. J.* **14**, (2019).

- 87. Chen, Y. *et al.* The enhanced effect and underlying mechanisms of mesenchymal stem cells with IL-33 overexpression on myocardial infarction. *Stem Cell Res. Ther.* **10**, 295 (2019).
- 88. Coumans, F. A. W. *et al.* Methodological Guidelines to Study Extracellular Vesicles. *Circ. Res.* **120**, 1632–1648 (2017).
- 89. Tortajada, M. M., Montón, C. G., Genis, A. B. & Roura, S. Extracellular vesicle isolation methods: rising impact of size-exclusion chromatography. *Cell. Mol. Life Sci.* **76**, 2369–2382 (2019).
- 90. Livshits, M. A., Khomyakova, E., Evtushenko, E. G. & Laz, V. N. Isolation of exosomes by differential centrifugation: Theoretical analysis of a commonly used protocol. *Sci. Rep.* **5**, **17319**, (2015).
- 91. Yuana, Y., Levels, J., Grootemaat, A., Sturk, A. & Nieuwland, R. Co-isolation of extracellular vesicles and high-density lipoproteins using density gradient ultracentrifugation. *J. Extracell. Vesicles* **3**, (2014).
- 92. Li, P., Kaslan, M., Lee, S. H., Yao, J. & Gao, Z. Progress in Exosome Isolation Techniques. Theranostics **7**, 789–804 (2017).
- 93. Tengattini, S. Chromatographic Approaches for Purification and Analytical Characterization of Extracellular Vesicles: Recent Advancements. *Chromatographia* **82**, 415–424 (2019).
- 94. Yang, D. *et al.* Progress, opportunity, and perspective on exosome isolation efforts for efficient exosome-based theranostics. *Theranostics* **10**, 3684–3707 (2020).
- Gimona, M., Pachler, K., Laner-plamberger, S., Schallmoser, K. & Rohde, E. Manufacturing of Human Extracellular Vesicle-Based Therapeutics for Clinical Use. *Int. J. Mol. Sci.* 18, 1190, (2017).
- 96. Chen, S., Sun, F., Qian, H., Xu, W. & Jiang, J. Preconditioning and Engineering Strategies for Improving the Efficacy of Mesenchymal Stem Cell-Derived Exosomes in CellFree Therapy. *Stem Cells Int.* **1779346**, (2022).
- 97. Park, K., Bandeira, E., Shelke, G. V, Lässer, C. & Lötvall, J. Enhancement of therapeutic potential of mesenchymal stem cell-derived extracellular vesicles. *Stem Cell Res. Ther.* **10**, 288 (2019).
- 98. Grangier, A. *et al.* Technological advances towards extracellular vesicles mass production. *Adv. Drug Deliv. Rev.* **176**, **11384**, (2021).
- 99. Zhu, J. *et al.* Myocardial reparative functions of exosomes from mesenchymal stem cells are enhanced by hypoxia treatment of the cells via transferring microRNA-210 in an nSMase2-dependent way. *Artif. cells, nanomedicine, Biotechnol.* **46**, 1659–1670 (2018).
- 100. Gu, J. & Chen, Y. Exosomes Derived from Hypoxia-Treated Human Adipose Mesenchymal Stem Cells Enhance Angiogenesis Through the PKA Signaling Pathway. Stem Cells Dev. 27, 456–465 (2018).
- 101. Garcia, N. A., Ontoria-Oviedo, I., González-King, H., Diez-Juan, A. & Sepúlveda, P. Glucose starvation in cardiomyocytes enhances exosome secretion and promotes angiogenesis in endothelial cells. *PLoS One* 10, 1–23 (2015).
- 102. Pinto, A. et al. Immune Reprogramming Precision Photodynamic Therapy of Peritoneal

- Metastasis by Scalable Stem-Cell-Derived Extracellular Vesicles. ACS Nano 15, 3251–3263 (2021).
- 103. Ib, F., Montesinos, J., Area-gomez, E. & Guerri, C. Ethanol Induces Extracellular Vesicle Secretion by Altering Lipid Metabolism through the Mitochondria-Associated ER Membranes and Sphingomyelinases. *Int. J. Mol. Sci.* 22, 8438 (2021).
- 104. Munir, J., Yoon, J. K. & Ryu, S. Therapeutic miRNA-Enriched Extracellular Vesicles: Current Approaches and Future Prospects. *Cells* **9**, 2271 (2020).
- 105. Wang, W., Xu, X., Li, Z., Lendlein, A. & Ma, N. Genetic engineering of mesenchymal stem cells by non-viral gene delivery. *Clin. Hemorheol. Microcirc.* **58**, 19–48 (2014).
- 106. Zhang, L. et al. Exosomes from microRNA-126 overexpressing mesenchymal stem cells promote angiogenesis by targeting the PIK3R2- mediated PI3K / Akt signalling pathway. J. Cell. Mol. Med. 25, 2148–2162 (2020).
- 107. Gnecchi, M. *et al.* Evidence supporting paracrine hypothesis for Akt- modified mesenchymal stem cell-mediated cardiac protection and functional improvement. *FASEB J.* **20**, 661–669 (2006).
- 108. Renaud-Gabardos, E. *et al.* Therapeutic Benefit and Gene Network Regulation by Combined Gene Transfer of Apelin, FGF2, and SERCA2a into Ischemic Heart. *Mol. Ther.* **26**, 902–916 (2018).
- 109. Ban, J. J., Lee, M., Im, W. & Kim, M. Low pH increases the yield of exosome isolation. *Biochem. Biophys. Res. Commun.* **461**, 76–79 (2015).
- 110. Lopatina, T. et al. Platelet-derived growth factor regulates the secretion of extracellular vesicles by adipose mesenchymal stem cells and enhances their angiogenic potential. Cell Commun. Signal. 12, 26 (2014).
- 111. An, Y. et al. Exosomes from Adipose-Derived Stem Cells (ADSCs) Overexpressing miR-21 Promote Vascularization of Endothelial Cells. Sci. Rep. 9, 12861 (2019).
- 112. Fierro, F. A., Kalomoiris, S., Sondergaard, C. S. & Nolta, J. A. Effects on Proliferation and Differentiation of Multipotent Bone Marrow Stromal Cells Engineered to Express Growth Factors for Combined Cell and Gene Therapy. *Stem Cells* **29**, 1727–1737 (2011).
- Cunha, B. et al. Bioprocess integration for human mesenchymal stem cells: From up to downstream processing scale-up to cell proteome characterization. J. Biotechnol. 248, 87–98 (2017).
- 114. Yuan, Y., Kallos, M. S., Hunter, C. & Sen, A. Improved expansion of human bone marrow-derived mesenchymal stem cells in microcarrier-based suspension culture. *J. Tissue Eng. Regen. Med.* **8**, 210–225 (2014).
- 115. Bellani, C. F. *et al.* Scale-Up Technologies for the Manufacture of Adherent Cells. *Front. Nutr.* **7**, (2020).
- 116. Mas-Bargues, C. *et al.* Relevance of oxygen concentration in stem cell culture for regenerative medicine. *Int. J. Mol. Sci.* **20**, (2019).
- 117. Mark, P. *et al.* Human mesenchymal stem cells display reduced expression of CD105 after culture in serum-free medium. *Stem Cells Int.* **2013**, (2013).

- 118. Wang, D. *et al.* Different culture method changing CD105 expression in amniotic fluid MSCs without affecting differentiation ability or immune function. *J. Cell. Mol. Med.* **24**, 4212–4222 (2020).
- 119. Das, R. *et al.* Preparing for cell culture scale-out: establishing parity of bioreactor and flask expanded mesenchymal stromal cell cultures. *J. Transl. Med.* **17**, 241 (2019).
- 120. Anderson, P., Carrillo-Gálvez, A. B., García-Pérez, A., Cobo, M. & Martín, F. CD105 (Endoglin)-Negative Murine Mesenchymal Stromal Cells Define a New Multipotent Subpopulation with Distinct Differentiation and Immunomodulatory Capacities. *PLoS One* 8, 1–13 (2013).
- 121. Ahmed, L. New Approaches for Enhancement of the Efficacy of Mesenchymal Stem Cell-Derived Exosomes in Cardiovascular Diseases. *Tissue Eng. Regen. Med.* (2022).
- 122. Collino, F. *et al.* Adipose-derived mesenchymal stromal cells under hypoxia: Changes in extracellular vesicles secretion and improvement of renal recovery after ischemic injury. *Cell. Physiol. Biochem.* **52**, 1463–1483 (2019).
- 123. Salomon, C. *et al.* Exosomal Signaling during Hypoxia Mediates Microvascular Endothelial Cell Migration and Vasculogenesis. *PLoS One* **8**, 1–24 (2013).
- 124. Schop, D. *et al.* Growth, metabolism, and growth inhibitors of mesenchymal stem cells. *Tissue Eng. Part A* **15**, 1877–1886 (2009).
- 125. Reiner, A. T., Witwer, K. W., van Balkom, B., de Beer, J., Brodie, C., Corteling, R. L., et al. Concise Review: Developing Best-Practice Models for the Therapeutic Use of Extracellular Vesicles. *Stem Cells Transl. Med.* **6**, 1730–1739 (2017).
- 126. Dong, L. *et al.* Comprehensive evaluation of methods for small extracellular vesicles separation from human plasma, urine and cell culture medium. *J. Extracell. Vesicles* **10**, (2020).
- 127. Böing, A. N. *et al.* Single-step isolation of extracellular vesicles by size-exclusion chromatography. *J. Extracell. Vesicles* **3**, 1–11 (2014).
- 128. Lee, H. & Kang, K. T. Advanced tube formation assay using human endothelial colony forming cells for in vitro evaluation of angiogenesis. *Korean J. Physiol. Pharmacol.* **22**, 705–712 (2018).
- 129. Suarez-Arnedo, A. *et al.* An image J plugin for the high throughput image analysis of in vitro scratch wound healing assays. *PLoS One* **15**, 1–14 (2020).
- 130. Adlerz, K., Lembong, J., Olsen, T., Rowley, J. & Ahsan, T. Xeno-Free Manufacturing of MSC-EVs in Scalable Bioreactor Culture. *ISEV 2020 Virtual Meeting* https://www.roosterbio.com/wp-content/uploads/2019/10/RoosterBio_Poster_ISEV2019-_-APR-2019.pdf (2022).
- 131. Maacha, S. *et al.* Paracrine Mechanisms of Mesenchymal Stromal Cells in Angiogenesis. *Stem Cells Int.* **2020**, (2020).
- 132. Gai, C., Carpanetto, A., Deregibus, M. C. & Camussi, G. Extracellular vesicle-mediated modulation of angiogenesis. *Histol. Histopathol.* **31**, 379–391 (2016).
- 133. Bai, Y., Bai, L., Zhou, J., Chen, H. & Zhang, L. Sequential delivery of VEGF, FGF-2 and PDGF from the polymeric system enhance HUVECs angiogenesis in vitro and CAM angiogenesis. *Cell. Immunol.* **323**, 19–32 (2018).
- 134. Landskroner-eiger, S., Moneke, I. & Sessa, W. C. miRNAs as Modulators of Angiogenesis. *Cold Spring Harb. Perspect. Med.* **3**, (2013).

- 135. Tian, J., An, X. & Niu, L. Role of microRNAs in cardiac development and disease. *Exp. Ther. Med.* **13**, 3–8 (2017).
- 136. Hwang, H. & Mendell, J. T. MicroRNAs in cell proliferation, cell death, and tumorigenesis. 776–780 (2006).
- 137. Wang, H. *et al.* MiR-145 functions as a tumor suppressor via regulating angiopoietin-2 in pancreatic cancer cells. *Cancer Cell Int.* **16**, 65 (2016).
- 138. Xu, W.-X. *et al.* MiR-145: a potential biomarker of cancer migration and invasion. *Am. J. Transl. Res.* **11**, 6739–6753 (2019).
- 139. Wang, J., Bonacquisti, E. E., Brown, A. D. & Nguyen, J. Boosting the Biogenesis and Secretion of Mesenchymal Stem Cell-Derived Exosomes. *Cells* **9**, 660 (2020).
- 140. Climent, M. *et al.* TGFβ Triggers miR-143/145 Transfer From Smooth Muscle Cells to Endothelial Cells, Thereby Modulating Vessel Stabilization. *Circ. Res.* **116**, 1753–1764 (2015).
- 141. Oda, N., Abe, M. & Sato, Y. ETS-1 Converts Endothelial Cells to the Angiogenic Phenotype by Inducing the Expression of Matrix Metalloproteinases and Integrin β3. *J. Cell. Physiol.* **179**, 121–132 (1999).
- 142. Wang, S. *et al.* Effects of hepatocyte growth factor overexpressed bone marrow- derived mesenchymal stem cells on prevention from left ventricular remodelling and functional improvement in infarcted rat hearts. *Cell Biochem. Funct.* **30**, 574–581 (2012).
- 143. Simpkin, J. C., Yellon, D. M., Davidson, S. M., Wynne, A. M. & Smith, C. C. T. Apelin-13 and apelin-36 exhibit direct cardioprotective activity against ischemia- reperfusion injury. *Basic Res. Cardiol.* **102**, 518 (2007).
- 144. Zeng, X. J. *et al.* Apelin protects heart against ischemia / reperfusion injury in rat. *Peptides* **30**, 1144–1152 (2009).
- 145. Detillieux, K. A., Sheikh, F., Kardami, E. & Cattini, P. A. Biological activities of fibroblast growth factor-2 in the adult myocardium. *Cardiovasc. Res.* **57**, 8–19 (2003).
- 146. Virag, J. A. I. *et al.* Fibroblast growth factor-2 regulates myocardial infarct repair: Effects on cell proliferation, scar contraction, and ventricular function. *Am. J. Pathol.* **171**, 1431–1440 (2007).
- 147. Kumar, R. *et al.* Fibroblast Growth Factor 2-Mediated Regulation of Neuronal Exosome Release Depends on VAMP3 / Cellubrevin in Hippocampal Neurons. *Adv. Sci.* **7**, (2020).
- 148. Javidi-sharifi, N. *et al.* FGF2-FGFR1 signaling regulates release of Leukemia-Protective exosomes from bone marrow stromal cells. *Elife* **8**, (2019).
- 149. Seghezzi, G. et al. Fibroblast Growth Factor-2 (FGF-2) Induces Vascular Endothelial Growth Factor (VEGF) Expression in the Endothelial Cells of Forming Capillaries: An Autocrine Mechanism Contributing to Angiogenesis. J. Cell Biol. 141, 1659–1673 (1998).
- 150. Jin, S. et al. Conditioned medium derived from FGF-2- modified GMSCs enhances migration and angiogenesis of human umbilical vein endothelial cells. Stem Cell Res. Ther. 11, 68 (2020).
- 151. Kunduzova, O. *et al.* Apelin / APJ signaling system: a potential link between adipose tissue and endothelial angiogenic processes. *FASEB J.* **22**, 4146–4153 (2008).
- 152. Abreu, R. C. De *et al.* Native and engineered extracellular vesicles for cardiovascular therapeutics. *Nat. Rev. Cardiol.* **17**, 685–697 (2021).

- 153. Théry, C. *et al.* Minimal information for studies of extracellular vesicles 2018 (MISEV2018): a position statement of the International Society for Extracellular Vesicles and update of the MISEV2014 guidelines. *J. Extracell. Vesicles* **7**, 1535750 (2018).
- 154. Sivanantham, A. & Jin, Y. Impact of Storage Conditions on EV Integrity/Surface Markers and Cargos. *Life* **12**, 697 (2022).
- 155. Han, C. *et al.* Human umbilical cord mesenchymal stem cell derived exosomes encapsulated in functional peptide hydrogels promote cardiac repair. *Biomater. Sci.* **7**, 2920–2933 (2019).
- 156. Monguió-tortajada, M. *et al.* Acellular cardiac scaffolds enriched with MSC-derived extracellular vesicles limit ventricular remodelling and exert local and systemic immunomodulation in a myocardial infarction porcine model. *Theranostics* **12**, 4656–4670 (2022).
- 157. Born, L. J. *et al.* Sustained Released of Bioactive Mesenchymal Stromal Cell-Derived Extracellular Vesicles from 3D-Printed Gelatin Methacrylate Hydrogels. *J. Biomed. Mater. Res. Part A* (2021).

7. Supplementay information

Time (day) Static Standard Static Glucose Static Standard Static Glucose Static Standard Static Glucose Static Standard Static Glucose

Figure 7.1 Metabolite concentration profiles during hAT-MSC culture in static culture systems (Static – Standard and Static – Glucose).





ADVANCING CELL-BASED THERAPIES TOWARDS THE TREATMENT OF MYOCARDIAL INFARCTION

CAROLINA DRUMONDE SOUSA